TECHNICAL AND VOCATIONAL TRAINING INSTITUTE (TVTI)

School of Graduate Studies

FACULTY OF ELECTRICAL AND ELECTRONICS TECHNOLOGY AND INFORMATION AND COMMUNICATION TECHNOLOGY (DEPARTMENT OF ELECTRICAL AND ELECTRONICS TECHNOLOGY)

DESIGN AND ANALYSIS OF FUZZY-BASED CONTROLLER FOR THE HYBRID POWER SYSTEM IN SMART GRID

MSc Thesis for the Partial Fulfillment of

Master of Science in Electrical Automation and Control Technology Management

By,

WUBETU ABATE (MTR/772/13)

Supervisor,

DR. BISRAT GEZAHEGN

August 2022

Addis Ababa, Ethiopia

DESIGN AND ANALYSIS OF FUZZY-BASED CONTROLLER FOR THE HYBRID POWER SYSTEM IN SMART GRID

A Thesis submitted to

TECHNICAL AND VOCATIONAL TRAINING INSTITUTE (TVTI)

FACULTY OF ELECTRICAL, ELECTRONICS TECHNOLOGY, INFORMATION, AND COMMUNICATION TECHNOLOGY (DEPARTMENT OF ELECTRICAL AND ELECTRONICS TECHNOLOGY)

In partial fulfillment for the Degree

MASTER OF SCIENCE *in* ELECTRICAL AUTOMATION AND CONTROL TECHNOLOGY MANAGEMENT

By,

WUBETU ABATE (MTR/772/13)

Supervisor,

DR. BISRAT GEZAHEGN

DECLARATION

I here by declare that the work which is being presented in this thesis entitled "**Design and analysis of fuzzy based controller for the hybrid power system in smart grid"** is the original work of my own, has not been presented for a masters thesis in this or other universities and all sources of materials used for this thesis work have been fully acknowledged.

Name: Wubetu Abate (MTR/772/13)

Signature: _____

Place Addis Ababa

Date of Submission: _____

This thesis proposal has been submitted for examination with my approval as a TVTI advisor.



Dr. Bisrat Gezahegn _____ 30/08/2022

Advisor Signature Date

FACULTY OF ELECTRICAL, ELECTRONICS TECHNOLOGY, INFORMATION, AND COMMUNICATION TECHNOLOGY (DEPARTMENT OF ELECTRICAL AND ELECTRONICS TECHNOLOGY)

Thesis on

DESIGN AND ANALYSIS OF FUZZY-BASED CONTROLLER FOR THE HYBRID POWER SYSTEM IN SMART GRID

By,

Wubetu Abate (MTR/772/13)

APPROVED BY THESIS ADVISOR COMMITTEE

Name of the Advisor	Signature	Date
Dr. Bisrat Gezahegn	……..	30/08/2022
Name of Examiner Internal	Signature	Date
Zemenu Tamir	……..	
Name of Examiner, Internal	Signature	Date
Dr. Pechinathan Govindan	……..	31-08-2022
Name of Examiner, External	Signature	Date
Dr. Beteley Teka	……	29-08-2022
Name of Chairperson	Signature	Date

ACKNOWLEDGMENT

First, I would like to say glory to powerful God who helps me in my unabridged lifetime. Several individuals, including academic and supportive staff from the Electrical and Electronic department, I would like to acknowledge and thank my best friends as well as my family and relatives that helped me with my thesis both directly and indirectly while I was a graduate student. I would also like to express my sincere gratitude to my advisor Dr. Bisrat Gezahegn for sharing their unreserved skill, experience and knowledge. His guidance and support was a vital input to perform the work that is without his devoted participation of this thesis might not implement.

ABSTRACT

The user load is supplied with electricity by an autonomous decentralized distributed generation hybrid system, whether in grid-linked or standalone modes. In remote and inaccessible areas or areas that have low installed capacity, this kind of decentralized system is often needed. This study's purpose is to design and simulate distributed hybrid energy systems that combine solar and wind energy using Matlab Simulink linked grid in order to generate enough power for the specified power loads. To produce the necessary power for the selected grid, it combines wind turbine, photovoltaic renewable energy sources. Renewable sources are varied according to the solar irradiance and wind speeds while loads are kept constant. The DC load is connected directly to the DC bus, while AC load is connected via inverter. After the addition of the both system, if the power cannot sustain the load due no wind and foggy atmosphere, the battery system is incorporated to support the system. It incorporates the energy management system using fuzzy logic for the power balance of the system. For the better performance optimization, operational efficiency and the reliability of the system. solar power generation over wind generation 50% of the energy demand which is around 18.5 KW is covered by solar panels, 20% of the load demand, which is around 7.4 KW, is produced from wind, and the remaining 30% of the load demand, which is around 11.1 KW. In this study, fuzzy logic controllers are utilized to make wise decisions on combining the three energy sources to efficiently utilize the electricity provided stated above. These selections are determined by first determining the kind and quantity of available resources, then selecting the best alternative source. Modeled using Matlab/Simulink and written in the fuzzy rule editor is a proposed hybrid energy system.

***Key words**: Fuzzy Logic Controller (FLC), Battery (Bp), wind power (Wp), Solar power (Sp)*

TABLE OF CONTENTS

ACKNOWLEDGMENT iii
ABSTRACT iv
TABLE OF CONTENTS v
LIST OF FIGURES viii
LIST OF TABLES ix
ABBREVIATIONS x
CHAPTER ONE 1
INTRODUCTION 1
1.1 Background 1
1.2 Problem Statement 2
1.3 Objectives of this Thesis 2
1.3.1 General Objective 2
1.3.2 Specific objective 2
1.4 Significance of the Study 3
1.5 Limitations of the Study 3
1.6 Scope of the Study 3
1.7 Methodology 3
1.8 Outline of the Thesis 4
CHAPTER TWO 5
LITERATURE REVIEW 5
2.1 Introduction 5
2.2. Summary of Literature Review 11
2.3. Research Gap 12
CHAPTER THREE 13
HYBRID SYSTEM MODELING 13
3.1 Introduction 13
3.2 Model of the Photovoltaic System 13
3.2.1 Solar Cell Arrangement 13
3.2.2 Equivalent Circuit of Solar Cell 14
3.2.3 Factors that affect the efficiency of solar systems 19

3.2.4 System of Maximum Power Point Tracking (MPPT) 22
3.2.5 Methods of MPPT algorithms 29
3.3 Model of the Wind Power Generator 33
3.3.1 Mathematical Model of Wind Turbine 33
3.3.2 Permanent Magnet Synchronous Generator (PMSG) 35
3.3.3 Power Converter 37
3.3.3.1. AC-DC Converters (Uncontrolled Rectifiers) 37
3.4. Load Sharing of the Hybrid System 40
3.5. System Sizing 40
3.5.3. PV System Designing 40
3.5.4. Wind Generator Designing and Sizing 43
CHAPTER FOUR 44
CONTROLLER DESIGN 44
4.1.1 Proposed System Modeling 45
4.1.2 Flow chart 45
4.2 Fuzzy Logic Controller Design for the Hybrid System 47
4.2.1 Controller Description 47
4.2.2 Proposed Fuzzy Logic Controller 48
4.3.1 Membership function of demand (Pd) 49
4.3.2 Membership function of Utility power (Mp) 50
4.3.3 Membership Function of Solar Power (Sp) 50
4.3.4 Membership Function of Wind Power (Wp) 51
4.3.5 Battery membership function (Bp) 52
4.4.2 Membership function of Grid (Po) 52
CHAPTER FIVE 57
RESULTS AND DISCUSSION 57
5.1. Introduction 57
5.2. Solar Panel Simulation Result 57
5.3. Wind Turbine Simulation Result 60
5.4. Matlab System Model of (HES) For Distributed Generation System Using FLC 61
CHAPTER SIX 67

CONCLUSION AND RECOMMENDATION 67
6.1. Conclusion 67
6.2. Recommendation 67
6.3. Future work 67
REFERENCE 68
APPENDIX 71
CHARACTERISTICS OF SELECTED SOLAR PANEL 71

LIST OF FIGURES

Figure 3. 1 Solar Cell [33 ..... *14*
Figure 3. 2 Equivalent Circuit of Solar PV Cell[25] *15*
Figure 3. 3 I-V and P-V graphs illustrating a solar cell's characteristics[25] *16*
Figure 3. 4 I-V and P-V graphs of a Solar Panel [33] *17*
Figure 3. 5 Fill Factor of a Solar Cell[27] *18*
Figure 3. 6 Resistance in series[21] *20*
Figure 3. 7 Shunt resistance with solar cell[21] *21*
Figure 3. 8 Shunt resistance's influence on the I-V curve[21] *21*
Figure 3. 9 The effect of I-V properties of a solar cell[18] *22*
Figure 3. 10 a converter that tracks maximum power points[27] *23*
Figure 3. 11 Buck converter (Step-down)[13] *25*
Figure 3. 12 Schematic for a Boost (step up) Converter[13] *27*
Figure 3. 13 Cuk converter[13] *28*
Figure 3. 14 Flowchart of Perturb & Observe algorithm[30] *31*
Figure 3. 15 Flowchart of Incremental Conductance Method Algorithm[30] *32*
Figure 3. 16 Block diagram of wind power generation system[13] *33*
Figure 3. 17 Generator-connected circuits for diode rectifiers[14] *37*
Figure 3. 18 Boost Converter[14] *38*
Figure 3. 19 When to use the boost converter: (a) turn on; (b) turn off[7] *39*

Figure 4. 1 Block diagram of the proposed hybrid system *44*
Figure 4. 2 System block diagram *45*
Figure 4. 3 Flow chart of the small-scale hybrid distributed generation system *46*
Figure 4. 4 Fuzzy logic block diagram [13] *47*
Figure 4. 5 Fuzzy logic control technique in MATLAB *49*
Figure 4. 6 Membership function of demand (Pd) *49*
Figure 4. 7 Membership Function of Utility (Mp) *50*
Figure 4. 8 Solar power's membership function (Sp) *51*
Figure 4. 9 Wind power's membership function (Wp) *51*
Figure 4. 10 Membership function of (Bp) *52*
Figure 4. 11 Grid power (Po) membership function *52*
Figure 4. 12 Written Fuzzy Logic Rules *53*
Figure 4. 13 The proposed fuzzy inference system for the battery system *55*
Figure 4. 14 The membership function plot of the input variable (discharging mode) *55*
Figure 4. 15 The membership function plot of the input variable (charging mode) *56*
Figure 4. 16 The fuzzy control rules for the battery system. *56*

Figure 5. 1 The smart hybrid system's Simulink model *57*
Figure 5. 2 The solar power system's Simulink model..... *58*
Figure 5. 3 The characteristics of solar energy in terms of V-I and P-V *58*
Figure 5. 4 The load voltage under different radiation and temperature. *59*
Figure 5. 5 The voltage and current generated by the PV array and the voltage and current after the converter. *59*
Figure 5. 6 The wind turbine system's Simulink model *60*
Figure 5. 7 The load voltage under different wind speed. *60*
Figure 5. 8 The input and output power of the wind turbine system *61*
Figure 5. 9 when there is availability to utility power, fuzzy logic rule viewer..... *62*
Figure 5. 10 when there is no availability to utility power, fuzzy logic rule viewer..... *62*
Figure 5. 11 The load voltage under different radiation, temperature, and wind speed..... *63*
Figure 5. 12 When utility power is in a condition of variable load, fuzzy logic rule viewer..... *63*
Figure 5. 13 The realization of the whole system model in Simulink *64*
Figure 5. 14 Case one of the fuzzy logic controller output..... *65*
Figure 5. 15 Case two of the fuzzy logic controller output..... *65*
Figure 5. 16 Fuzzy logic controller output case three..... *66*

Figure A. 1 Voltage vs Current Simulation Result *72*
Figure A. 2 Current vs Power Simulation Result *73*
Figure A. 3 Voltage vs power Simulation Result *73*

LIST OF TABLES

Table 3.1: Solar panel specifications[29] *41*
Table 3.2: Technical details of the 200W cyclone wind turbine[29]..... *43*

ABBREVIATIONS

DG…….Distributed Generation

FLC……Fuzzy Logic Controller

HAWT……..……Horizontal Axis Wind Turbine

IC……...Installed Capacity

KW……Kilo Watt

MW…….…..Mega Watt

MWH…….…...Mega Watt Hour

NME……..……National Metrology Agency

PI……..….Proportional Integral

PID……....Proportional Integral Derivative

PL……..Peak Load

PV…….....Photo Voltaic

SM…….....Synchronous Machine

SSHDG…….Small Scale Hybrid Distributed Generation

VAWT……..Vertical Axis Wind Turbine

CHAPTER ONE
INTRODUCTION

1.1 Background

Any country has access to a variety of critical energy sources, and electrical energy has greatly aided in the rapid industrialization and economic growth of many nations. It is impossible to exaggerate the value and usefulness of electrical energy to the world. Industrial, commercial, and residential sectors all benefit from electrical energy. Electrical energy is used in manufacturing, telecommunications, domestic (lighting, heating, cooling, entertainment), and commercial operations. Maintaining energy resources in the most efficient manner should be given sufficient priority [1].

The accessibility of cheap, reliable, and safe electricity sources is essential for a country's economic success. Thus, humankind’s quest for secure, long-lasting sources of energy has always been a fascinating mission because of the strong reliance of modern life on electricity, either in large/small cities or everywhere. Today, electricity is a need for all commercial and noncommercial activities as well as for every citizen's survival. Most of the remote towns, disruption of electricity is a serious problem throughout the year. The outages of the electricity network and its area go on a long distance and service restoration takes a very long time, because of this, every aspect of residents', health centers, small and medium enterprise, business and non-business day-to-day life is adversely impacted, especially in large hospitals with delicate loads for power [2].

A contemporary supply of unique energy to a selected location (site) is becoming a major challenge for obtaining reliable electricity even though they are connected to the grid. The efficiency of the continuous production of energy from renewable sources improved by taking into account the possibility of combining different sources to create a hybrid energy system, thus also significantly reducing the intermittency and volatility of the production of energy, to prevent issues brought on by artificial, environmental, and meteorological uncertainty. It is understood that Ethiopia has enormous renewable energy resources, and the livelihood of its people will be advantageous if these resources are used effectively. A hybrid renewable energy system integrates

two or more renewable energy sources into a single unit and has a control system that enables it to produce the power of the desired quality [3]. Solar and wind energy sources exhibit unpredictability and randomness. Solar energy is unreliable because the level of solar radiation is affected by environmental and climatic conditions such as temperature and clouds [4]. Although the wind has tremendous power, it is extremely unpredictable in nature. As a result, wind energy is also regarded as unreliable. Energy storage systems can help to increase the stability and reliability of renewable energy systems. As a result, a hybrid system that combines solar PV, a wind turbine, and a battery storage system is generally more reliable than either wind or solar PV alone [5].

1.2 Problem Statement

It has been a major challenge to achieve the reliability of electrical energy in towns, and if the issue is not resolved with an appropriate measuring solution, it will remain difficult in the future. It is understood that modern life is heavily dependent on electricity everywhere people live, but it is very difficult to obtain sufficient electricity. This problem is getting worse in different industrial, commercial, and social institutions, such as academic colleges, micro and small enterprises, and health institutions. Today, in several micro industries and general hospitals, the majority of hospitals have power-sensitive load departments. We still have daily power outages in the hospital emergency room, maternity ward, neonatology division, and operating room. When this happens, numerous infants, expectant mothers, and emergency room surgical patients risk dying. My motivation is to contribute to the development of a green and active backup power supply.

1.3 Objectives of this Thesis

1.3.1 General Objective

The general objective of the research is to design and simulate the hybrid energy system of the grid-connected smart power system using a fuzzy logic controller.

1.3.2 Specific objective

This study seeks to develop a system that will address the following:

- To study the influence of power interruptions.

- To explore the solution to the challenge of power disruption.
- To study the methodology for hybrid smart sustainable electricity irrespective of changes in weather conditions.
- To analyze the various sources of energy for a hybrid power system.
- To design the fuzzy controller to improve the performance of the hybrid power system.
- To model and simulate the control system of the combined designed backup system using a fuzzy logic controller on Matlab Simulink.

1.4 Significance of the Study

Due to the use of the suggested hybrid energy system for the fuzzy logic controller distributed generation backup system, the frequency of power interruption on the grid was reduced. Because of this analysis, these and similar problems will be reduced by the disruption control in hospitals, affecting human life and sensitive materials.

1.5 Limitations of the Study

The limitations would be that, as opposed to using a random signal generator, the recommended distributed hybrid generating system cannot be completely described to provide an accurate signal for the controller in Matlab/Simulink.

1.6 Scope of the Study

This thesis looks into the technological and financial viability of systems that are connected to solar, wind, and batteries. Among the various renewable energy resources, the study only focuses on solar and wind energy resources. Based on the required total energy, it selects the optimal solar panels, wind turbines, and batteries. This study does not have any practical application; instead, it forecasts and models the hybrid system using MATLAB/Simulink software.

1.7 Methodology

The following methodologies were employed: a review of relevant literature was conducted. The fuzzy logic will regulate the system's energy flow to meet demand continuously and to a high

standard. By simulating the proposed method, MATLAB/SIMULINK is used to evaluate its performance.

1.8 Outline of the Thesis

The study is organized into six chapters. The first chapter is a general introduction to the thesis, which includes general details on electric power demand, and the introduction of the incentive for the use of renewable energy. A solid history or literature review and state the art for hybrid renewable energy systems is presented to the reader in the second chapter and each portion is introduced in a separate section. The methodology for designing the HRES, the system design of each part of power generation, and its controller using the Fuzzy logic system discussed in chapter three. Generally, it begins with modeling solar, wind, and battery systems and then how to size the whole system in a necessary form. Chapter Four begins with small-scale hybrid power generation, distributed generation definition, explanation of the Simulink layout and process description, and conceptual framework from a theoretical point of view of the fuzzy controller and how fuzzy logic works. Chapter Five briefly addresses the simulation results and discussions, (the Fuzzy logic controller and hybrid component simulation results in Matlab/Simulink 2020a. Chapter Six offers the study of a major conclusion, some future work, and recommendations as well.

CHAPTER TWO

LITERATURE REVIEW

2.1 Introduction

This section examines earlier works that were either directly or indirectly connected to the thesis statement of this study. Because of the high demand for energy and the scarcity of traditional energy sources, such as fossil fuels, renewable energy sources have gained popularity among researchers. In order to increase the effectiveness and dependability of renewable energy sources, numerous research papers have been produced. Hybrid energy generation is based on fuzzy systems and was published in so many articles. It takes great and substantial care to identify and review research papers, which are publicly available and offered research papers. The author's research focuses on modeling, simulation, and control of a grid-tied hybrid power system.

Author [6] aimed to develop a hybrid power source system that is effective and affordable in order to improve people's lives, particularly in remote places without electricity from the main grid. This article explains the hybrid system, which combines a diesel generator with solar panels, wind turbines, energy storage technology, and power electronics. He feels hybrid and/or renewable energy sources are cost-competitive over the course of the system, despite the significant upfront investment they demand. The author employs a Genset as a backup power system in this work. However, using a generator has a significant impact on environmental pollution. Furthermore, Weather-dependent renewable energy sources include solar and wind power. As a result, a control system is critical for ensuring continuous power supply and preventing system components from being damaged, as well as harvesting the maximum potential of solar and wind energy for the corresponding wind speed and irradiation.

According to [7] a model was developed to specify the balancing of influences on power quality in a wind-diesel hybrid system. This study's main objective is to lessen the impact of voltage flicker and variation caused by wind turbines on the electrical system. The simulation results demonstrate the FC/ELZ system's ability to compensate for flicker and voltage fluctuation. The results show that the proposed system improves the output power quality of the FCWT, increases the reliability

of the micro-grid due to its high energy density, and reduces the fuel consumption of the diesel-generator; as a result, the fuel cost, pollution, and fuel transfer to the micro-grid are reduced. This paper, like the previous one, used a generator as a backup power system. As a result, it has an environmental impact. Furthermore, only wind provides a complete guarantee of continuous power supply, and he did not use any type of controller mechanism.

A study was carried out [8] with the aim of electrifying a community of 100 homes with a health center and a school. He talked about how installing a PV-Wind hybrid system might enhance people's lives in remote places where the main grid has not yet reached for energy. Using HOMER software, he produced results that differ according on the prevalence of renewable resources. The hybrid setup system used in his study has energy prices that range from 30 to 40 cents per kilowatt-hour. He clarified that this value is exorbitant when compared to both the domestic and the present global electricity tariff. This expense shouldn't be taken into consideration, though, considering the nation's electrical scarcity and the low rate of electricity use in rural areas. The relationship between power supply and demand is time-varying and nonlinear, making it difficult to anticipate. In order to handle varied fluctuations in power supply and demand, a supervisory control system is needed to manage power intermittency, power peak shaving, and long-term energy storage. To deal with these problems, no control mechanism was employed in this paper.

The current study's [9] objective was to simulate the best control strategies for managing the flow of electricity from wind generators to the grid during wind power peaks and from the grid to the electrolyzer during periods of low wind speed, enabling the production of 4-5 kg of electrolytic hydrogen for both stationary and portable applications. The simulation results show that the cost of electricity generated by wind energy is higher than Uganda's commercial energy costs. The commercial cost of Ugandan electricity is 19.12 US cents per kWh, but Kampala has COE of 35.26 US cents per kWh and Tororo has a COE of 42.48 US cents per kWh. The environmental benefit of saving 169,819 kg of CO2 and 140,959 kg of CO2 emissions is the gain in this case. The wind is the only power source considered in this paper. However, in WECS, power will be available whenever there is sufficient wind speed. As a result, the system cannot guarantee a continuous power supply.

The author [10] intended to connect photovoltaic generators, fuel cells, and electrolyzers. SimPower Systems and MATLAB/Simulink are used in this work to model and simulate results. The PV generator is 2880 W, while the FC delivers a 200 W power plant at 1000 (w/m2) solar, and the current and available power from the PV generator decrease due to radiation variation. The system's primary power source is solely photovoltaic (PV) panels. Only PV has no guarantee of continuous power supply because it is weather dependent and power is only available when the sun shines. A control system is also required. Furthermore, he did not use any kind of controller mechanism.

Another work by the author [11] demonstrates how to design a hybrid power system for remote areas. It concentrates on PV and FC systems. In other words, the photovoltaic (PV) panels provide the majority of the power for the hybrid system, with backup provided by additional fuel cells (FC). The best hybrid system architecture and control scheme was determined for this work using the Hybrid Optimization Model for Electric Renewable (HOMER) optimization software. As a result of the increase in fuel consumption in the FC from 0.03 to 0.05 L/hr./Kw.

Author [12] devised a method for optimally sizing system components to meet load requirements while minimizing system-annualized costs and maximizing power supply reliability. In this work, a Wind-PV-FC-Battery Hybrid System was built and simulated using the (HOMER), and the operational and economic parameters that are commonly used in rural India were compared.

The optimized result shows that the system's operating cost is Rs 84,962. The system's total net present value is Rs 47, 999, 37.12. According to energy, photovoltaic's produce 65 percent of total electrical energy, while wind turbines produce the remaining 35 percent. The system generates 1626kWh of electricity per year. Because of the erratic nature of wind and solar energies, a control system is required for a long-term power supply. The author did not consider the control system in this work.

According to the author [13], the goal was to demonstrate the system's performance under various conditions using a typical load profile. The goal of this paper is to design a hybrid photovoltaic (PV)/fuel cell (FC) energy system for stand-alone applications. The system's primary energy source is photovoltaic, with a fuel cell serving as a long-term storage system and backup. MATLAB/Simulink was used to create a design and simulation model for the hybrid system.

Simulations of power management are run for a typical winter and summer day. In all scenarios, the load demand is maintained constant. The simulation results show the effectiveness of the overall power management strategy, and the power flows between the various energy sources and load demand are successfully balanced in both the winter and summer situations. However, because PV is weather dependent, there is no guarantee of continuous power supply because power will be available whenever sunlight is available.

Author [14], possesses increasing demands for electricity on a daily basis that met at a sufficient rate without non-renewable energy resources. Renewable energy sources, like wind and solar power, are widespread and environmentally friendly. Though being the most effective means of meeting the world's energy needs, these renewable energy sources are unpredictable when exposed to the environment. The greatest method for utilizing these available resources would be to deploy hybrid solar and wind renewable energy systems like these.

According to [15], In this article, hybrid solar, microhydro, and biomass power systems are constructed for Barsoma village using fuzzy logic-based control. By detecting the kind and quantity of available resources, An intelligent decision is made regarding how to utilize the power produced by the three energy sources stated above using a fuzzy logic controller. The fuzzy rule editor's appropriate alternative source fuzzy rule selection and Matlab/Simulink modeling of each component of the proposed hybrid system are additional steps.

Author [16], creates a model of a fuzzy logic controller for electrical energy derived from biogas production. A fuzzy logic algorithm was created to help with the power supply to the load to increase the biogas performance of this system. Three operations for fuzzy logic are used to make a decision: the fuzzification procedure, the rule base inference engine, and the process of defuzzification. For the simulation of the constructed model, MATLAB SIMULINK was used. The results showed that for biogas electric power production with a fuzzy logic controller, the power output increased by 3.65 kWh, which is an increase of 45.6 percent with the introduction of a fuzzy logic controller. The applicability of the strategy was shown by the findings. When forecasting the output of biogas, the fuzzy logic controller model produced lesser variances and demonstrated greater predictive performance.

In paper [17] Owing to the high rate of population growth, the daily rise in energy demand is shown in this article. Due to the enormous demand for energy, fossil fuel sources are rapidly running out. The climate is negatively impacted by the increased use of fossil fuels, which contributes to global warming. There is therefore a need to find free, easily available, and environmentally friendly renewable energy solutions. The paper discusses biomass & its sources, methods of production of biomass energy, costs associated with biomass, and benefits and drawbacks.

According to [18], a comprehensive analysis of the mathematical modeling, hybrid renewable energy system topologies, and system management techniques is presented in this study. The optimization methods that could increase the system's economic attractiveness are also illustrated in this article. Future trends in renewable energy are being driven by severe environmental conditions and an abundance of life. The use of solar and wind energy as complementary sources of energy has the potential to significantly reduce global energy consumption. Due to low wind speeds and being more unpredictable than solar energy, wind energy systems might not be physically practicable everywhere. As a result, the combined use of various renewable energy sources is growing in popularity as an alternative to "Hybrid Renewable Energy Systems" of energy that produce oil. Due to advancements in renewable energy technology and a large rise in the price of fossil fuels, these hybrid energy systems are becoming more and more common in remote power generation applications.

Author [19], introduces the capacity to enhance power transmission through the hybrid generation system with grid interconnection. This hybrid energy system typically combines solar and wind power. This research proposes the concept of comprehensive power monitoring approaches to achieve the best and continuous output power from these renewable energy systems at any moment. The key concept of this maximum power point tracking controller used for the control of the direct current to DC boost convertor, through simulation using Matlab/Simulink, the output of this (MPPT) dependent hybrid system observed.

Author[20], explores that since it is abundant and environmentally friendly, renewable energy, such as wind and solar energy, is perfect for power generation. This paper is about system integration for grid-connected Hybrid Renewable Energy Source (HRES) power management, and fuzzy logic-based controller design. Through a common current source interface, the hybrid system connects a photovoltaic (PV) array multiple-input dc-dc converter, a wind turbine, and battery storage. The electrical system can employ this converter to include renewable energy sources. A two-level control system with a fuzzy logic controller is introduced, enabling power management between the generation of intermittent renewable energy (RE), energy storage, and the grid, as well as local controllers for the photovoltaic wind turbine. The simulations were carried out using MATLAB and Simulink.

According to[21], In this paper, a single energy source is not a smart choice to maintain the consistency of the supply of electricity. It combines a wind turbine, a diesel generator, and a solar photovoltaic system with an integrated battery bank. Using HOMER software, a techno-economic analysis of the suggested hybrid system model was conducted.

Author [22], presents a plan on how the Addis Abeba Institute of Technology can generate renewable energy (AAiT). In order to ensure that the primary load is met by the solar energy source that is available and that additional sources are complementary when the primary supply is insufficient, renewable energy sources are hybridized. The four backups for the PV system that are being assessed are batteries, diesel generators, two-hybrid batteries or diesel generators, and grid systems. In HOMER software, the configurations created for finding the best system have been modeled.

In [23] a 36W PV module is modeled and simulated with varying irradiation and temperature. The incremental conductance (INC) and perturbation and observation (P&O) methods were used as MPPT techniques. The P&O algorithm is simple to use and requires less hardware than the incremental conductance technique. However, the power loss is slightly higher when compared to the incremental conductance technique. The development of an intelligent controller for maximizing the electricity provided by sources, simulated, and evaluated in [24], with the capacity to effectively manage the power flow between an energy storage system and a PV-wind hybrid power system. The perturb and observe (P&O) approach is described for comparison with neural

network controllers (NNC), which are utilized to accomplish the MPP for PV modules. The NNC enables the PV system to reach its maximum power point more quickly and with minimal fluctuations at a steady state. P&O, incremental conductance, and FLC MPPT techniques for photovoltaic applications are discussed in [25].

The traditional P&O and incremental conductance algorithms are modified to allow the hill-climbing controller to track the maximum power point under varying irradiation. Furthermore, because the maximum power point voltage curve is not linear, it adjusts the reference voltage increment to match the operating point. The efficiency is around 99.4 percent, and the results of the efficiency tests are used to compare the performances of the adjusted P&O and incremental conductance algorithms, as well as the fuzzy logic control. This paper concludes that the adjusted hill-climbing algorithms outperform the fuzzy logic control (FLC) performance.

2.2. Summary of Literature Review

The majority of the papers reviewed for this thesis are about electrifying rural areas with solar or wind systems combined with a fuel cell or a generator. However, PV and wind are complementary in nature and cannot provide energy independently throughout the day. This results in a lack of dependability and stability in the supply system. However, no control mechanisms are used in these papers. In comparison to previous research, the main objective of this work is to develop a plan for managing the power flow of a hybrid renewable energy system that consists of numerous renewable energy sources (solar and wind energy) and many energy storage systems (battery and fuel cell). The storage system improves the overall system's reliability and stability while the control system maximizes solar and wind energy for the matching wind speed and irradiation. The main energy storage method in this work is batteries for short- to medium-term energy storage, and hydrogen fuel cells for long-term energy storage.

Traditional methods of power flow monitoring and control in a hybrid system lack the efficiency needed to respond quickly to complex hybrid systems, from the literature review so far. The application of artificial intelligence to key problems relating to the optimal dimensioning of both renewable energies and energy storage has also begun to explore by researchers.

2.3. Research Gap

The research gap formulated from the previous thesis work during literature review of the power management of hybrid renewable energy sources has also benefited from performance improvements resulting from the adoption of artificial intelligence (AI) techniques such as fuzzy logic systems. Many researchers use renewable resources for standalone energy that is wind and solar, solar and biomass, and geothermal. Biomass, and geothermal renewable resources is has a significant impact on environmental pollution. The hybrid renewable energy sources of photovoltaics, wind, and batteries were suggested in this study to lessen grid power failures. Fuzzy logic used for the decision-making of usable and sufficient power sources between HRES and supplies the most powerful full source to the load when the main commercial supply is disconnected.

CHAPTER THREE

HYBRID SYSTEM MODELING

3.1Introduction

Renewable energy effectively addresses environmental issues as well as a country's resource shortage. However, because they use natural energy, they are vulnerable to climate change and unstable. On rainy days, for example, solar power cannot provide enough energy. A solution to this weakness could be the hybridization of multiple renewable energy systems. Hybrid renewable energy systems can utilize a variety of renewable energy sources and function adaptably in a range of climatic situations to create a reliable power supply. When multiple renewable energy sources are combined into a single hybrid system, the benefits of one source offset the disadvantages of the others. To satisfy the power system's need for energy, hybrid power systems combine a number of renewable energy generators and storage components. It primarily consists of PV generators and wind turbines, but other sources of electrical energy are added to meet the energy demand. Before developing a hybrid power system, it is critical to understand the energy demand and the resources available at that location. The location's potential for solar energy, wind energy, and other resources must be researched by energy planners. This will assist them in determining what type of hybrid power system will best meet the demand.

As a result, improved efficiency and overall cost reduction are possible. This chapter describes the mathematical models of photovoltaic systems, wind turbine systems, and the connection between the Connected Power Grid. To simulate the technical performance of the PV arrays and wind turbine, a detailed dynamic simulation in MATLAB Simulink will be performed.

3.2Model of the Photovoltaic System

3.2.1 Solar Cell Arrangement

The photovoltaic effect, naturally physical and chemical phenomena, is what allows a solar cell, also known as a photovoltaic cell, to convert light energy directly into electricity. It is a type of photoelectric cell, meaning that its electrical properties, such as current, voltage, or resistance,

change when exposed to light. Modules, more commonly referred to as solar panels, are constructed from individual sun cell equipment. A single silicon solar cell junction in simple terms generates a 0.5 to 0.6 volt maximum open-circuit voltage. There is a need for a solar cell, a PN junction with a wide surface region. The N-type material is kept thin to allow light to pass to the PN junction.

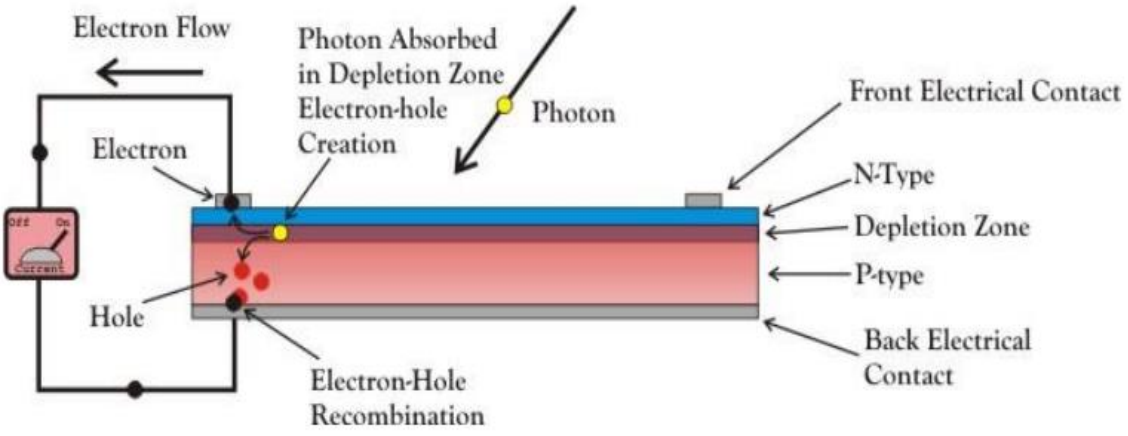


Figure 3. 1 Solar Cell [33

Light to travel in units of energy called photons. Within the PN junction's depletion zone, electrical current is generated. The depletion region, as previously discussed with the diode, is the field surrounding the PN junction where the silicon type N electrons have diffused through the material type P holes. In N-Type silicon, a photon of light that passes through one of these atoms displaces one electron, leaving a free electron and a hole in its place. There is ample room for the hole and free electron to leave the depletion region. When the electron from the back electrical touch hits the P-type silicon, it combines with the hole to restore electrical neutrality.

3.2.2 Equivalent Circuit of Solar Cell

The analog circuit seen in Figure 3.2 is used to further illustrate the PV cell's characteristics. A current source, a diode, and a series resistance are components of the PV model. The parallel resistance effect is seen in the very low leakage resistance of the cell in a single module. Under conditions of constant temperature and constant incident light radiation, the output of the current source, which represents the current emitted by the photons, is constant.

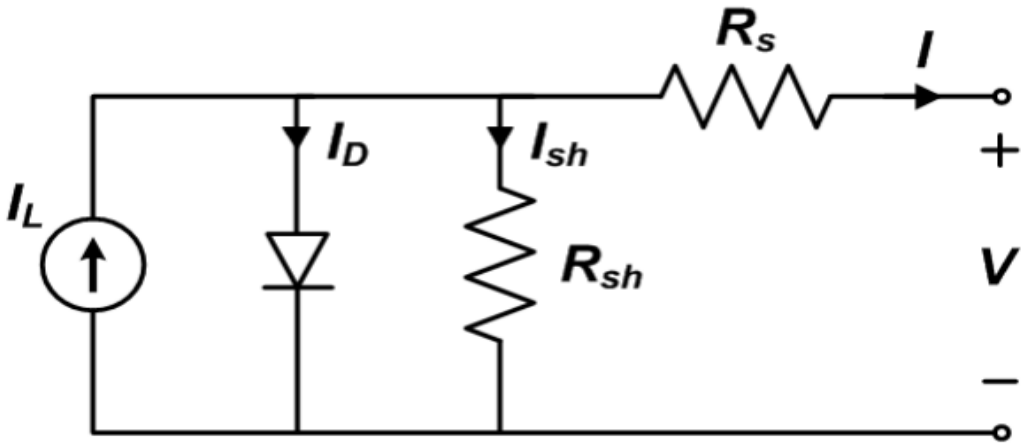


Figure 3. 2 Equivalent Circuit of Solar PV Cell[25]

The current-voltage (I-V) curves were acquired by keeping the cell's temperature constant while exposing those to a constant amount of sunlight, adjusting the load resistance, and measuring the current generated. Two points normally pass through when an I-V curve is drawn:

Short-circuit current (I_{SC}): This is the current generated when the solar cell's positive and negative terminals are shorted together and the inter-terminal voltage is zero, which corresponds to zero-load resistance.

Open-circuit voltage (VOC): This is the voltage between the positive and negative terminals of an open circuit when there is no current flowing, which is equivalent to an infinite load resistance. Current-voltage relationship of a PV cell is given in equation (3.1):

$$I = I_{SC} + I_D \tag{3.1}$$

$$I_D = I_S \left[\frac{qV_D}{e^{nKT}} - 1\right] \tag{3.2}$$

Now from equations (3.1) and (3.2)

$$I_D = I_{SC} - I_S \left[\frac{qV_D}{e^{nKT}}\right] \tag{3.3}$$

Where,

I = output current (A)

I_{SC} = short circuit current (A)

I_S= reverse saturation current (A)

V_D = voltage (V) across the diode

q = electron charge (1.6x C)

K = Boltzmann's constant ($1.38064852 \times 10^{-23}$ m^2 kg s^{-2} K^{-1})

T = junction temperature (K)

n = diode ideality factor (1~2)

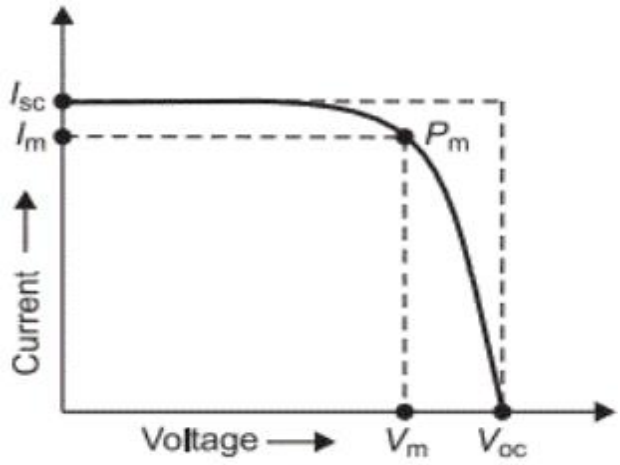


Figure 3. 3 I-V and P-V graphs illustrating a solar cell's characteristics[25]

In figure 3.3 illustrates the current-voltage (I-V) characteristics of a typical silicon photovoltaic cell operating in a typical environment. The power output of a solar cell is the product of its current and voltage (I-V). When the multiplication is done point by point for all voltages from short-circuiting to open-circuit conditions, the power curve above is generated for a specific radiation intensity.

The voltage around the solar cell is at its maximum when it is open-circuited, and the current is at its minimum (zero) when it is not connected to any loads. This value is referred to as the solar cell open circuit voltage, or Voc. The voltage around the shorted solar cell is at its minimum (zero) at the opposite end, i.e., the positive and negative leads are linked, but the short circuit current, or ISC, flowing out of the cell is more than its maximum. Consequently, the ideal operation of a photovoltaic (or panel) cell is defined as being at the maximum power point. We've examined the Solar Cell I-V Characteristic Curve up to this point for a single solar cell or plate. However, some solar arrays are constructed from smaller, connected PV panels. The I-V curve of the PV array is simply a scaled-up version of the I-V characteristic curve of a single solar cell, as shown in figure 3.4.

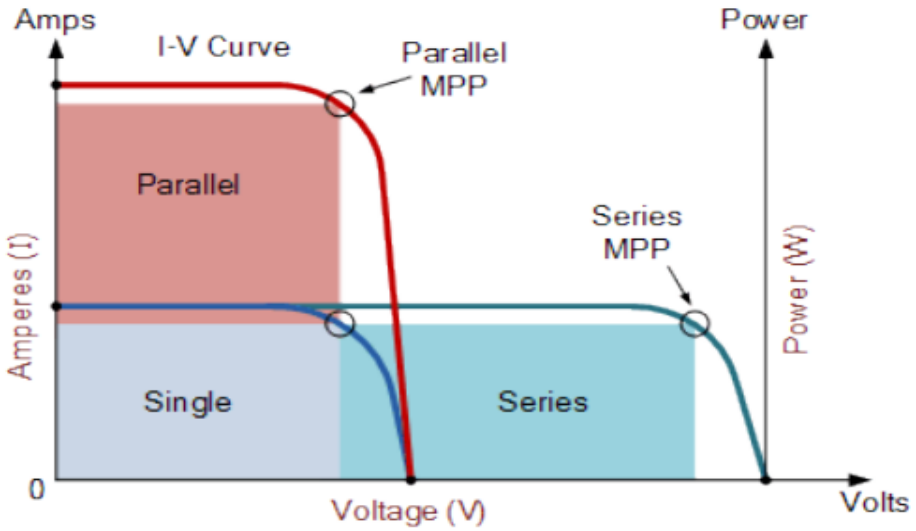


Figure 3. 4 I-V and P-V graphs of a Solar Panel [33]

To maximize the voltage or current power of the solar arrays, photovoltaic panels are connected or interconnected in series, parallel, or both. The voltage rises if the array panels are connected together in a series combination. The current increases when connected in parallel. These various solar configurations will still generate electricity in watts as a function of current voltage times, (P = V x I). Even if the solar panels are connected, the upper right corner of the array will still have a maximum power point (MPP).

The short-circuit current and the open-circuit voltage are the ultimate current and voltage from a solar cell. At any of these operating stages, the power from the solar cell is, however, zero. The parameter that determines the maximum power of a solar cell with ISC and VOC is the "fill factor," more commonly known by its abbreviation "FF." The ratio of the solar cell's maximum power to the combination of the VOC and ISC is defined as FF. The area of the largest rectangle that can fit in the I-V curve and the graphic squareness of the solar cell are both measured by the FF. The FF is illustrated in figure (3.5).

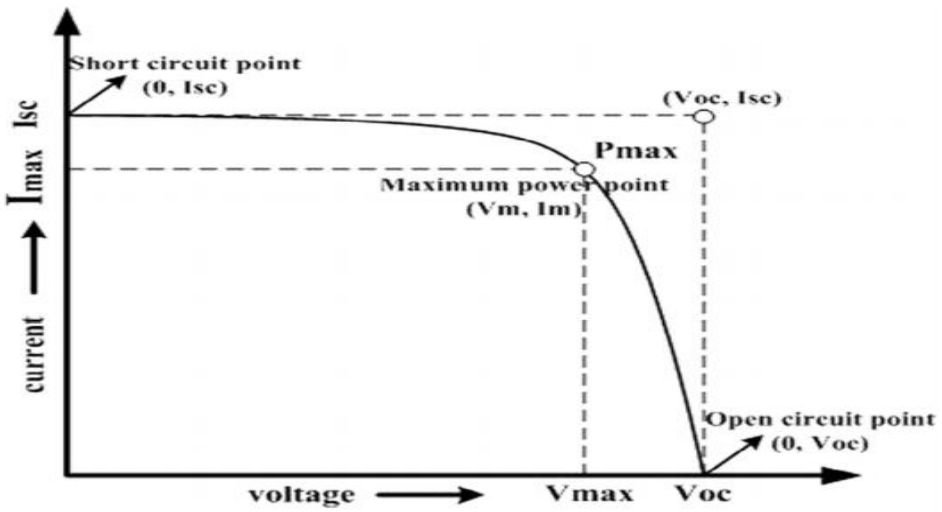


Figure 3. 5 Fill Factor of a Solar Cell[27]

As FF is a measure of the "squareness" of the IV curve, a solar cell with a higher voltage has a higher FF potential, as the "rounded" portion of the IV curve takes up less space. It is possible to calculate the maximum theoretical FF of a solar cell by extracting the power from a solar cell's voltage and finding where it is equal to zero. Thus:

$$\frac{d(IV)}{dV} = 0$$

$$V_{MP} = V_{OC} - \frac{nKT}{q} ln\left(\frac{qV_{MP}}{nKT} + 1\right) \tag{3.4}$$

To solve the above equation, Lambert functions are required, but using iteration to calculate VMP is a simpler approach. In equation (3.4) just applies VOC to VMP; IMP and FF must be determined using different equations.

$$FF = \frac{V_{OC} - ln(V_{OC} + 0.72)}{V_{OC} + 1} \tag{3.5}$$

Where,

V_{OC} known as a "normalized V_{OC}":

$$V_{OC} = \frac{q}{nKT} V_{OC} \tag{3.6}$$

According to equation (3.6), a greater voltage would have a better FF potential. There are, however, relatively uncommon major variations within a given material system in open-circuit voltage. For instance, there is a difference of about 120 mV in the highest open-circuit voltage maximum FFs of 0.85 and 0.83, respectively, in one light between the silicone particular model

and the average commercial solar cell. For instance, the FF of a GaAs solar cell may be near to 0.89. Also shows the importance of the ideality factor, also known as the "n-factor." of a solar cell. Strong n-values not only cause the FF to weaken but also cause low open-circuit voltages because they normally indicate high recombination. The IV curve calculation is most frequently used to determine the FF, which is defined as the maximum power divided by the product of the I_{SC} and VOC,

$$FF = \frac{V_{MP} I_{MP}}{V_{OC} I_{SC}} \tag{3.7}$$

3.2.3 Factors that affect the efficiency of solar systems

3.2.3.1 Temperature Effect

Solar cells are temperature sensitive, as are all other semiconductor materials. As a semiconductor's band gap narrows with increasing temperature, many semiconductor material properties are affected. With increasing temperature, a semiconductor's band gap closes, increasing the energy of the electrons within the material. Therefore, less energy is required to break the link. In the semiconductor bond model, lowering the bond energy also lowered the band gap. As a result, as the temperature increased, the band gap shrank. The solar cell characteristic that is most impacted by temperature rise is the open-circuit voltage.

The I_0 temperature dependence causes the open-circuit voltage to drop with temperature.

$$I_0 = qA \frac{Dn_i^2}{LN_D} \tag{3.8}$$

Where,

q : The electrical charge indicated for the constants on the page

A : the region;

D : the Silicon Material Parameters page's description of silicon's minority carrier diffusivity as a function of doping;

L : is the length of diffusion for the minority carrier;

N_D: doping is;

n_i: is the intrinsic concentration of the carrier given on the Page for Silicon Material Parameters.

Many of the constants in the previous equation are somewhat temperature-dependent, but the intrinsic carrier's concentration, ni, has the biggest impact. The energy of the band gap and the energy of the carriers affect the intrinsic carrier's concentration, with lesser band gaps resulting in a larger intrinsic carrier concentration (with higher temperatures).

Effect of Series Resistance

The flow of current through the solar cell's emitter and base, the resistance of the metal's contact with the silicone, and the resistance of the metal's contact with the top and rear metal all have a role in serial resistance in solar cells. Extremely high values of series resistance can also reduce the short-circuit current, although its primary effect is to reduce fill factor.

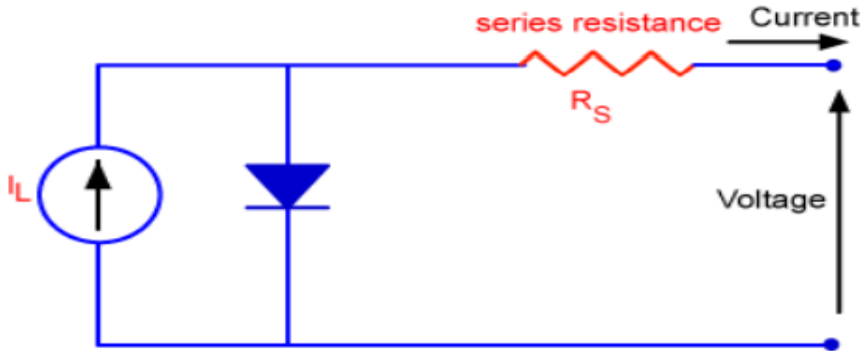


Figure 3. 6 Resistance in series[21]

$$I = I_L - I_0 \left[\frac{q(V + IR_S)}{e^{nKT}} \right] \tag{3.9}$$

Where:

I : cell output current,

I_L: light-generated current,

V: voltage across the cell terminals,

T : temperature;

K: constants,

q : constants,

n : ideality factor,

R_S : is the cell series resistance.

Due to the presence of the current, the formula serves as an example of an implicit function on both sides of the equation, and must be solved using numerical methods. In figure 3.8 demonstrates how the series resistance affects the IV curve.

However, the series resistance has a significant impact on the I-V curves close to the open-circuit voltage. The slope of the I-V curve at the open-circuit voltage point is an easy method for calculating the series resistance of a solar cell.

3.2.3.2 Effect of Shunt Resistance

Instead of poor solar cell design, significant power losses brought on by the presence of shunt resistance, or RSH, are typically the result of manufacturing errors. Low shunt resistance causes power losses in solar cells by giving the current generated by light an alternative channel. There is a bigger impact when this current is lost to the shunt.

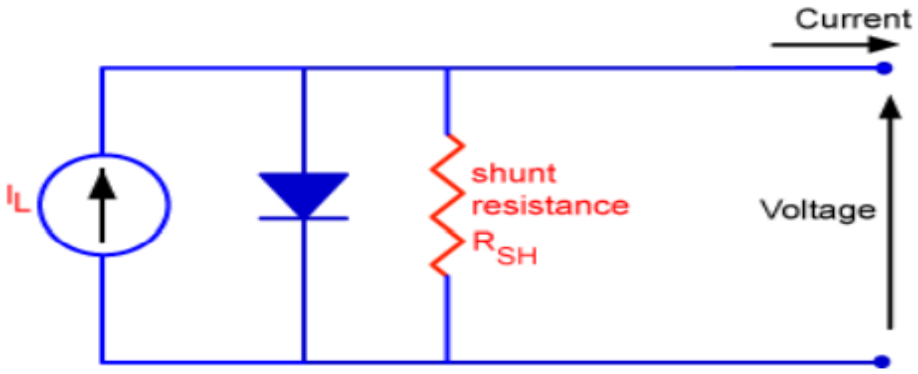


Figure 3. 7 Shunt resistance with solar cell[21]

When shunt resistance is present, the solar cell's equation is:

$$I = I_O \left[\frac{qV}{e^{nKT}}\right] - \frac{V}{R_{SH}} \tag{3.10}$$

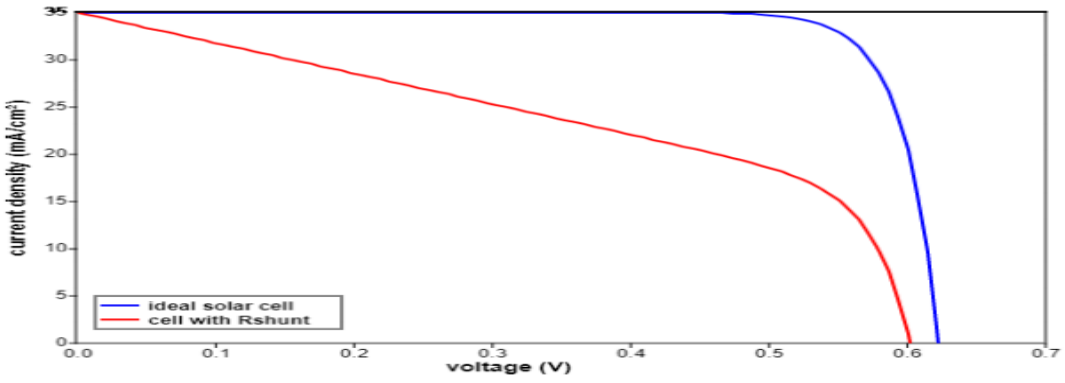


Figure 3. 8 Shunt resistance's influence on the I-V curve[21]

3.2.3.3 Intensity of Light's Effect

All solar cell parameters, such as short-circuit current, open-circuit voltage, FF, efficiency, and the impacts of series and shunt resistances, have an impact on the amount of light that enters a solar

cell. The number of suns is a measure of the frequency of light on a solar cell, where 1 sun corresponds to the usual illumination of 1.5AM or 1 kW/m2. A "flat plate" module is referred to as a PV module designed to operate under one solar condition, whereas those using extreme sunlight are referred to as "concentrators."

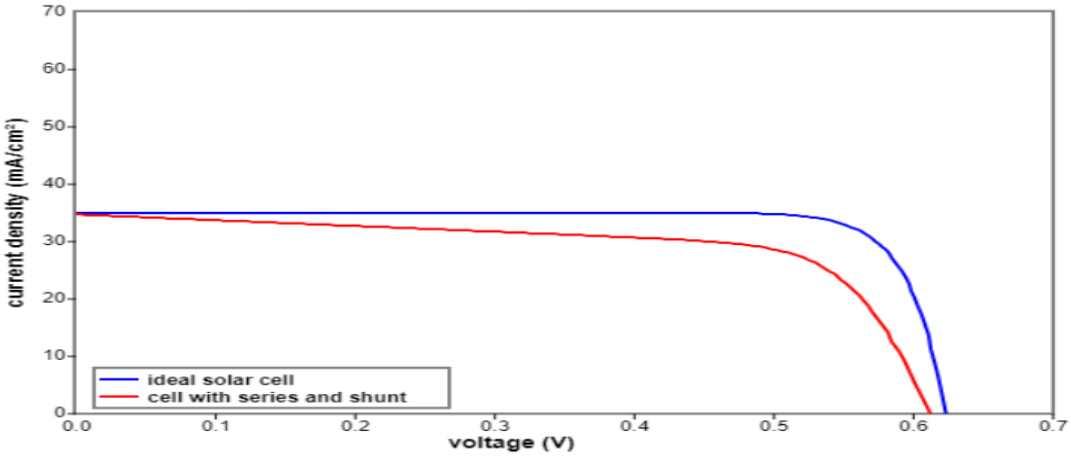


Figure 3. 9 The effect of I-V properties of a solar cell[18]

A solar cell that is a concentrator is made to function when there are several lights present. When sunlight is present, optical components concentrate or direct the incident so that a narrow beam of intense light shines on a solar cell. Concentrators may offer a variety of advantages, including improved performance over single-sun solar cells and possibly lower costs. A device operating under ten suns would have ten times the short-circuit current of a similar device working under one sun since the short-circuit current from a solar cell varies linearly with light intensity. Instead, the benefits of efficiency are extracted from the open-circuit voltage's logarithmic short-circuit dependence. The cost of a concentrated PV system may be less than that of a comparable flat-plate PV system due to the smaller area of solar cells required.

3.2.4 System of Maximum Power Point Tracking (MPPT)

Because MPPT ensures that the system consistently works at its peak power point across a period of fluctuating weather conditions, it is essential for the solar generation to operate the system at high power efficiency.

Between the PV array and the load is a mounted electrical device called the MPPT system. For maximum electricity transfer to the load, the PV system is operated with an MPPT control

algorithm and a AC to DC inverter or DC-DC switching power converter. As the solar panel produces electricity, the maximum power it can produce varies depending on the weather and the load's electrical characteristics. By altering the task ratio of the power converter, the MPPT's primary goal is to balance these two characteristics [25]. In the following figure, the MPP matching is shown in figure 3.12.

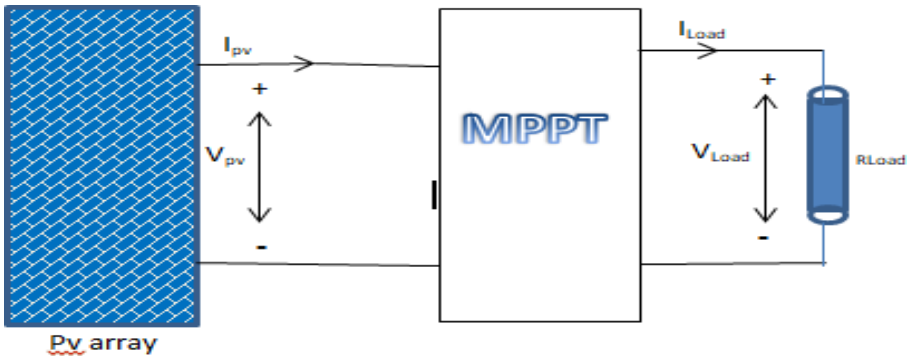


Figure 3. 10 a converter that tracks maximum power points[27]

3.2.4.1 Parameters of MPPT controller performance

When assessing the effectiveness of a new or improved MPPT control algorithm for superior design, three aspects are considered: dynamic responsiveness, steady-state error, and tracking efficiency [25].

The Complex Reaction:

For an MPPT control algorithm to keep up with the MPP amid abrupt changes in atmospheric conditions, it must be quick in its approach. The device loses less solar energy the faster the MPPT algorithm tracks the sun's energy.

An error of the steady state:

If the MPPT control algorithm can stop monitoring and force the device to sustain operation for as long as possible at this optimum operating point. This is challenging to effectively implement in an actual MPPT system because to the active perturbation mechanism in MPPT algorithms and the constant variation in solar insolation and temperature. The effectiveness of the PV system is negatively impacted by this phenomena.

Performance tracking:

Efficiency monitoring is a critical stage in determining how well an MPPT control algorithm monitors the MPP and how much, in comparison to competing approaches, it enhances the PV

system's overall performance. Monitoring performance is described in this research [28] as the discrepancy between the PV array's actual and predicted power over a specific time frame. To determine the efficiency of the tracking, we used the equation shown below:

$$\eta_{MPPT} = \frac{1}{n}\sum_{i}^{n}\frac{p_{actual,i}}{p_{max,i}} \tag{3.11}$$

3.2.4.2 DC-DC Converter for Photovoltaic System

The primary part of the MPPT system is the DC-DC converter transfer mode. These are commonly utilized in DC power supplies and DC motor drives to convert uncontrolled DC inputs into balanced DC outputs or to serve as inverted inputs at the desired voltage and current levels [29]. By monitoring the duty ratio and managing the input voltage at the PV array MPP, an MPPT makes use of the same converter to accomplish load matching for maximum power transmission. To ensure that the solar module is always working at its highest power point and giving the desired input voltage level to the inverter, the photovoltaic module is connected to the inverter using DC-DC converters. The converter task ratio was managed by Maximum Power Point Monitoring Algorithms (MPPT).

Isolated and non-isolated converters are the two categories into which converters are frequently split. A compact, high-frequency electrical isolation transformer is used in isolated topologies to provide the necessary DC isolation between the input and output of the DC converter. By altering the ratio of transformer turns, the output voltage can be altered. In the power supply transfer mode, these converter types are utilized (half bridge and full bridge are the most common). Converters without an insulating transformer are not isolated [29].

Three kinds are distinguished in non-isolated converters: step down (buck), step up (boost), and step up and step down (buck-boost).

3.2.4.3 Step-Down (Buck) Converter

In this type of DC-DC converter, V_O consistently provides an output voltage that is lower than the DC input voltage. The buck converter is used in PV applications such as battery charging and voltage step-down in water pumping systems.

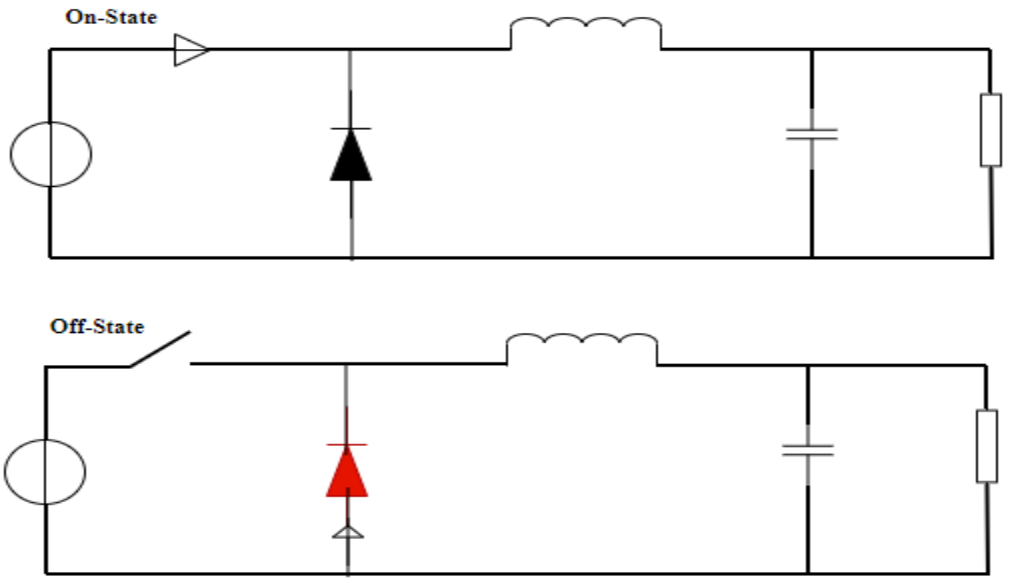


Figure 3. 11 Buck converter (Step-down)[13]

In figure 3.13 the circuit current is Zero starting with the open (off-state) switch. When the switch is first closed (on the state), the current will start to grow. In reaction to the changing current, the inductor will produce an opposite voltage across its terminals. The source voltage is offset by this drop in voltage, which lowers the net voltage across the load. The voltage across the inductor increases as the rate of current shift slows down over time, which also raises the voltage at the load. The inductor stores energy in the form of a magnetic field during that time. If the switch is opened while the current is still changing, there will always be a voltage drop across the inductor, resulting in a net voltage at the load that is lower than the input voltage source. The voltage source will no longer be a part of the circuit, when the switch is reopened (off position), and the current will decrease.

Contrary to the on-state drop, the decreasing current results in a voltage drop across the inductor, making the inductor a current source. The energy stored in the inductor's magnetic field enables a current to pass through the load. This current, which flows when the source of input voltage is unplugged, exceeds the average input current when combined with the current flowing during the on-state (being zero during off-state). In theory, the "increase" in average current compensates the voltage drop and maintains the integrity of the power supplied to the load. During the off state, the inducer releases its stored energy into the circuit. Before the inductor completely discharges, if the

switch is opened and closed once more, the voltage at the load will still be higher than zero (on the state).

The mathematical paradigm:

$$\frac{V_o}{v_d} = \frac{D}{1-D} \tag{3.12}$$

So that

$$L = \frac{R(1-D)^2}{2F_S} \tag{3.13}$$

$$C = \frac{D}{(Rf_S\left(\frac{\Delta V_o}{V_o}\right))} \tag{3.14}$$

3.2.4.4 Boost Converter

The boost converter's purpose is to increase the DC voltage from one that is lower to one that is greater. The boost converter has an inductor, a capacitor, a diode, and a MOSFET. It makes use of a switching transistor that is connected in parallel to control the output voltage. The transistor is biased "OFF" (switch open), and electrical current only travels through the inductor to the load since the transistor switch is effectively linked in parallel with the output. Electrical energy from the PV module goes through the inductor and MOSFET in the Boost Converter circuit when the MOSFET is completely on before returning to the supply. Since the MOSFET can actually produce a short circuit at the output, none of it results. As a result, the inductor receives more current because its inner path back to the source is shorter. The MOSFET connects the anode to the ground, causing diode D to become reverse biased. As the capacitor begins to drain via the load, the voltage level at the output practically stays constant.

When the switch is on:

$$V_S = V_L \tag{3.15}$$

$$I_{L.on} = \frac{V_S}{L}\int dt \tag{3.15}$$

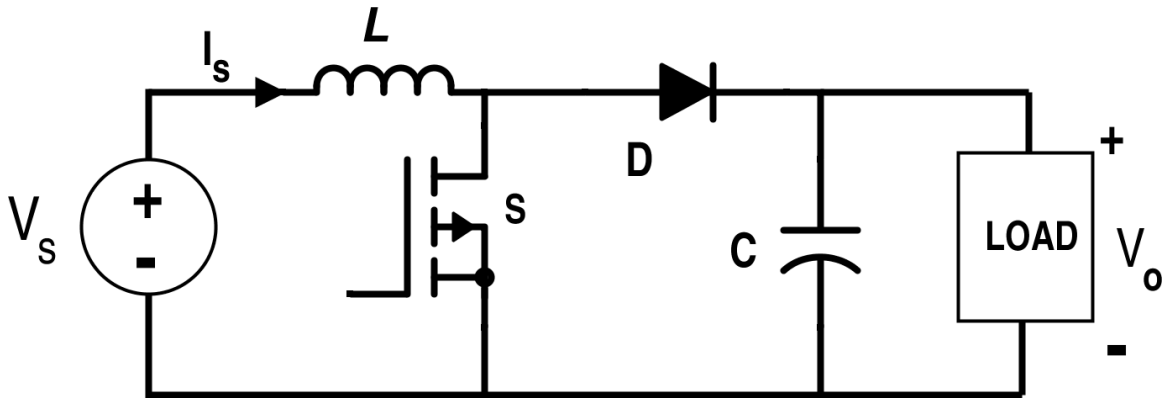


Figure 3. 12 Schematic for a Boost (step up) Converter[13]

The input supply is now connected to the output through the inductors and diode series once the MOSFET has been entirely switched off. The induced energy stored in the inductor is transferred to the output by V_S as the inductor field decreases via the currently forward biased diode. All of this causes the induced voltage to reverse via the inductor *L* and add to the input supply voltage, which results in the following:

$$V_S - V_o = V_L \tag{3.17}$$

$$I_{L,off} = \frac{V_s - V_L}{L} \int dt \tag{3.18}$$

The ratio of output to the input voltage is represented by:

$$\frac{V_o}{V_S} = \frac{1}{1 - D} \tag{3.19}$$

$$\frac{I_o}{I_{in}} = (1 - D) \tag{3.20}$$

Where, D = Duty ratio, Vo = Output voltage, Vs = Input Voltage of PV module, $I0$ = Output current and Iin = Input current

The equation used to calculate minimum inductance is:

$$L_{min} > \frac{(1 - D)^2 DR}{2f} \tag{3.21}$$

Where,

D = Duty cycle

f = Switching frequency

$Lmin$ = Minimum inductance

3.2.4.5 *Cuk (Buck-Boost) Converter*

Utilizing the duality idea, the Cuk converter is built on a Buck-Boost topology circuit. It is clear that the Cuk converter has a Boost converter as its input circuit and a Buck converter as its output circuit. As a result, the Cuk converter is similar to the Buck-Boost converter in that it provides an output voltage that is controlled by negative polarity to the input voltage terminal [28, 29].

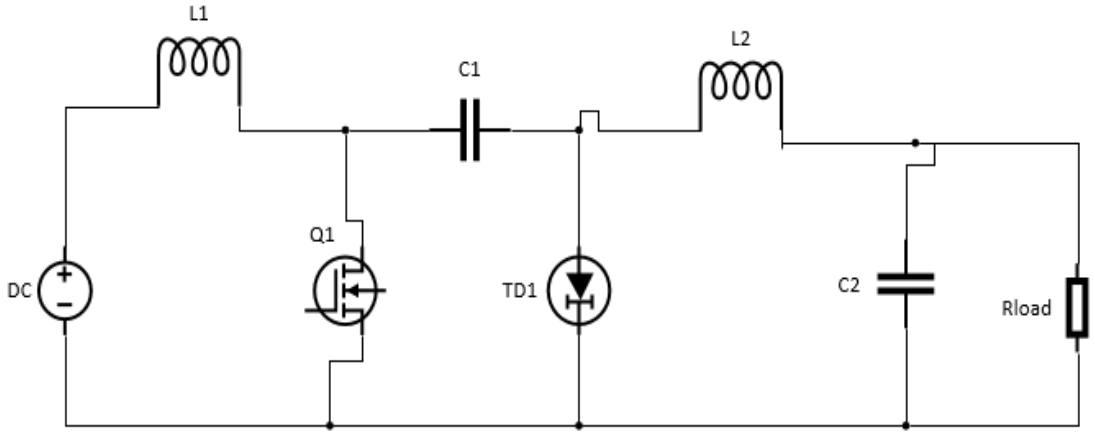


Figure 3. 13 Cuk converter[13]

When an inductor is turned off, it discharges and its voltage acts as the output voltage (negative). When an inductor is turned on, both its charges and its voltage are input voltage (positive).

A comparative study from different points of view was carried out in the literature [29][31] between some widely used topological ones to monitor the PV array's highest power. The Buck-Boost converter has the advantage of consistently obeying to the MPP under all conditions, including solar radiation global radiation, cell temperature, and connected load, as shown in reference. This is in contrast to separate Buck and Boost converters [32]. But at a given price, the specific Boost and Buck varieties are the most effective converters. The author in [33] found that in contrast to the others, each topology has its pros and cons. For instance, some of them, like SEPIC and Cuk converters, have minimal current ripples and can offer input-output isolation. The output voltage needs to be increased or decreased in order to make the Buck and Boost converter suitable for water pumping systems.

The Cuk and SEPIC converters' benefit is that they can draw current from a PV array with ripple. [27] and have a steady input current. In comparison to the Boost converter, the Cuk, SEPIC, and Buck-Boost converters contain more passive components and place greater pressures on the switch or transistor in terms of current, voltage, and switching power. This also affects the overall performance of the system [26], because the switched current and voltage are higher than an individual buck or boost for the same output power. In order to get the desired AC voltages that are delivered to the AC equipment, the higher voltages must also feed the inverter. To maximize the energy harvest from solar systems, boost converters were created. Transformers must be huge and strong for much more than a few watts when used for voltage conversion at mains frequencies of 50–60 Hz. This makes them expensive, and they are resistant to energy losses in their windings and because of eddy currents in their cores.

It was decided to use a DC-DC boost converter in this work since it is an essential part of the PV inverter system and improves the overall system performance. Because of the higher input voltage operation, less input current is required for a given amount of power, which lowers losses. It is in charge of regulating and boosting the D.C output voltage of the P.V system. The PV device's voltage was raised in this study to a higher constant voltage of 680V so it could power an inverter. A boost converter operating in continuous conduction mode was developed to do this.

3.2.4.6 DC-AC converter for photovoltaic system

A technique called pulse width modulation (PWM) switching is used to monitor the length of the opening of each switch. A balanced three-phase output voltage is obtained from a triangular wave PWM switch that is contrasted with three 120-phase shifted sinusoidal control voltages. Each switch in the inverter receives from the PWM switch a duty ratio, D, and this duty ratio control whether the switch is opened or closed [8].

3.2.5 Methods of MPPT algorithms

A PV device's power can be maximized using a variety of strategies, from basic voltage relationships to several sample-based assessments of more complex situations. Because the MPP of a PV module varies with solar radiation and temperature, maximum power point tracking (MPPT) techniques are required in photovoltaic applications. As a result, using MPPT algorithms

is required to get the most power out of a PV module. Several techniques for detecting the maximum power point have been improved and published. These methods differ in several ways, including the number of sensors required, the complexity, and the cost of implementation, the speed, tracking correction. The most commonly used MPPT methods are listed:

3.2.5.1 Constant Voltage Method

The simplest process is the constant voltage system. The VMP is simply represented by a single voltage using this method. This value may sometimes be programmed by connecting an external resistor to the control IC's current source pin. The resistor in this scenario might be a component of a network that also includes an NTC thermostat, enabling temperature 25 to compensate for the value. For each of the several irradiance fluctuations, the system would capture around 80% of the maximum power that is possible. The average degree of irradiance would decide the actual results. The findings could be higher in cases of low levels of irradiance [28].

3.2.5.2 Open Circuit Voltage Method

V_{OC} uses V_{OC} to measure V_{MP} to enhance this process. Once the device obtains the V_{OC} value, VMP is determined by,

$$V_{MP} = k * V_{OC} \tag{3.22}$$

The value of k is normally between 0.7 and 0.8. To compensate for any temperature change, it is important to update the VOC periodically. Sampling the VOC value can also help correct changes in temperature and changes in irradiance to some degree. Input current monitoring may indicate when to re-measure the VOC. The logarithmic function of the irradiance determines the value of k, which rises in value as the irradiance rises. It is important to take this into account in addition to the VOC process.

3.2.5.3 Perturb and Observe Method

Easy input arrangements and limited calculated parameters are used in this algorithm. In this method, a disturbance is periodically administered to the module voltage and the resulting output power is compared with that of the previous disruptive cycle[27]. Minor disruption to the system was introduced in this algorithm. This disruption causes the solar module's power to differ. If the energy increases because of the disturbance, so the disturbance continues in the same direction. The power at the MPP is zero after the peak power is reached and the next instant decreases thus

the disturbance reverses as seen below after that. In the PV system, the P&O algorithm will be used to track MPP.

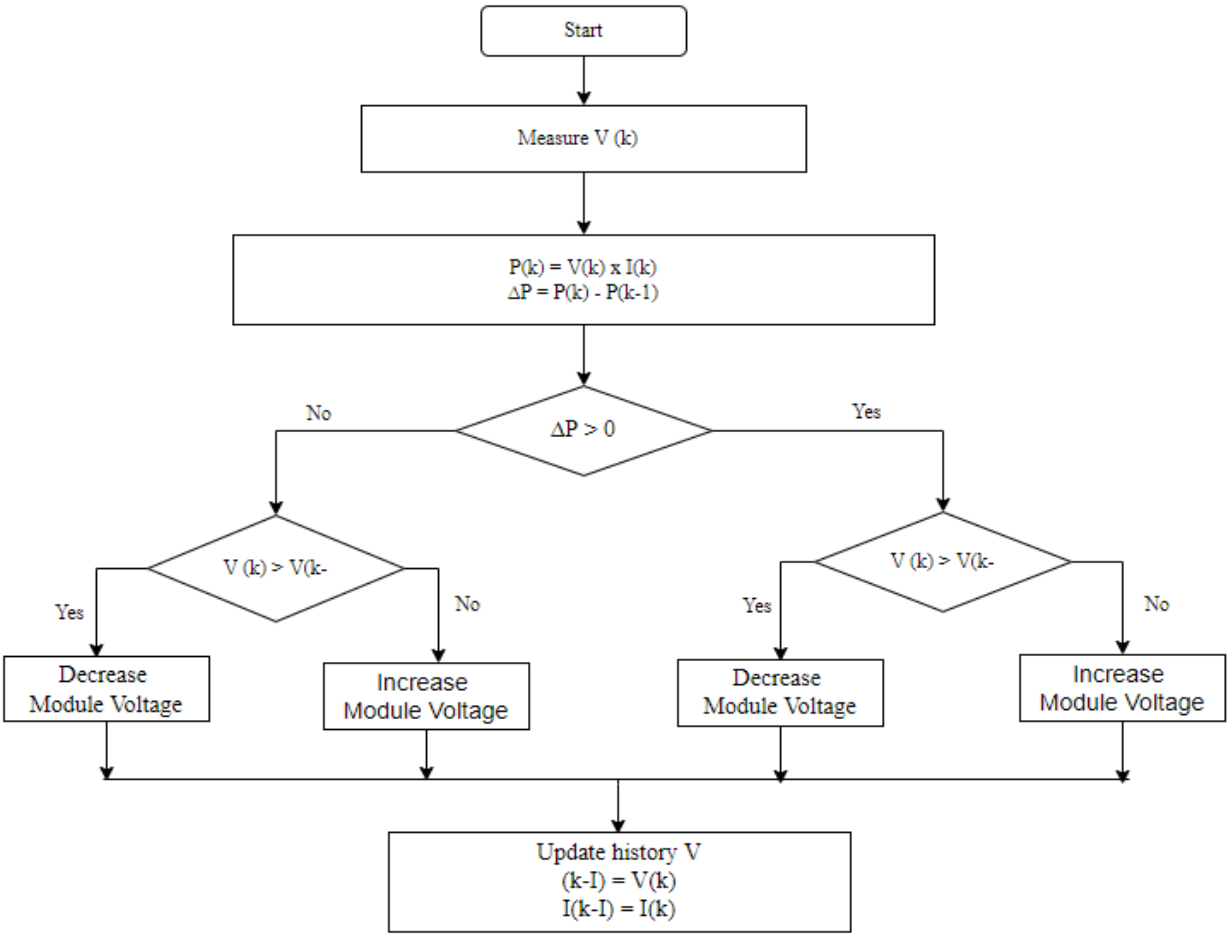


Figure 3. 14 Flowchart of Perturb & Observe algorithm[30]

3.2.5.4 Incremental Conductance Method

The Incremental Conductance Approach is designed to follow an observation based on a P-V characteristic curve. The technique of incremental conductance is based on the fact that the slope of the power curve's PV array is zero at the MPP, positive at the left of the MPP, and negative at the right of the MPP.

This can be offered by,

$$\frac{dP}{dV} = \frac{d(V.I)}{dV} = I\frac{dV}{dV} + V\frac{dI}{dV} \tag{3.23}$$

$$= I + V\frac{dI}{dV}$$

MPP is reached when $\frac{dP}{dV} = 0$ and

$$\frac{dI}{dV} = -\frac{I}{V} \tag{3.24}$$

$$\frac{dP}{dV} > 0 \text{ Then } Vp < Vmpp$$

$$\frac{dP}{dV} = 0 \text{ Then } Vp = Vmpp$$

$$\frac{dP}{dV} < 0 \text{ Then } Vp > Vmpp$$

So if the MPP is on the right side, $< -\frac{I}{V}$ and then to enter the MPP, the Photo Voltaic voltage must be decreased. It has been known to increase the PV performance, decrease power loss and the device cost in order to find the MPP IC technique that can be used. Then, using the current and previous voltage and current values, the gradual changes, dI (change in current) and dV (change in voltage), are determined.

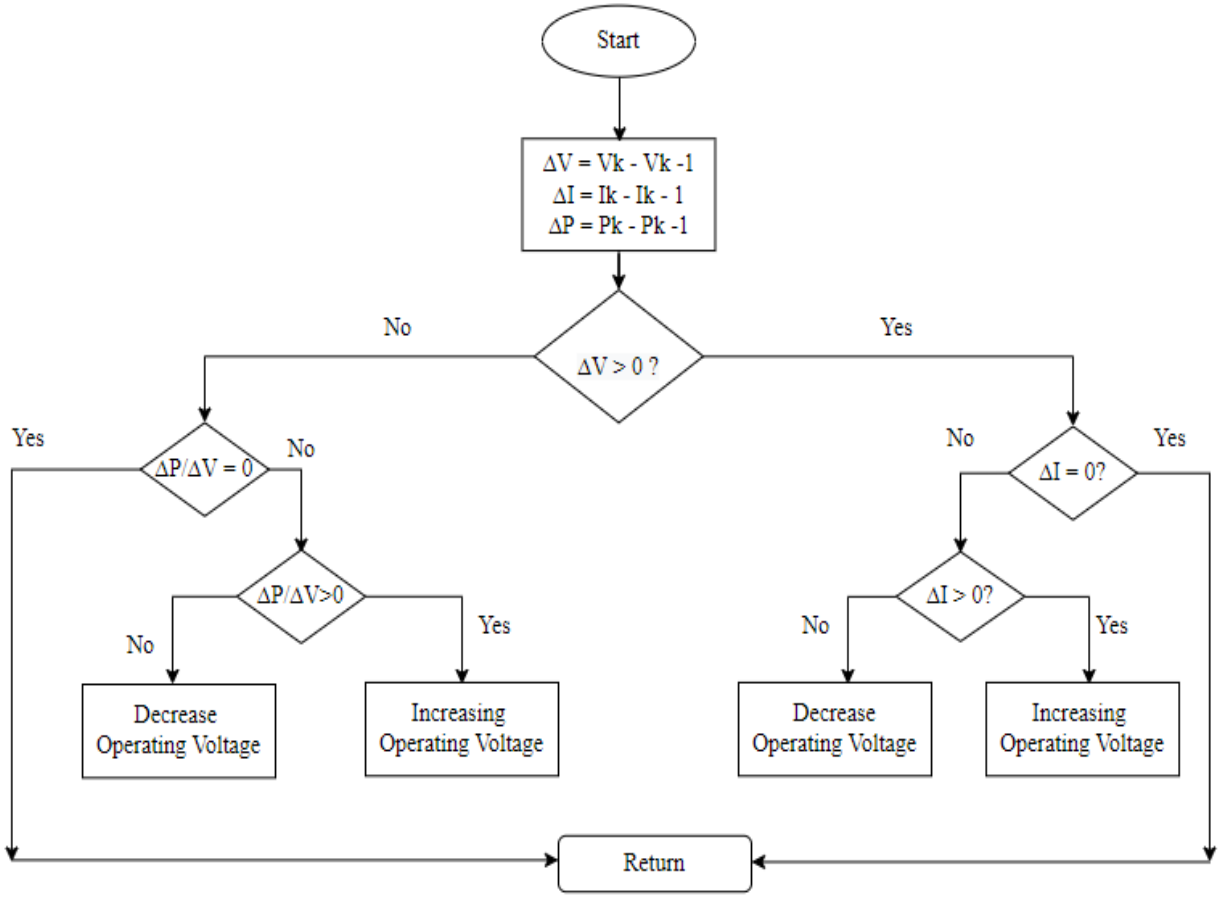


Figure 3. 15 Flowchart of Incremental Conductance Method Algorithm[30]

3.3 Model of the Wind Power Generator

Figure 3.19 depicts the wind power generation system configuration. It consists of a wind turbine, a PMSG, a PWM rectifier, a capacitor filter, a PWM inverter, and a utility grid. The drive shaft connects the wind turbine to the PMSG directly. The three-phase IGBT rectifier with capacitor filter transforms the alternating current generator voltages into direct current voltages. A coupling resistor or inducer is used by the inverter to connect to the utility grid. A machine-side control is used to track the maximum available power point regardless of the wind speed. In order to ensure that the relevant grid connection conditions are met, grid-side control is also used.

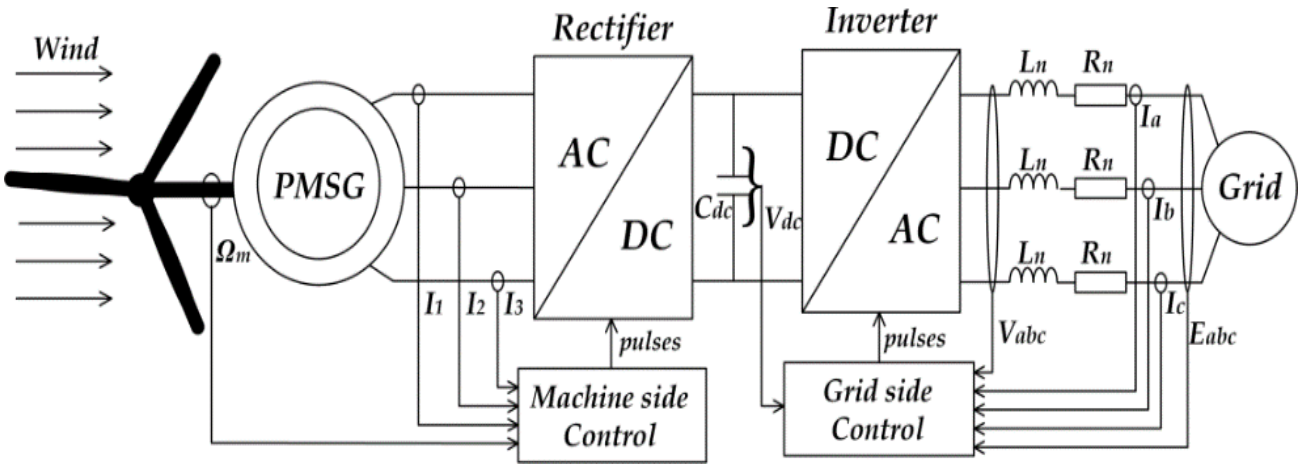


Figure 3. 16 Block diagram of wind power generation system[13]

3.3.1 Mathematical Model of Wind Turbine

A wind turbine's purpose is to transform the kinetic energy of the wind into mechanical energy. The actuator disk theory and the blade element theory are the two main theories that have been used to evaluate and describe the aerodynamic behavior of wind turbines in the literature. The kinetic energy of the wind can only be fully captured by wind turbine blades, according to energy balances and the Bernoulli equation [13]:

$$\frac{g\omega_{mech}}{dt} = \frac{T_{turb} - T_{em,gen}}{J_{turb}} \tag{3.25}$$

The wind turbine's mechanical speed of rotation is denoted by ω_{mech}, its output torque is denoted by T_{turb}, its electromagnetic torque is denoted by $T_{em,gen}$, and the moment of inertia of the system

composed of the wind turbine and the combined generator is denoted by J_{turb} is. The output power of a wind turbine is tied to T_{turb}, which can be seen here.

$$P_{out} = P_{turb} = T_{turb} \tag{3.26}$$

Additionally, in equation (3.26), its input power of the wind speed:

$$P_{in} = P_{wind} = \frac{1}{2}\rho A v^3 wind \tag{3.27}$$

The relationship between T_{turb} and P_{wind} expressed as

$$P_{turb} = C_P P_{wind} = C_P \frac{1}{2}\rho A v_{wind}^3 \tag{3.28}$$

Where,

$$C_P = \frac{P_{out}}{P_{in}} \tag{3.29}$$

Therefore, T_{turb} expressed as

$$T_{turb} = C_P \frac{1}{2}\rho A \frac{R^3}{\lambda^3}\omega_{wind}^2 \tag{3.30}$$

The wind power coefficient C_P for a particular wind turbine is often a function of $\frac{V_{wind}}{\omega_{mech}}$ and beta where V_{wind} is wind speed and beta in general is a constant. Therefore, C_p is regarded as a function of $\frac{V_{wind}}{\omega_{mech}}$. The tip speed ratio (TSR) is described as:

$$\lambda = \frac{R\omega_{mech}}{v_{wind}} \tag{3.31}$$

C_p is additionally considered as a result of λ.

For $C_P = C^{opt}{}_p$the corresponding Tip Speed Ratio is represented as λ^{opt},

i.e. $C_P(\lambda^{opt}) = C^{opt}{}_p$; the relation between λ^{opt}

and ${\omega_{mech}}^{opt}$ can be stated as:

$$\lambda^{opt} = \frac{R\omega^{opt}{}_{mech}}{v_{wind}} \tag{3.32}$$

Where λ^{opt}usually is a constant for a given wind turbine and ${\omega_{mech}}^{opt}$ usually is dependent on wind speed v_{wind}. The plot of C_p versus $mech$ for a given wind speed is shown in figure 3.20. We can see from the graph that there is a value of ω_{mech} at which C_p has the highest value. Let ${C_p}^{opt}$ be the highest possible value of C_p, and ${\omega_{mech}}^{opt}$ be the corresponding value of ω_{mech}.

When the wind turbine is operational, we hope that the wind power coefficient C_p remains at ${C_p}^{opt}$, allowing the wind turbine to efficiently convert the input power into output power. In other words, we hope the mechanically rotational speed of the wind power, ω_{mech}, can keep at ${\omega_{mech}}^{opt}$ who would usually change in response to the wind speed.

The small wind turbines have fixed blades, which mean that $\beta = 0$. An aerodynamic stall strongly advised with this design to reduce turbine efficiency above a certain wind speed. C_P commonly expressed in the literature as a function of the coefficients λ and β.

$$\begin{cases} C_P(\lambda,\beta) = 05176\left(\frac{116}{\lambda} - 0.4\beta - 5\right)e^{\frac{-21}{\lambda}} + 0.0068\lambda \\ \frac{1}{\lambda} = \frac{1}{\lambda+0.08\beta} - \frac{0.035}{\beta^3+1} \end{cases} \tag{3.33}$$

Now let be the pitch angle $\beta = 0$

$$C_P = 0.5716\left(\left(\frac{1}{\lambda} - 0.035\right)116 - 5\right)e^{-21\left(\frac{1}{\lambda}-0.035\right)} + 0.0068\lambda \tag{3.34}$$

So that power coefficient reaches a maximum of 0.41 when $\lambda = 0.72$.

3.3.2 Permanent Magnet Synchronous Generator (PMSG)

In direct-driven wind power production systems, permanent magnet synchronous machines/generators (PMSM) play a crucial role in transforming mechanical energy into electrical energy. It is necessary to do mathematical modeling research on the steady state and dynamic characteristics of wind energy conversion systems in order to develop machine control algorithms and PMSG. Several fundamental presumptions must be established before developing the PMSM's mathematical model, including the following:

1. There is very little damping in the magnets and rotor.
2. Effects of magnetic saturation are ignored.
3. Hysteresis losses and Eddy's current are disregarded.
4. The stator windings' induced back electromotive force (EMF) is sinusoidal.
5. Along the air gap, the stator windings are dispersed sinusoidally.

The generator's electrical angular frequency is influenced by the mechanical rotor speed and number of generator poles n_p.

$$f_e = \frac{n_p}{2} f_r = \frac{n_p}{2}\frac{\omega_r}{2\pi} \tag{3.35}$$

$$\omega_e = 2\pi f_e = \frac{n_p}{2}\omega_r \tag{3.36}$$

Where,

f_e: electrical frequencies

f_r : rotor angular frequencies (in hertz)

The PMSG, and (ω_e) is The electrical angular frequency of the generator. A full-rating power converter and a PMSG make up the generation system. In evaluations of power systems, it is assumed that the magnetic flux distribution surrounding the synchronous generator's air gap is sinusoidal.

The state space relationship between the PMSM's terminal voltages and phase currents is described as:

$$\begin{aligned} v_{as} &= R_s i_{as} + \frac{d}{dt}\lambda_{as} \\ v_{bs} &= R_s i_{bs} + \frac{d}{dt}\lambda_{bs} \\ v_{cs} &= R_s i_{cs} + \frac{d}{dt}\lambda_{cs} \end{aligned} \tag{3.37}$$

Where v_{as}, v_{bs} , and v_{cs} are the three-phase stator voltages in a, b, and c at just that point, and i_{as}, i_{bs} , and i_{cs} are the instant three-phase stator currents.

The author [33] is credited with introducing the dq0 Park's transformation, which is necessary to streamline the study of synchronous machinery models. Analyzing the PM synchronous machine normally involves using the well-known machine model in a dq-reference frame that rotates synchronously with the rotor, where the d-axis is aligned with the magnet axis and the q-axis is orthogonal to the d-axis. Stator voltages, stator currents, and flux linkages are the time-varying quantities that make up the phase quantities in three-phase systems like PMSMs. Converts the AC numbers into time-independent DC quantities.

The transformation can be expressed as follows:

$$\begin{bmatrix} u_d \\ u_q \\ u_0 \end{bmatrix} = \sqrt{\frac{2}{3}} \begin{bmatrix} cos(\theta_r) & cos\left(\theta_r - \frac{2\pi}{3}\right) & cos\left(\theta_r + \frac{2\pi}{3}\right) \\ cos(\theta_r) & sin\left(\theta_r - \frac{2\pi}{3}\right) & sin\left(\theta_r + \frac{2\pi}{3}\right) \\ \frac{\sqrt{2}}{2} & \frac{\sqrt{2}}{2} & \frac{\sqrt{2}}{2} \end{bmatrix} \begin{bmatrix} u_a \\ u_b \\ u_c \end{bmatrix} \tag{3.38}$$

The parks transformation in reverse is:

$$\begin{bmatrix} u_a \\ u_b \\ u_c \end{bmatrix} = \sqrt{\frac{2}{3}} \begin{bmatrix} cos(\theta_r) & -sin(\theta_r) & \frac{\sqrt{2}}{2} \\ cos\left(\theta_r - \frac{2\pi}{3}\right) & -sin\left(\theta_r - \frac{2\pi}{3}\right) & \frac{\sqrt{2}}{2} \\ cos\left(\theta_r + \frac{2\pi}{3}\right) & -sin\left(\theta_r + \frac{2\pi}{3}\right) & \frac{\sqrt{2}}{2} \end{bmatrix} \begin{bmatrix} u_d \\ u_q \\ u_0 \end{bmatrix} \tag{3.39}$$

3.3.3 Power Converter

The model of the AC/DC/AC converter in renewable energy systems is based on a commonly used two-level voltage source converter topology. The converter has good capabilities for correctly and swiftly reacting, as well as for efficiently transporting generated power from wind turbines to the grid. Insulated Gate Bipolar Transistors, Power MOS Field Effect Transistors, and Gate Turn Off Thyristors (IGBTs) are some of the most well-liked power electronics semiconductors on the market right now [20]. IGBT modules are utilized in AC/DC/AC converters in the power industry. A bipolar power transistor is used in combination with a switch to transmit huge currents and an isolated gate FET as the control component, the IGBT combines the advantages of MOSFETs and bipolar transistors. Applications requiring medium- to high-power use the IGBT.

The switching frequency of an IGBT can reach up to 40 kHz, and it has a more simpler control scheme than a GTO. High-power IGBT modules can connect many devices at once and manage a lot of current.

3.3.3.1. AC-DC Converters (Uncontrolled Rectifiers)

Unregulated converters called uncontrolled rectifiers employ diodes to transfer power from an AC source to a DC circuit. An uncontrolled rectifier generates a fixed DC output voltage for a particular AC supply. The three-phase, full-wave diode bridge rectifier circuit is shown in figure 3.16.

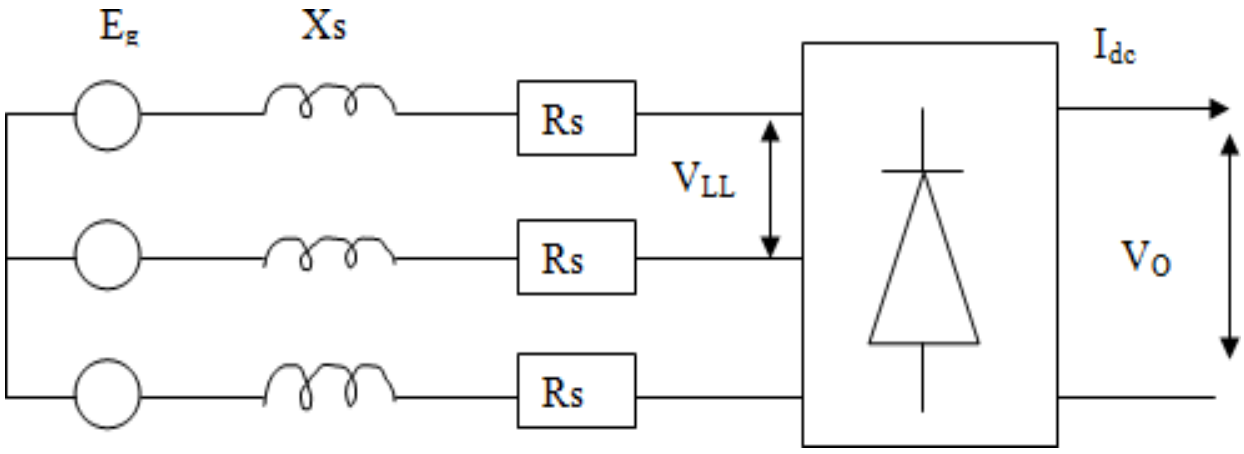


Figure 3. 17 Generator-connected circuits for diode rectifiers[14]

The following formulas determine the rectifier circuit's average output voltage is:

$$V_0 = \frac{1}{\frac{\pi}{3}} \int_{\frac{-\pi}{6}}^{\frac{\pi}{6}} \sqrt{6V_{LL}} cosCos(\omega t) d(\omega t) \quad (3.40)$$

$$V_0 = V_{rec} = \frac{\sqrt[3]{6}}{\pi} V_{LL} \quad (3.41)$$

Where,

V_{LL} : generator's nominal phase-to-phase voltage

3.3.3.2. DC-DC Boost Converters

The objective of a DC-DC converter is to convert an unpredictable DC input voltage from a variable load into a controllable DC output voltage. In some situations, rectifying a varying line voltage will supply the DC input voltage. Boost converters are a type of DC-DC converter that can adjust the current of the input source while boosting the voltage of the output load. A switching technique is widely used to manage the voltage output in boost converters.

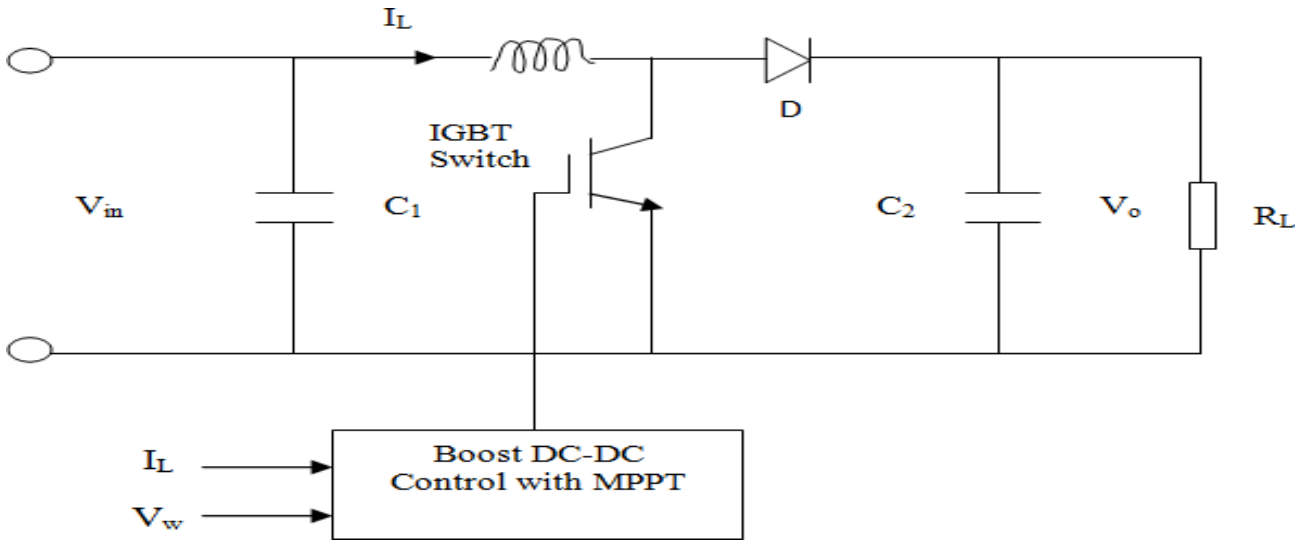


Figure 3. 18 Boost Converter[14]

The service cycle (D), is affected by the T_{on} and switching frequency f_s.

$$D = \frac{t_{on}}{t_{on}+t_{off}} = \frac{t_{on}}{T} = t_{on} f_s \quad (3.42)$$

The input to output voltage proportion in steady-state operation is $\frac{1}{1-D}$. The duty cycle is used to regulate the output voltage. $0<D<1$ is the duty cycle range.

$$t_{on} = DT$$

$$t_{off} = (1-D)T$$

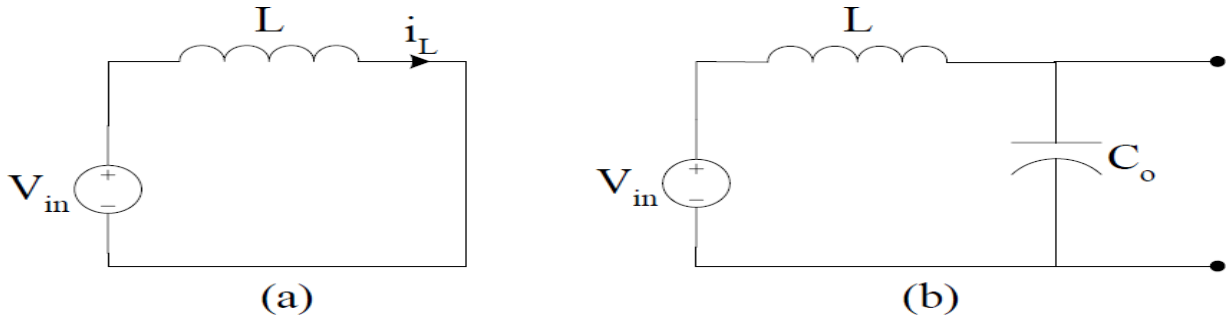


Figure 3. 19 When to use the boost converter: (a) turn on; (b) turn off[7]

The diode is reverse-biased when the switch is activated, isolating the output level. No energy flows from the input to the output due to the connection between the two, but the output does receive energy from the capacitor. Figure 3.23(a) depicts the identical circuit. The inductor voltage in this case is:

$$i_L(t) = \frac{1}{L}V_{in} + I_L(0)0 \geq t \leq DT \tag{3.43}$$

Where $I_L(0)$ is the inductor current at startup at $t = 0$, D is the duty cycle, and T is the time. The power switches are turned on for the next loop. The condition is given in Figure 3.23(b). The inductor would continue to push current through the diode D to the output circuit and charge it because the capacitor was fully charged the previous cycle. The inductor is discharging, and the diode is biased forward. The output stage receives energy from both the input and the inductor. The inductor voltage was measured as follows:

$$V_L - V_t - V_0 - L\frac{di_L}{dt} \Longrightarrow \frac{di_L}{dt} - \frac{V_t - V_0}{L} \tag{3.44}$$

$$i_L(t) = \frac{1}{L}(V_{in} - V_o)(t - DT) + I_L(DT)\ DT \leq t \geq T \tag{3.45}$$

Over one switching time, the average inductor voltage is zero in a steady state, so

$$V_{LON}t_{ON} + V_{LOFF}t_{OFF} = 0$$

$$V_tDT + (V_t - V_o)(1 - D)T = 0 \tag{3.46}$$

$$V_0 = \frac{1}{1 - D}V_i$$

The selection of the inductor, however, is an important design factor for a high-power converter. In order to minimize the size and weight of the inductor, a low inductance value desired. The minimal critical inductance value of the converter for CCM functioning is as follows:

$$L_{CR,BOOST} = \frac{V_0 - V_{in}}{2P}\frac{V_{in}^2}{V_0}T_s \tag{3.47}$$

The output and input capacitor values are also provided, as determined by the voltage ripple of the capacitor.

$$C_1 = \frac{\Delta I_L}{8\Delta V_{in}} T_s \quad (3.48)$$

$$C_2 = \frac{V_0 D_m}{R_L \Delta V_0} T_s \quad (3.49)$$

Equation also gives the inductor ripple current:

$$\Delta L_L = \frac{V_0 - V_{in}}{2L} \frac{V_{in}}{V_0} T_s \quad (3.50)$$

.

3.4. Load Sharing of the Hybrid System

Hybrid energy generation technologies, such as solar, wind, and batteries, are effective, particularly in smart grids with high power sensitivity. Solar power generating outperforms wind power generation and battery storage in terms of production costs and other advantages. This paper, it assumed that 50% of the energy demand generated from solar panels is about 18.5 KW, 20% of the load demand generated from wind is about 7.4 KW, and the remaining 30% of the load demand generated from battery technology is about 11.1 KW.

3.5. System Sizing

System sizing is a technique used to determine the proper voltage and current ratings for each component of a solar, wind, and battery system in order to satisfy the load's electrical requirements. By describing all the load profile of the smart grid, the average power demand in watt-hours per day was obtained. Geographical location showing solar radiation, amount of inclination of the tilt angle plate, and average daily sun hours, wind speed and amount of battery resource are included.

3.5.3. PV System Designing

The first phase in designing a solar photovoltaic system is determining the total power and energy consumption of all the loads that the solar photovoltaic system needs to supply, as different sizes of PV modules can generate different amounts of electricity, as described in the previous section. Selecting the PV module's size is the next step because different PV module sizes produce different quantities of electricity.

The total energy requirement of the system or total watt-hours rating of the system = Total connected load (kilowatts) × Operating hours = 18.5KWh.

- The actual power output of a PV panel = Peak power rating of selected solar panel × assumed operating factor = 150watt × 0.75 = 112.5watt.
- The power used at the end use is less (due to the lower combined efficiency of the system) Actual power output of a panel × combined efficiency = 112.5× 0.81 = 91.125watts.
- Energy produced by panel in a day = Actual power output × 24hours/day (peak equivalent) = 112.5× 24 = 2700 watts-hour.
- The number of solar panels required to satisfy the given estimated daily load = (Total watt-hour rating (daily load)/ (Daily energy produced by a panel) =18500watthour/2700watt-hour= 6.85= 7solar panels are required.

The solar photovoltaic module with a power rating of 150W is chosen for this function due to its mechanical and electrical advantages as well as the fact that its specifications (8.56A short circuit current and 22.5V open circuit voltage) fulfill the criteria. To produce the required solar electricity, a seven (7) solar panel array and each string of solar arrays with 27 solar cells connected in series (Ns) are recommended. a power of around 3.2KW per array is expected to be generated. With the selected PV cell's technical specifications taking its 30% performance into account, the output would be around 22.4 KW (i.e. seven arrays each producing 3.25KW). Seven parallel strings of 27 PV modules each, coupled in series, make up the total number of PV modules.

Table 3.1: Solar panel specifications[29]

150 W solar panel technical specification	
Maximum power	150W
Open circuit voltage	22.5V
Short circuit current	8.56A
Maximum power voltage	18.5V
Maximum power current	8.11A
Module efficiency	15.2%
Solar cell efficiency	17.1%

3.5.3.1. Suitable Storage Battery Sizing

If the need arises, a battery enables electrical energy transformed into chemical energy, stored and transformed back into electrical energy. Negative electrodes, positive electrodes, and electrolytes are the three basic building blocks of batteries. The negative electrode releases electrons to an outside load, and the positive electrode recognizes electrons from the load. Lead-Acid, Lithium Ion, Nickel-Cadmium, Nickel Metal Hydride, and Sodium Sulfur are the types of batteries. Today, the rechargeable lead acid battery is the most common battery for electricity storage, with cost being the key factor [17]. Batteries store direct current electrical energy for later use. However, this energy storage comes at a cost because lead acid batteries often reduce the output and efficiency of the PV system by 10%. The UB-8D AGM 250 AH, 12V-DC system is taken into consideration when developing the mathematical study for sizing the battery bank.

The quantity of energy storage needed, assuming three days of autonomy or days without sunlight, is:

$Erough = 216KWh * 3 = 648KWh$, and

Energy safety

$Esafe = \frac{Enough}{MDOD} = \frac{648KWh}{0.75} = 864KWh$, and

The battery bank capacity needed to be evaluated:

$C = Esafe/Vb = 864KWh/12 = 72000\ Amps\ h$

The whole amount of batteries provided by

$Nbatt/Vb = 864KWh/12 = 72000\ Amps\ h.$

The number of batteries in the series is equal to $Ns = V\frac{DC}{Vb} = \frac{48}{12} = 4$, and the number of parallel paths is equal to $Np = \frac{number\ of\ batteries}{NS} = \frac{288}{4} = 72.$

To improve the dependability of the system, the battery is charged both directly from the solar panels and through a rectifier from commercial A.C power.

3.5.3.2. The inverter's size

the inverter's efficiency at converting solar energy from the system's solar panels from direct current (DC) to alternating current (AC). Electricity varies when the power input rises and falls. If the input from the panels is within the window's viewing range, the inverter is assumed to be

operating at its optimum. The total watt-hours of all the appliances should always exceed the input rating of the inverter. The inverter's scale in standalone systems should be 25–30% larger than the sum of the appliances' wattages. Additionally, the inverter's capacity to withstand surge current during startup should be at least three times greater than that of the motor or compressor appliance type. The inverter should have a minimum output of 23 KW because the expected load is around 18.5 KW.

3.5.4. Wind Generator Designing and Sizing

The energy released during air movement as a result of atmospheric temperature variations is known as wind energy. The first phase used to determine the required power from wind energy for generation is to know the wind speed of the site. In this paper, to determine the performance of wind energy, monthly measurements of wind speed data from the chosen site for the last 4 years are used. The option of a wind turbine capable of producing the required power depends on the wind speed data collected and analyzed from the site to produce 7.4KW. The estimated and selected technical characteristics of wind turbines had shown in Table 3.2. It predicted that a wind speed of about 4 m / s will occur at an altitude of 40 m from the selected site, but it will require an increase in the height of the wind turbine tower if additional power is needed to produce power to generate the necessary power sufficiently. A three-blade cyclone wind turbine that is capable of producing a power of 150w picked. Considering this 50 wind turbines are designed to generate 7.4 KW. This particular three-blade wind turbine uses a stall to control the wind's fluctuating speed. This suggests that the wind turbine is protected at a greater wind speed by choosing the blade's attack angle so that turbulence occurs and when the wind speed exceeds the rated wind speed, the output power decreases.

Table 3.2: Technical details of the 200W cyclone wind turbine[29]

Diameter of Rotor (m)	2
Initial wind speed (m/s)	3
Normal wind speed (m/s)	5
Cutout wind speed	9
maximum power output (w)	200
voltage output (VDC)	12/24

CHAPTER FOUR

CONTROLLER DESIGN

4.1 Layout of the Hybrid Components

This section model and explains the power produced from the hybrid components and the Simulink/Matlab block diagram of the fuzzy logic controller. First, according to the designed system model the design of the solar panel power system is intended to give an output of about 18.5 - 20 kW and the next single wind turbine process is developed to give around 150W, to produce 7.4-8KW,and to generate 11.1 - 12KW power from the battery.

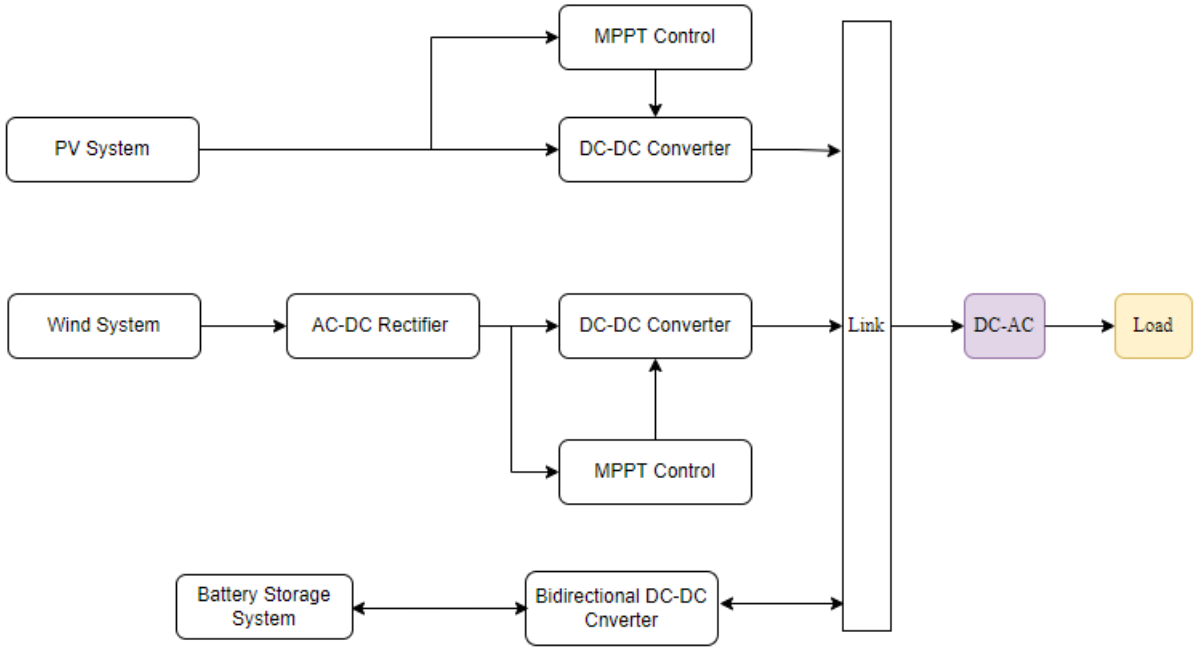


Figure 4. 1 Block diagram of the proposed hybrid system

A hybrid solar PV/wind power system with a battery storage system was modeled, studied, and simulated in this study. When the solar PV or wind systems are turned off, the other system can power the load.

4.1.1 Proposed System Modeling

In the absence of a primary commercial utility supply, the proposed small-scale distributed hybrid generation system uses battery, wind, and solar technology as a backup energy source. A fuzzy logic controller will govern the energy produced by these renewable energy sources.

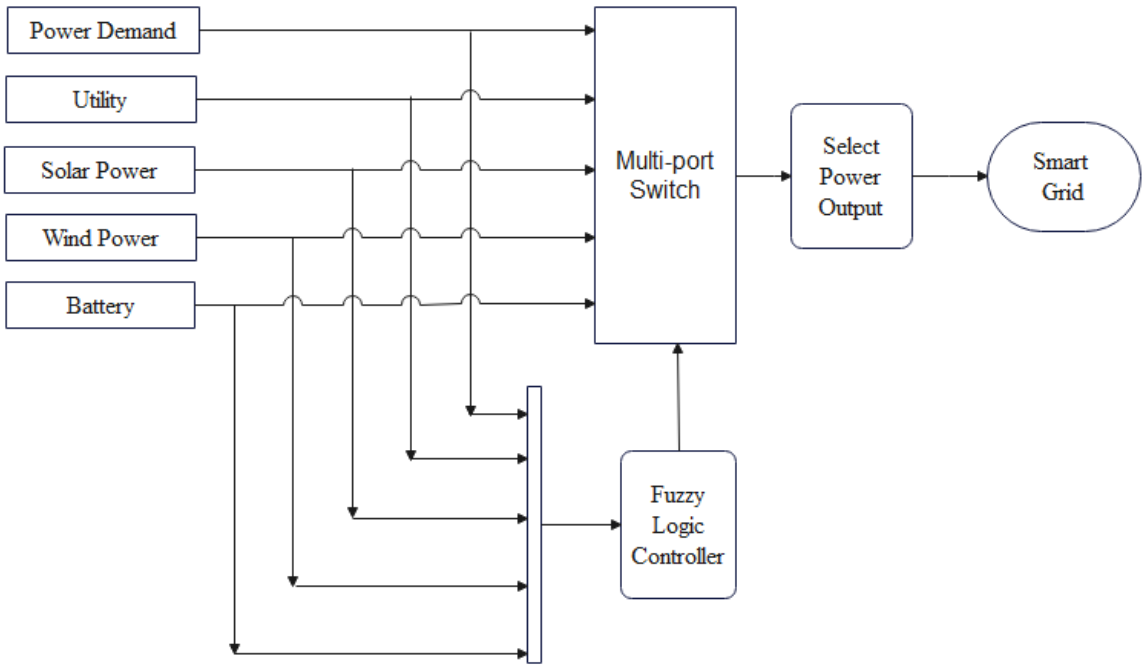


Figure 4. 2 System block diagram

In order to determine whether the current load is being served by the commercial main power or not, the system first checks its availability. If not, a smart multi-port switch is intelligently switched by the fuzzy logic controller based on the level of energy demand to the appropriate load demand output.

4.1.2 Flow chart

The flow chart below, figure 4.3, shows the power delivery system chain using fuzzy logic control. In these flow charts, the fuzzy logic controller provides a smart decision after the system started by sensing the form and quantity of available resources and choosing the required alternate source to supply electricity to power-sensitive load departments when the commercial main power supply is disrupted.

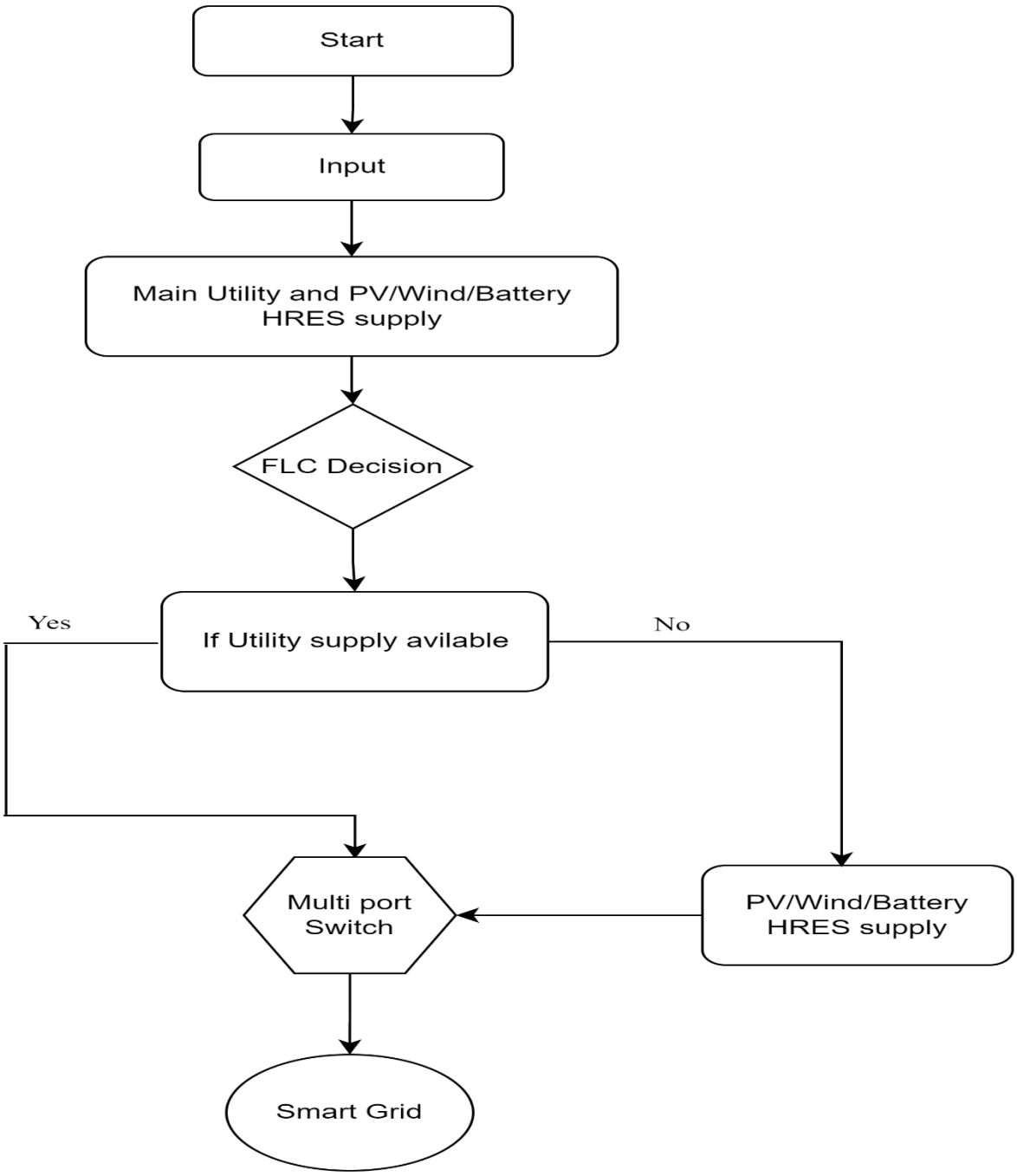


Figure 4. 3 Flow chart of the small-scale hybrid distributed generation system

4.2Fuzzy Logic Controller Design for the Hybrid System

4.2.1 Controller Description

In this paper, the fuzzy algorithm involves IFs...THEN rule. The fuzzy inference engine is the foundation, which makes it a logical generator of the fuzzy method. A judgment is based on fuzzy sets and the result is a fuzzy linguistic meaning [16, 17, 18]. The fuzzification Interface mainly covers input parameters. The input parameters are fuzzified to determine the predefined input function (membership functions). It can in various forms, be triangular, sinusoidal, trapezoidal and exponential. The membership functions are defined by setting the X-axis input selected and the number of Y-axis membership variable input groups. The features of membership will vary between zero and one. To determine the fuzzy sets and the operation, the rule-based interface matrix is used as a conditional function. For a fuzzy system, a rule is written as follows: if x is A, Y is B then z is C Where, A and B = Set of conditions met and z = Set of results deduced. The fuzzy value is transformed into a crisp value by the defuzzification interface. There are several interface defuzzification methods: max-membership, centroid, mean bisector and KarnikN average weight [19, 20]. Fuzzy logic is a rule-based framework that connects the output command to the data input using linguistic fuzzy principles. Fuzzy rules are if-then rules that are interpreted by an expert to cover all probable scenarios that must pass through the system. The complete components of the fuzzy logic system are shown in figure 4.4.

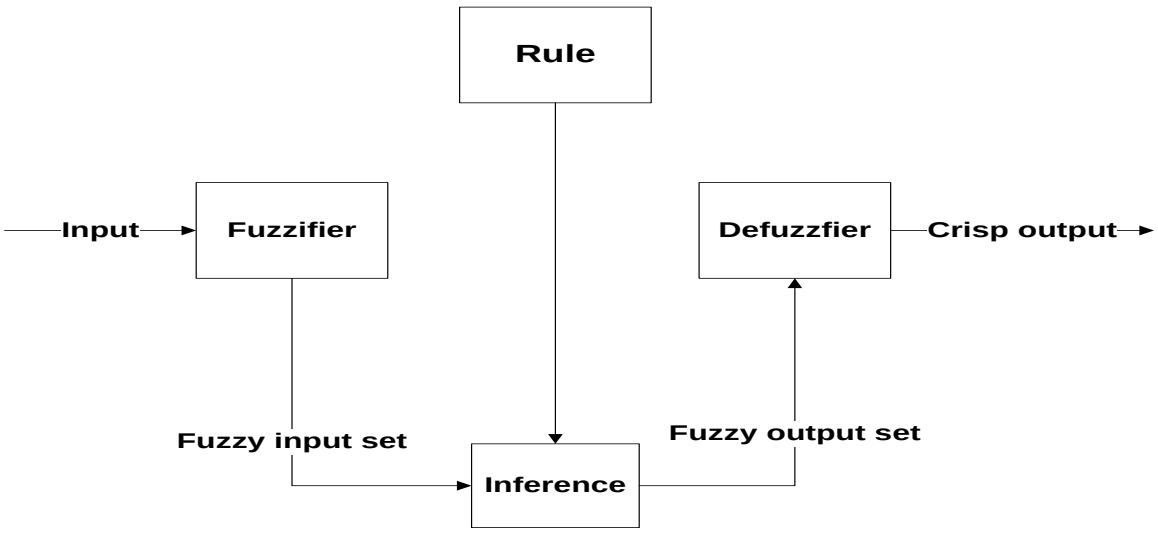


Figure 4. 4 Fuzzy logic block diagram [13]

A control mechanism's purpose is to maintain certain device objectives at various desired values. A linear system, which relates its inputs directly to the outputs, is the ideal control system. In reality, however, instability affects the regulated performance of the system and causes a deviation from the proposed set points. Like an open loop system and a closed loop system, the control mechanism is divided into two main designs. The closed-loop system utilizes the input of the signal to correct the output of the controller to reach the desired value. The key control characteristics, such as stability, precision, response speed, sensitivity, and representation, are included in the study of control theory [32]. It is difficult to gain control of a complex system as HRES using conditional methods. Therefore, FLC is also a more effective approach since it encompasses a wide variety of potential working conditions with a reasonable degree of ambiguity or lack of knowledge in the future. FLC is reasoning which is closer to the human decision-making style that gives the FLC the priority chosen as HRES for the management of a complex system. The system is very complex, nonlinear, unpredictable, has a lot of uncertainty, and its mathematical model is somehow complicated, so the best alternative is to use one of the smart, expert-based systems, such as the fuzzy logic control system. In light of intermittent power generation, the fuzzy logic will regulate the system's energy flow to meet demand continuously and to a high standard. The FLC has two key states in this document, such as supplying the RES to the load when the utility is not available and isolating the RES energy when the main commercial utility in the case of a multi - port switch and the rules are based on system requirements and updated by trial and error. To model, evaluate and analyze the framework, Matlab Simulink was used.

4.2.2 Proposed Fuzzy Logic Controller

Utility supply (Mp), demand power (Pd), solar power (Sp), wind power (Wp), and battery(Bp) are the five variable inputs for the proposed fuzzy logic controller, which provides a single crisp output.

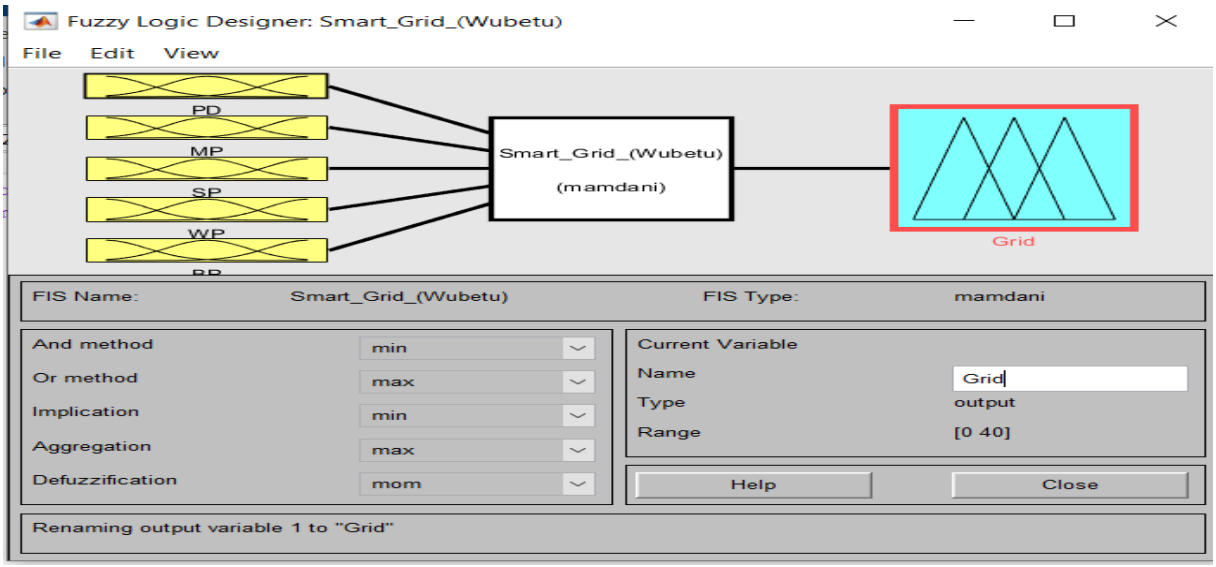


Figure 4. 5 Fuzzy logic control technique in MATLAB

4.3 Membership function

4.3.1 Membership function of demand (Pd)

Each of the input language variables with three linguistic variables called low, medium, and high is the demand power, and the fuzzy sets are: high (10 20 30) (22 30 40 40) (22 30 40 40), medium (10 20 30) and low (0 7.5 7.5 17.5),.

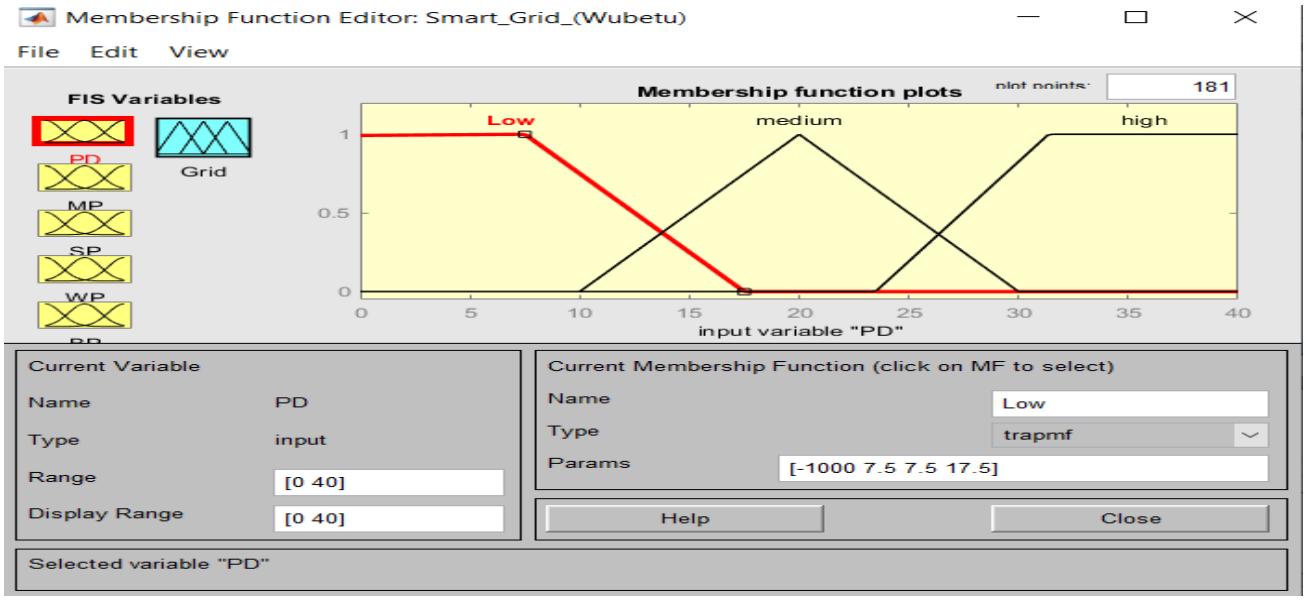


Figure 4. 6 Membership function of demand (Pd)

4.3.2 Membership function of Utility power (Mp)

The second input language variable, utility power, has two linguistic values and is OFF and ON and the fuzzy sets are: OFF (0 2 2 4), and ON (2.5 5 40 40).

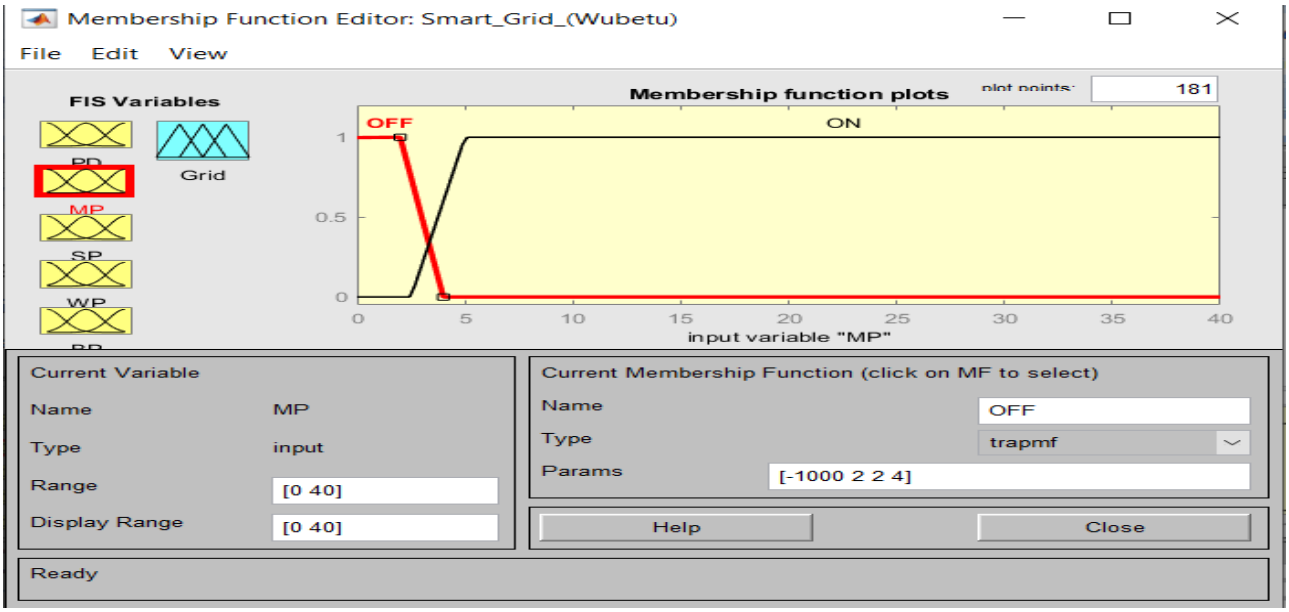


Figure 4. 7 Membership Function of Utility (Mp)

4.3.3 Membership Function of Solar Power (Sp)

The third language variable, solar power (Sp), contains three linguistic values: high (12 16.5 20 20), medium (5 10 15), and low (0 3 38.5). The fuzzy sets are high (12 16.5 20 20), medium (5 10 15), and low (0 3 38.5),

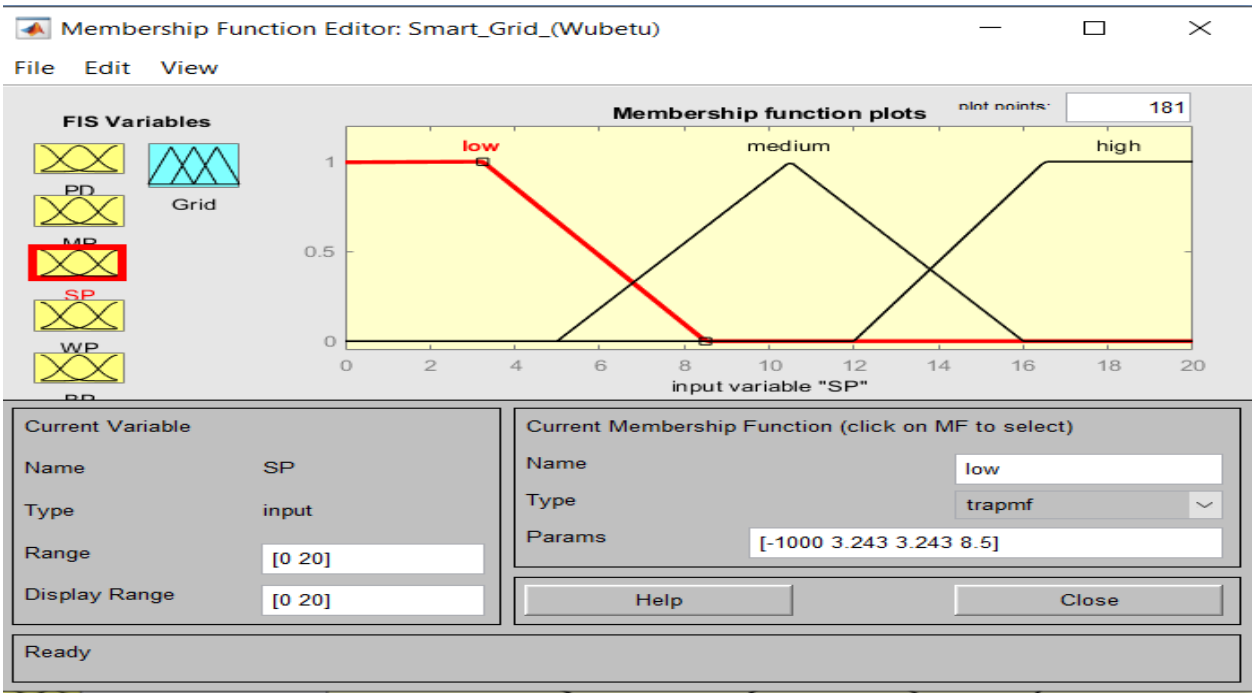


Figure 4. 8 Solar power's membership function (Sp)

4.3.4 Membership Function of Wind Power (Wp)

The fourth language variable, wind power (Wp), contains three linguistic values: low, medium, and high. The fuzzy sets are: high (5 7 8 8) , medium (1, 75, 4, 25), and low (0, 1.51, 3.5).

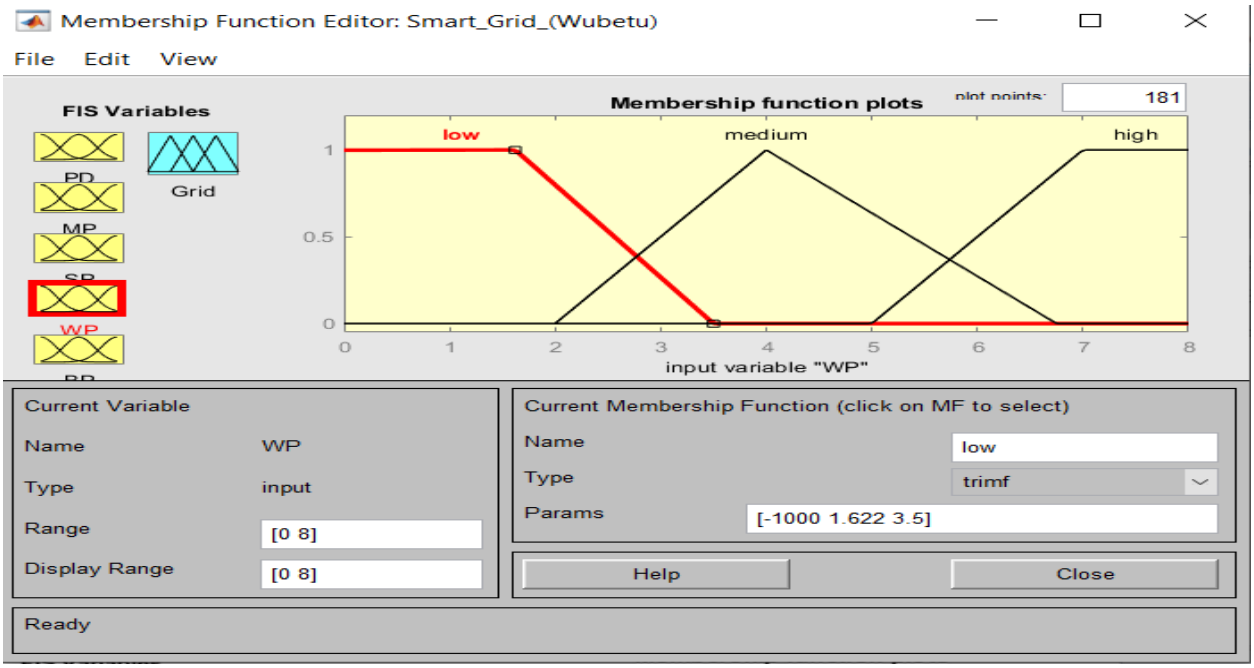


Figure 4. 9 Wind power's membership function (Wp)

4.3.5 Battery membership function (Bp)

Battery power (Bp) is the fifth linguistic variable having three linguistic values called low, medium and high and the fuzzy sets are: High (8 11 12 12), Medium (2.75 6.5 10.5), and Low (0 2.5 2.5 6).

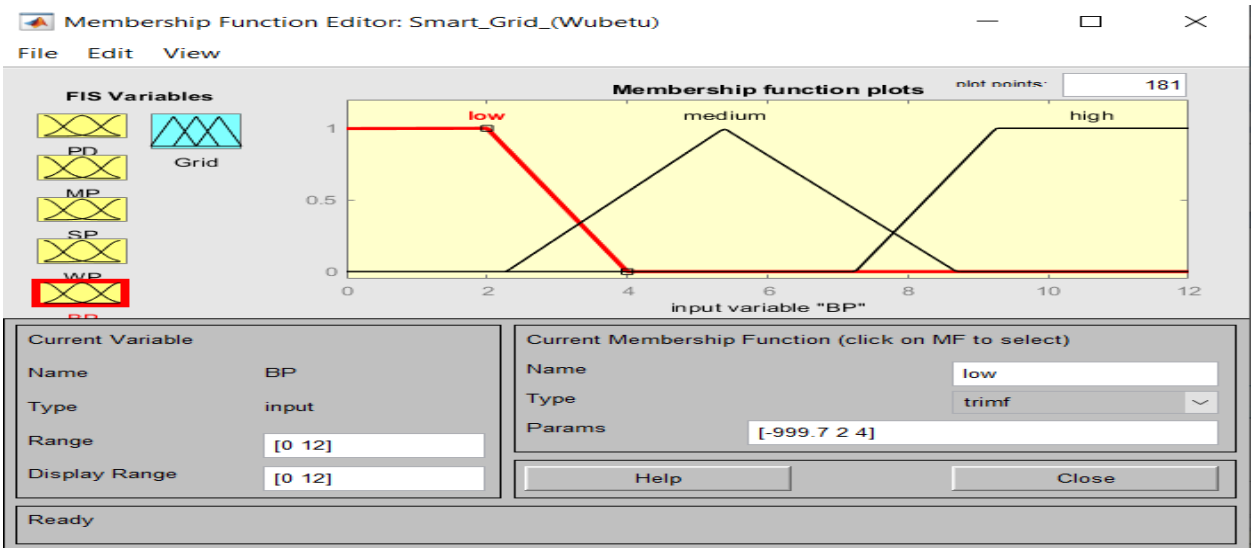


Figure 4. 10 Membership function of (Bp)

4.4.2 Membership function of Grid (Po)

There are only five Sp values in the Grid power, $Sp + Wp, Sp + Bp, Sp + Wp + Bp$, and Mp only and the fuzzy sets are: Sp only BP (15 22.5 30), SP+ WP (10 15 20), SP+ WP + BP (25 32 37) + (-6 0 6 12), SP, MP only (35 37 40 40).

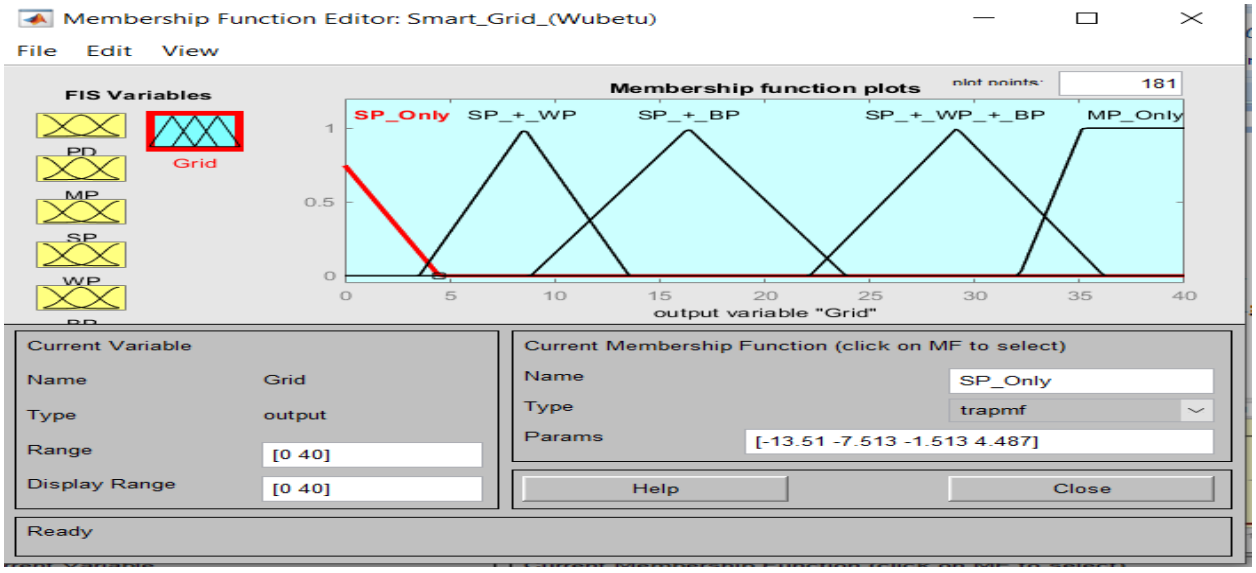


Figure 4. 11 Grid power (Po) membership function

4.4 Proposed Fuzzy Logic Control Written Rules

In this paper, IF THEN rules for controlling and take judgments to perform the required purpose, and in compliance with those written in the rule editor, the overall system model run.

Fuzzy logic control rules listed below:

1. If (PD is Low) or (MP is OFF) or (SP is low) or (WP is low) or (BP is high) then (Smart_Grid is SP_+_BP) (1)
2. If (PD is Low) or (MP is OFF) or (SP is low) or (WP is medium) or (BP is high) then (Smart_Grid is SP_+_BP) (1)
3. If (PD is Low) or (MP is OFF) or (SP is low) or (WP is high) or (BP is low) then (Smart_Grid is SP_+_WP) (1)

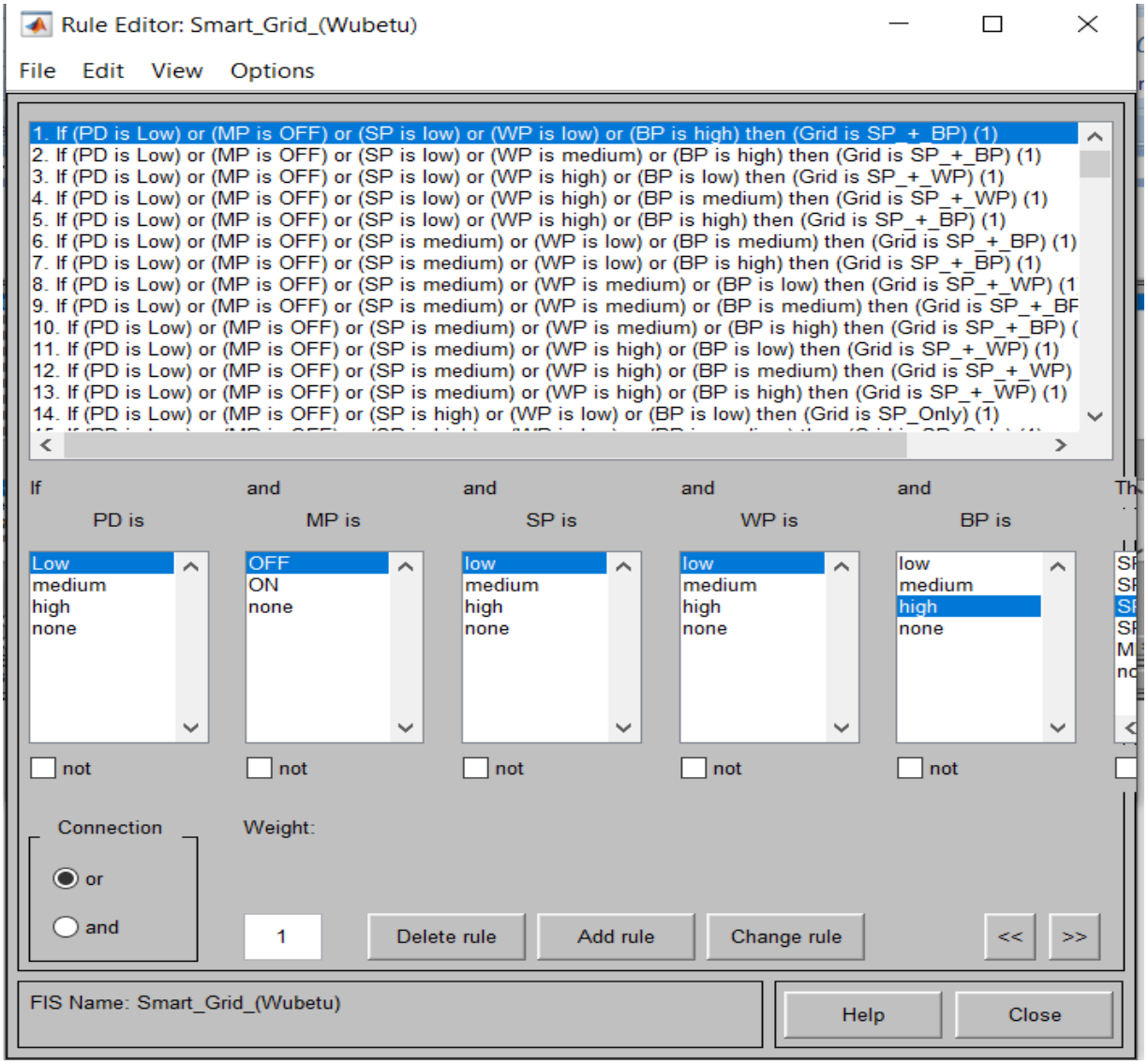


Figure 4. 12 Written Fuzzy Logic Rules

4.5 Fuzzy Logic Controller for Power Battery Management

Power electronic converters, loads, and the dynamic interplay of the hybrid PV/wind/battery system may result in reduced system power quality or stability issues. Therefore, in the hybrid system, administration and control of the power distribution system are essential. Since solar and wind energy sources change over time, the operating system mode must be flexible. The day is dominated by solar energy, whereas the night may be dominated by wind energy. The power flow between the PV, wind, and battery systems is controlled and managed by two fuzzy logic control (FLC) systems. While the second FLC is used to manage PV and wind systems in a variety of weather conditions, the first FLC is utilized to regulate battery charging and discharging (solar irradiance and wind speed). This fuzzy logic controller controls the charging and discharging modes of the proposed hybrid system. The fuzzy control input variable is Error (P), which is calculated using equation (4.1):

$$error(\Delta P) = P_{pv} + P_{wind} - P_{Load} \tag{4.1}$$

Where,

P_{pv} - The photovoltaic system's power output

P_{wind} - The wind energy system's output power

P_{Load} - The power load

The fuzzy controller is charging when Error (ΔP) is a positive number, and discharging when Error (ΔP) is a negative number.

The Fuzzy Logic Toolbox was used to create the suggested fuzzy controller for the battery system in MATLAB. This controller, as shown in Figure 4.13, has two output variables, Battery Charge (BC) and Battery Discharge (BD), and one input variable, Error (P).

The membership functions of the input variable Error (ΔP specify whether the variable is charged or discharged. The Error input variable has a value range of -500 to 500. As previously stated, when Error (P) is a negative number between 0 and -500, the battery is discharging, and when it is a positive value between 0 and 500, the battery is charging, as illustrated in figures 4.13 and 4.14.

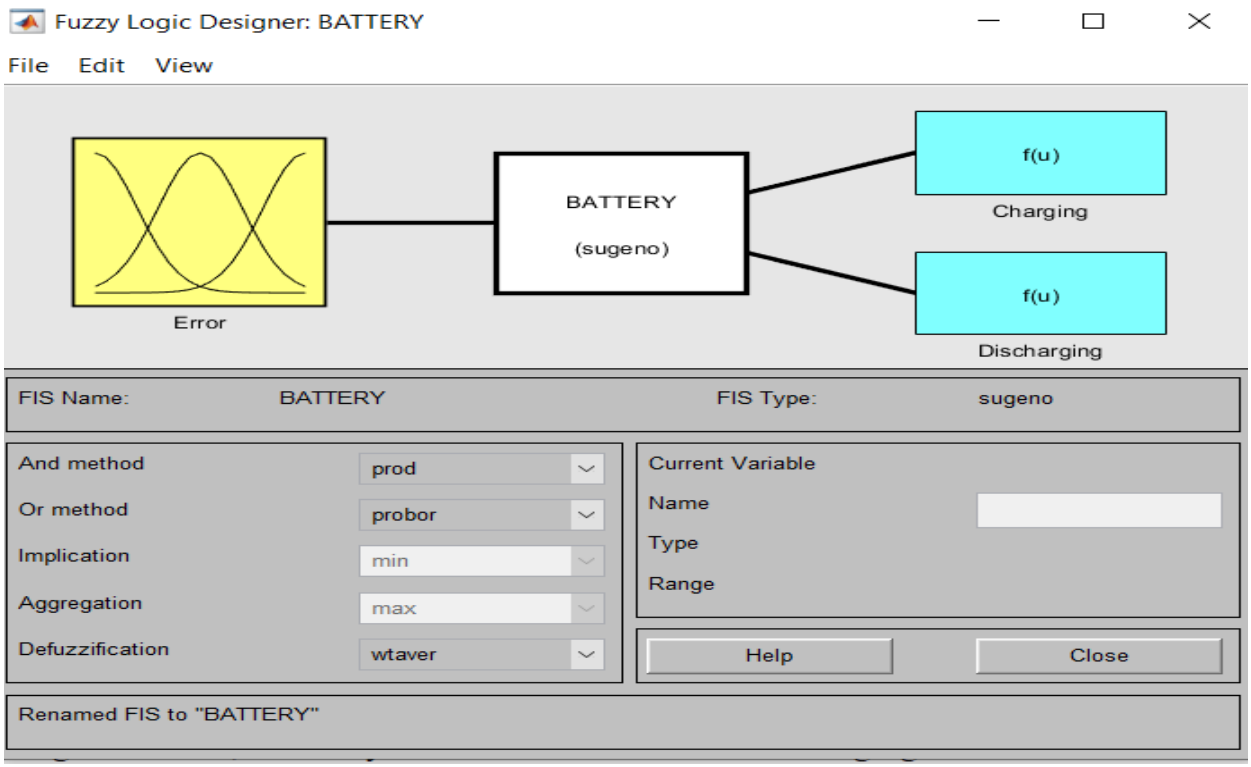


Figure 4. 13 The proposed fuzzy inference system for the battery system

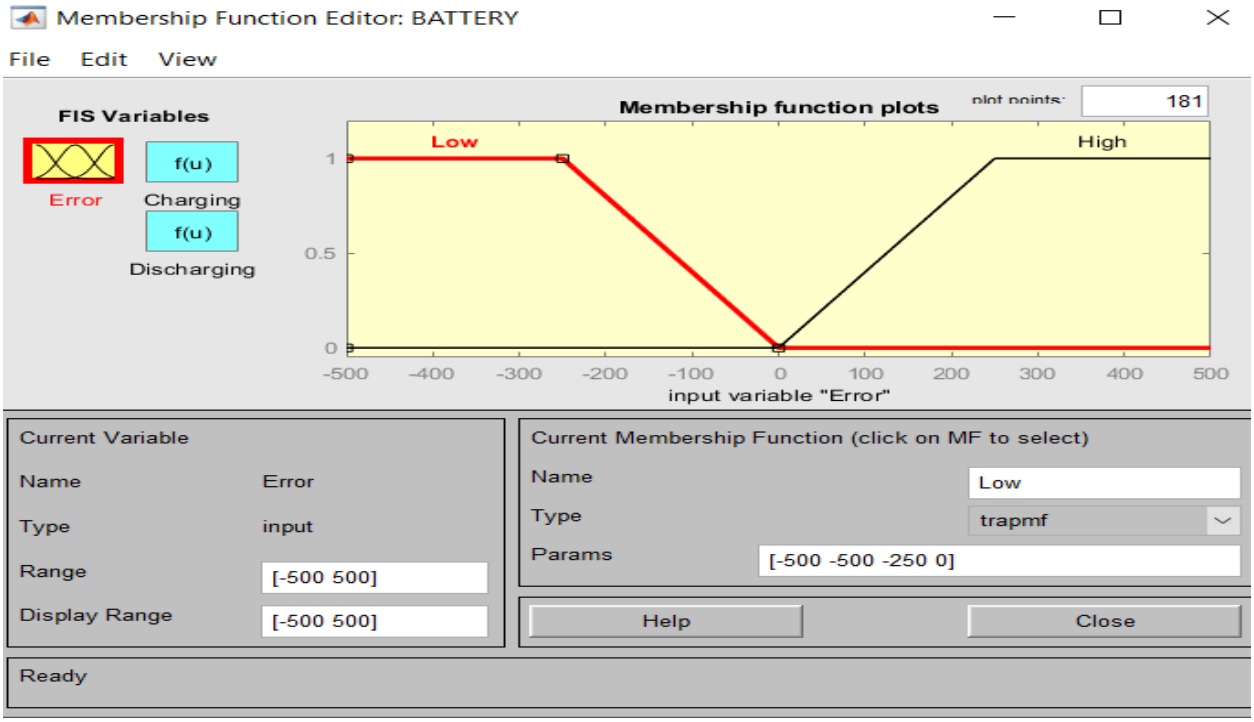


Figure 4. 14 The membership function plot of the input variable (discharging mode)

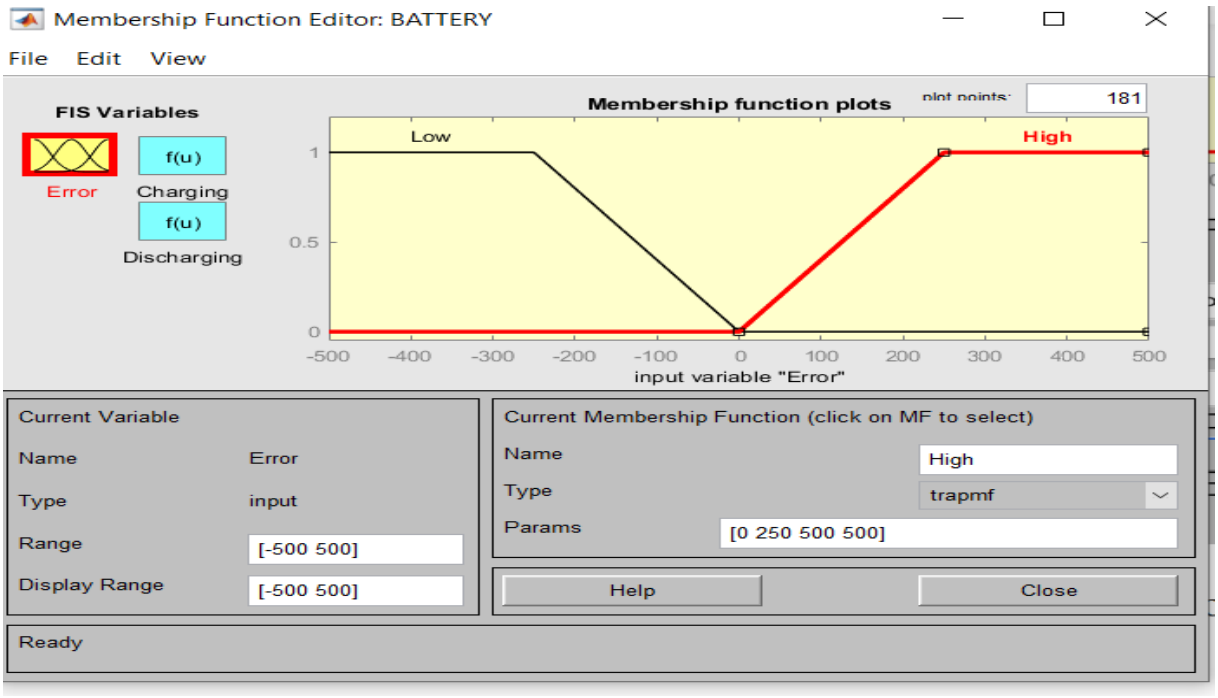


Figure 4. 15 The membership function plot of the input variable (charging mode)

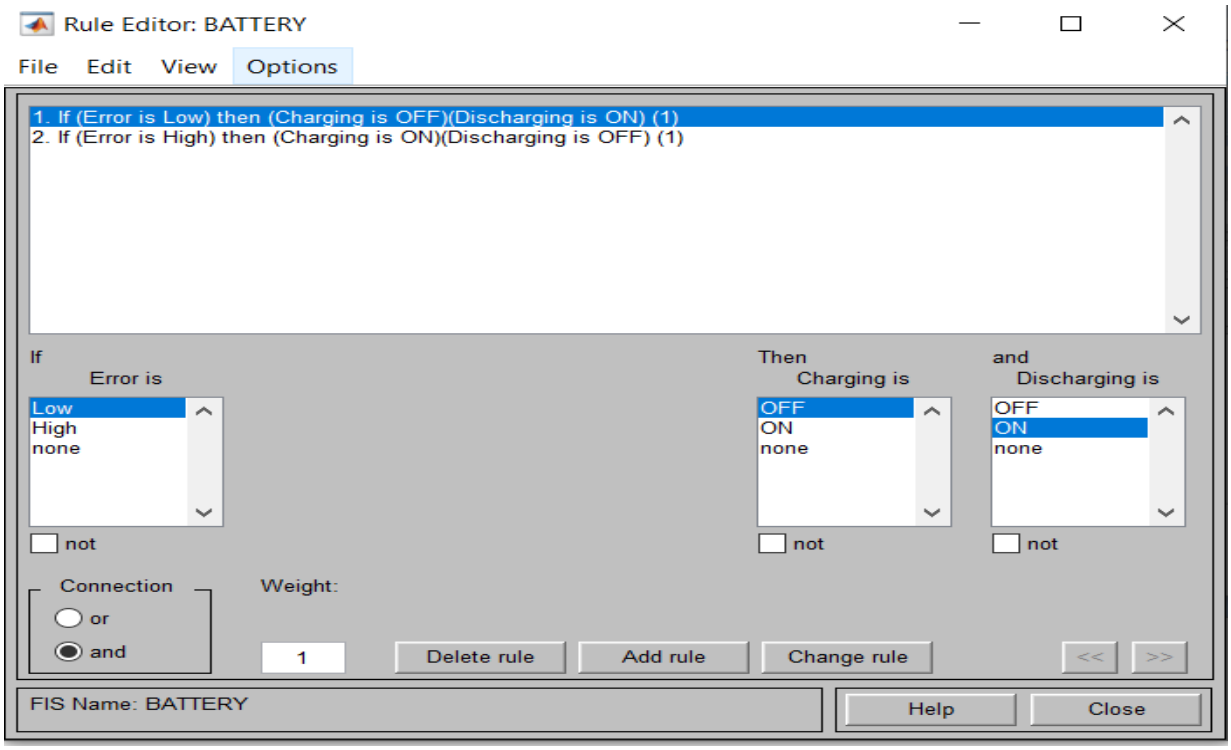


Figure 4. 16 The fuzzy control rules for the battery system.

CHAPTER FIVE

RESULTS AND DISCUSSION

5.1. Introduction

MATLAB/Simulink will be used in this chapter to simulate the designed hybrid system. Two operation modes are simulated in order to show the proposed hybrid system's stability. The smart hybrid system's Simulink model is illustrated in Figure 5.1.

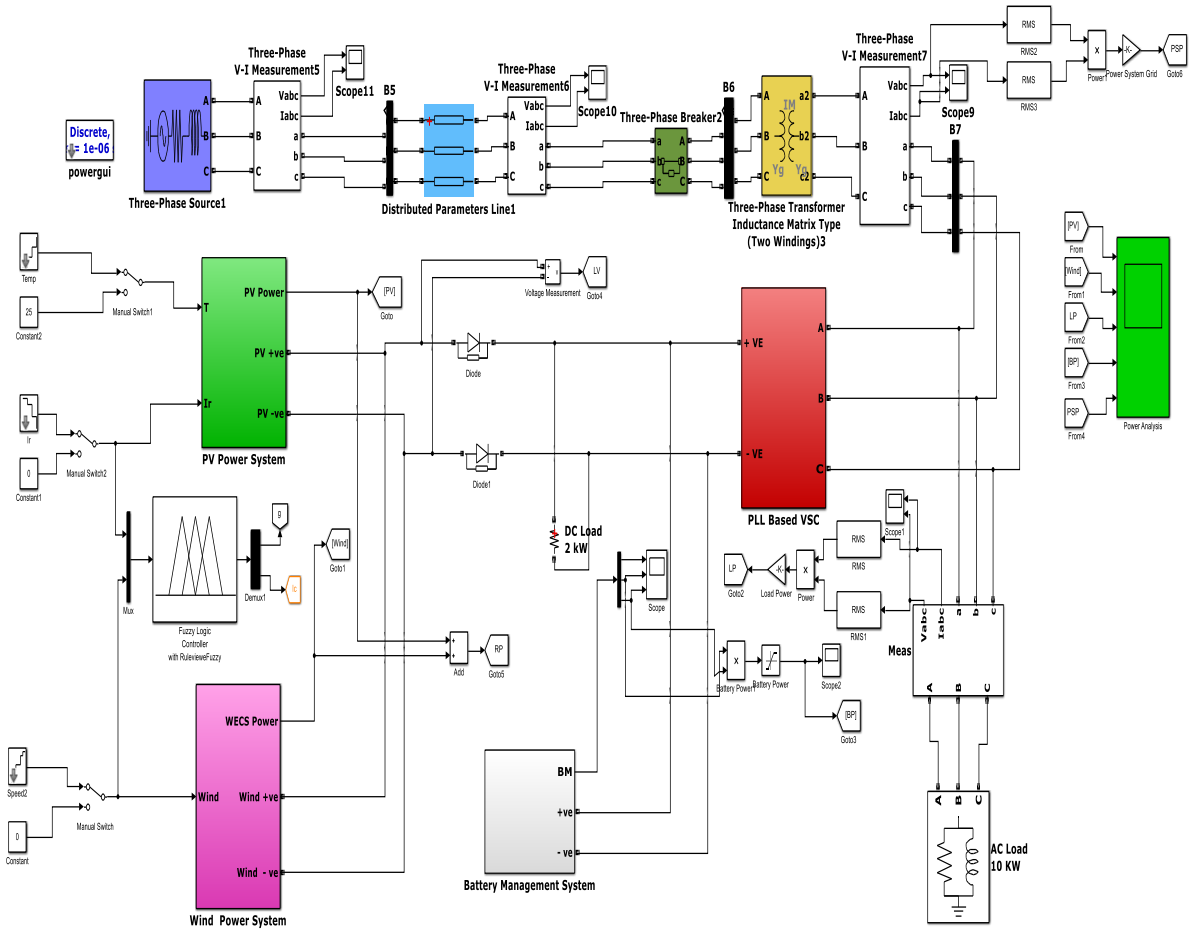


Figure 5. 1 The smart hybrid system's Simulink model

5.2. Solar Panel Simulation Result

The suggested solar array will provide between 18.5 and 20 KW of power, as illustrated in figure 5.2, which also shows the power vs voltage and current versus voltage curves.

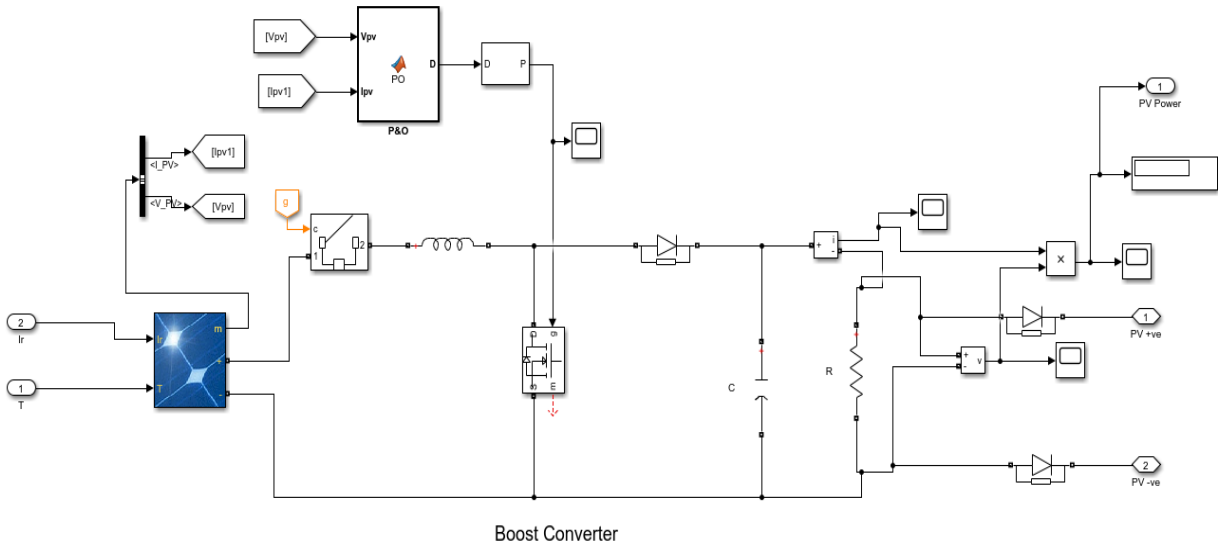


Figure 5. 2 The solar power system's Simulink model

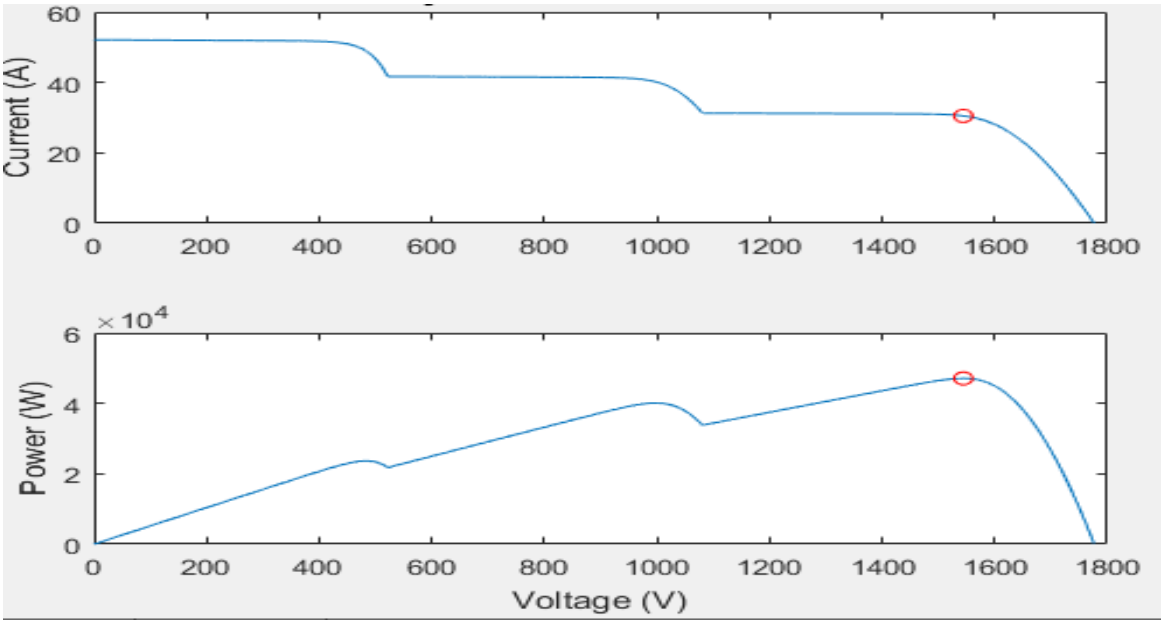


Figure 5. 3 The characteristics of solar energy in terms of V-I and P-V

When only the PV system turned on and the wind and battery systems are turned off completely; the solar radiation ranges from 250 to 1000 w/m2 it will be in the medium to high range. The temperature ranges from 25 to 45 degrees Celsius. The load frequency is set to 50Hz and an active power of 37.6kW recommended. Despite the fact that the wind speed is zero (off) and the radiation and temperature are variable, the load voltage remains constant, as illustrated in figure 5.4.

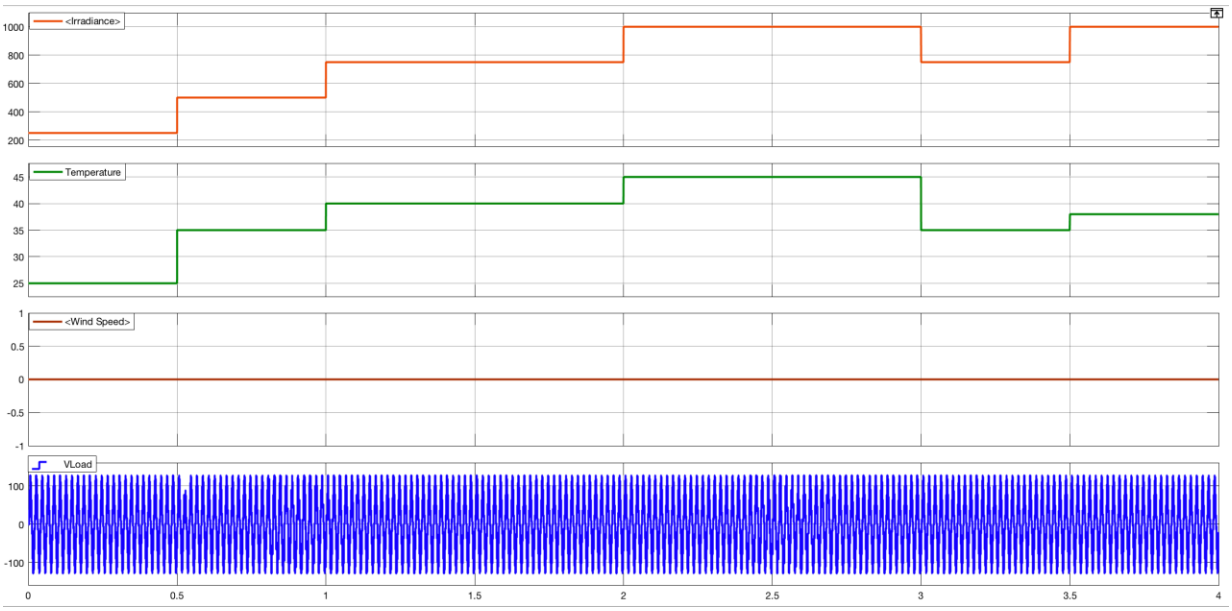


Figure 5. 4 The load voltage under different radiation and temperature.

The PV array's actual maximum voltage is around 30.5V, with a 48V output voltage after the DC-DC converter. As shown in figure 5.5, the maximum input current is around 8A, and the output current is around 0.3A.

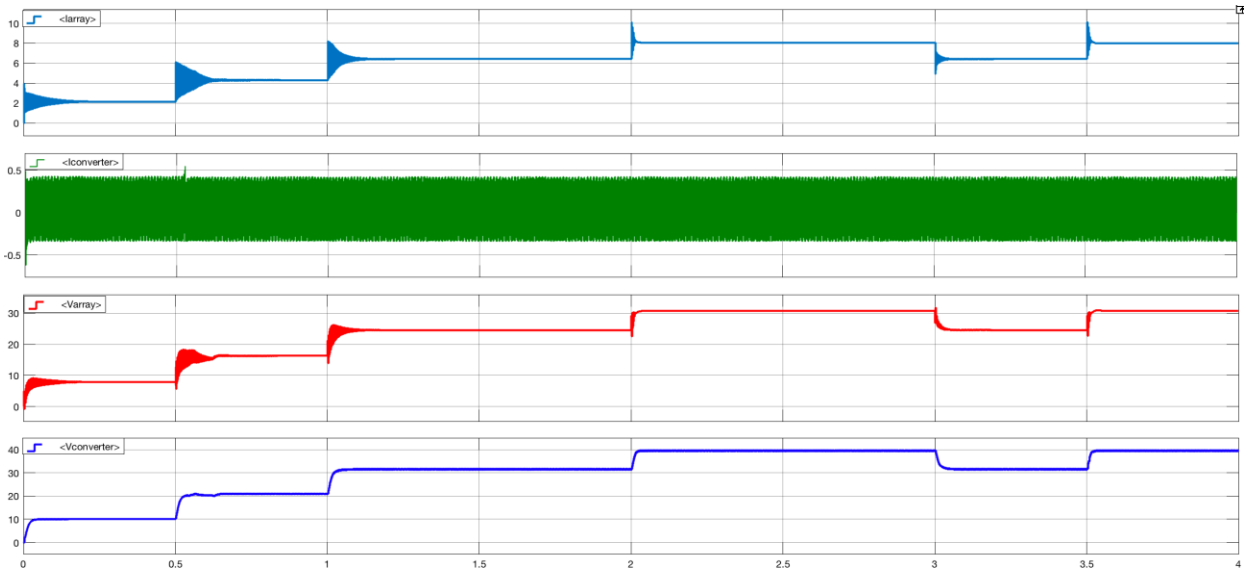


Figure 5. 5 The voltage and current generated by the PV array and the voltage and current after the converter.

5.3. Wind Turbine Simulation Result

A single wind turbine can generate 294.5W, as shown by the results of the Matlab simulation in figure 5.6, and at a given wind speed of around 4 m/s, a single wind turbine can be observed generating an active power of about 294.5W.

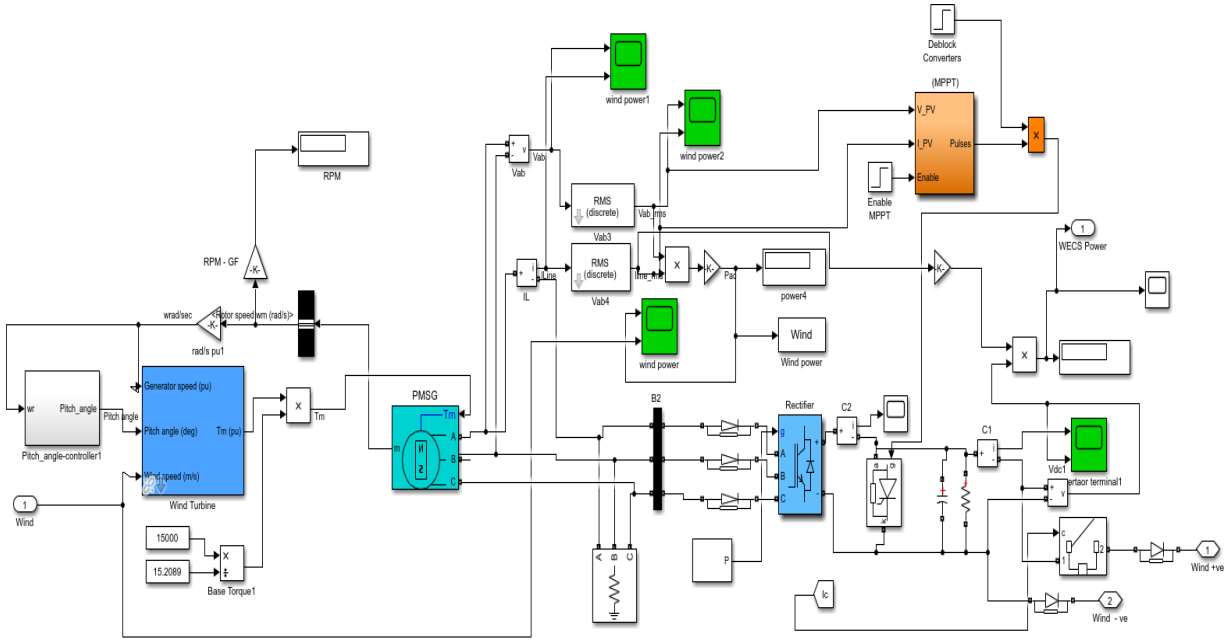


Figure 5. 6 The wind turbine system's Simulink model

When the wind power system turned on but all other systems turned off. Wind speeds range from 4 to 12 m/s. The load voltage remains constant under varying wind speed, as shown in figure 5.7.

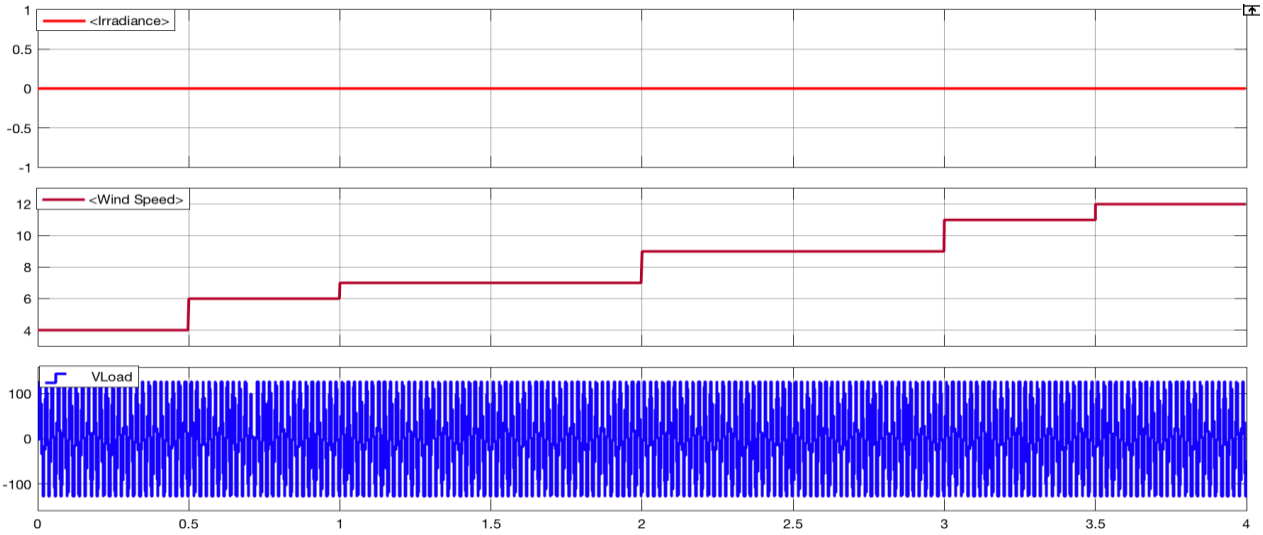


Figure 5. 7 The load voltage under different wind speed.

In the PMSG, the maximum power value is around 294.5W and the maximum output power of the wind power system is 247.4W. As a result, the proposed wind power system will have an efficiency of 84%, as shown in figure 5.8. This efficiency only applies to electrical power after the PMSG. It does not apply to wind turbines because their efficiency is determined by mechanical power and other factors. The maximum AC voltage after the PMSG is approximately 195V and the wind power system's maximum output voltage is 200V.

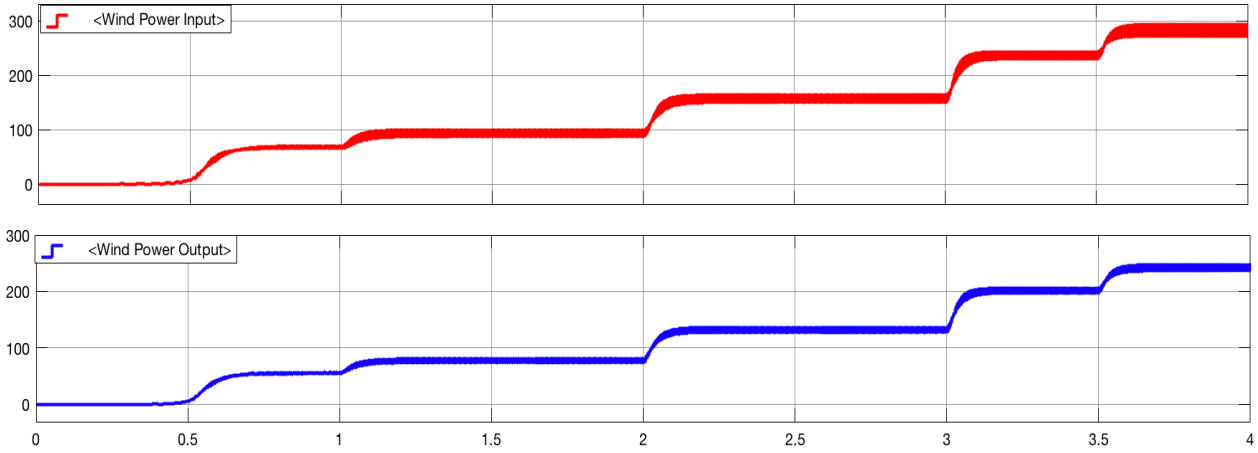


Figure 5. 8 The input and output power of the wind turbine system

5.4. Matlab System Model of (HES) For Distributed Generation System Using FLC

All of these input sources could every once in a while vary due to the intermittent nature of renewable energy sources, so a for each of the five variables, to determine if the controller can recognize this variance and choose the best course of action with regard to the multi-port switch. By purposefully setting all of the two renewable energy sources, namely solar power and wind power, to zero, a typical example of how to use Matlab simulation to determine whether a system is running according to written criteria is provided. The decision in the case in point to supply the demand power, which is around 38.5 kW from the commercial main power, and the output power of 38.8 kW further demonstrate the right use of the fuzzy rule in this typical circumstance.

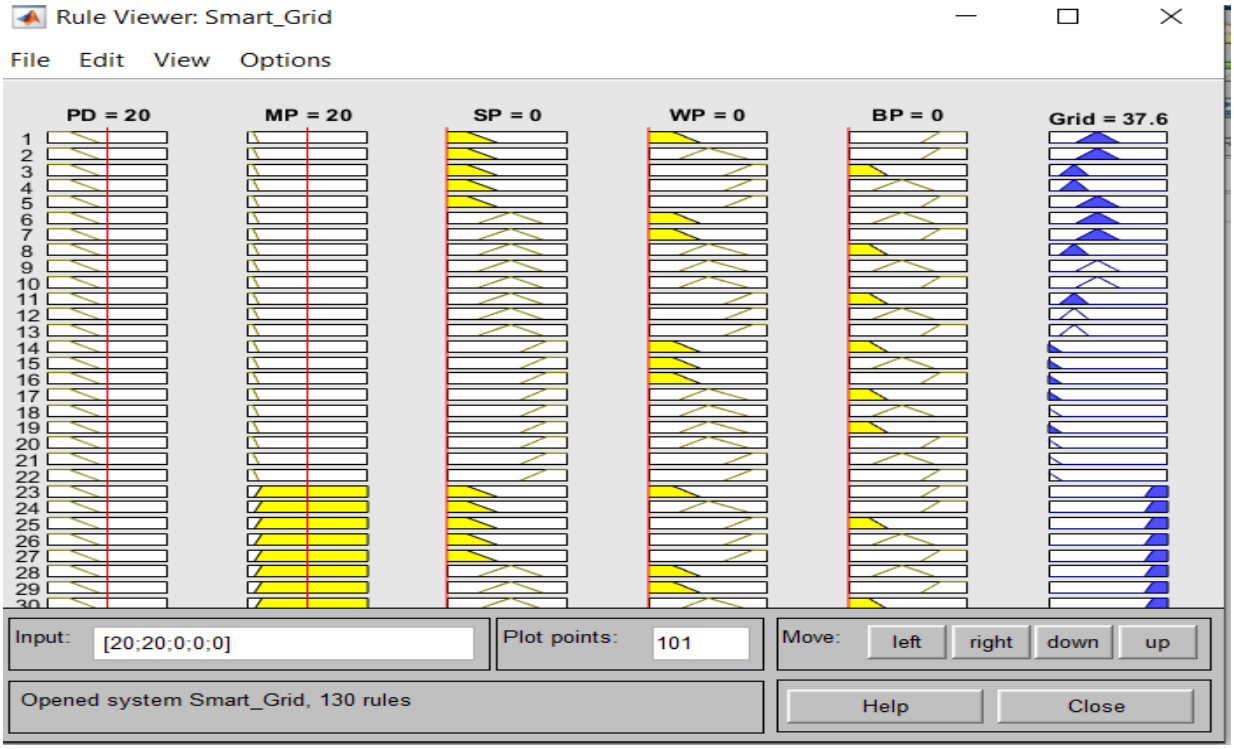


Figure 5. 9 when there is availability to utility power, fuzzy logic rule viewer

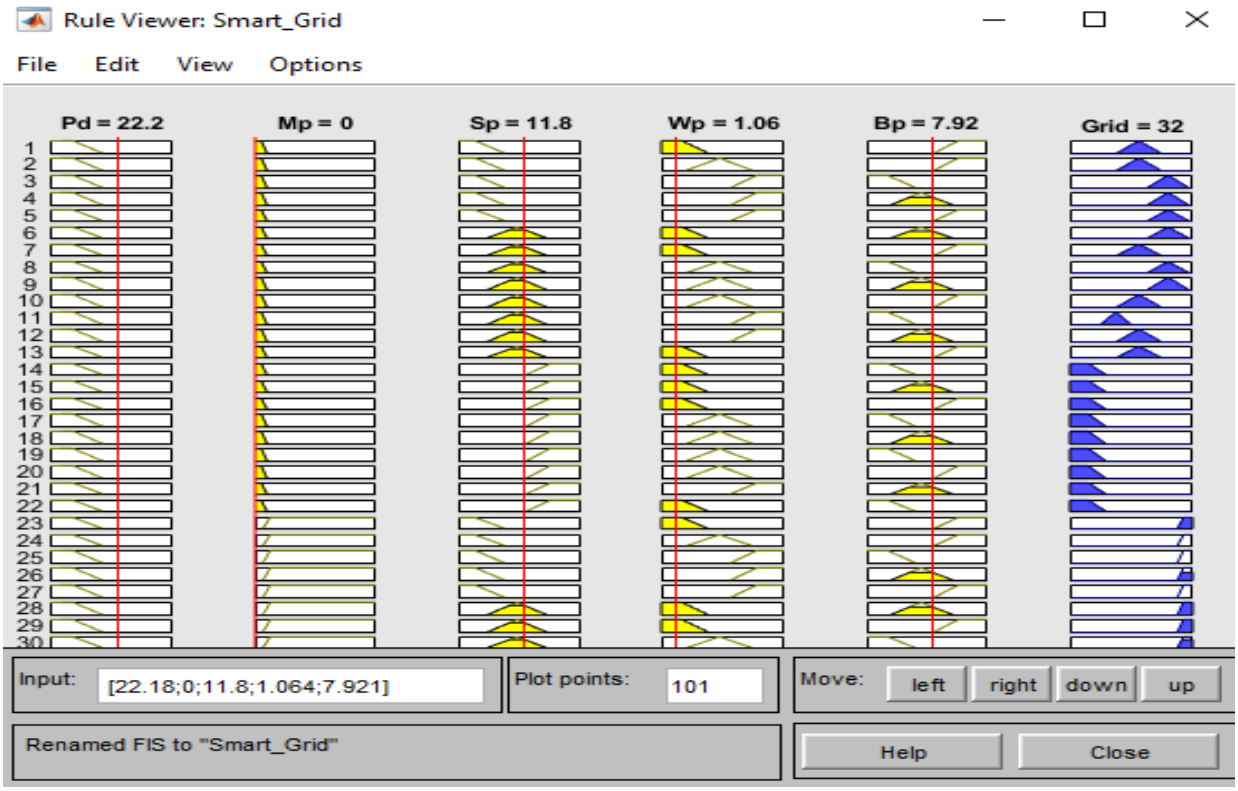


Figure 5. 10 when there is no availability to utility power, fuzzy logic rule viewer

When the PV and wind systems are completely off at first, then when both systems are running at the same time. When the PV and wind systems are turned off, the battery is in discharging mode, supplying the load and maintaining a constant voltage level on the load side. When the PV and wind systems are operational, the battery will be in the discharging mode for a short period before switching to the charging mode. The desired load voltage is achieved under varying weather conditions, as shown in Figure 5.11.

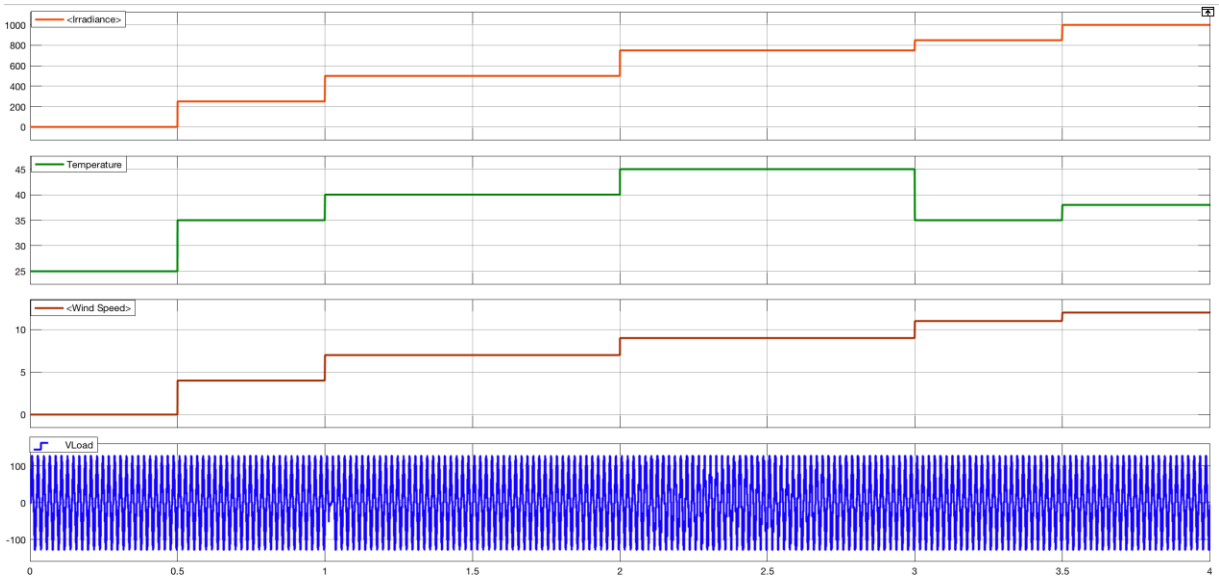


Figure 5. 11 The load voltage under different radiation, temperature, and wind speed



Figure 5. 12 When utility power is in a condition of variable load, fuzzy logic rule viewer

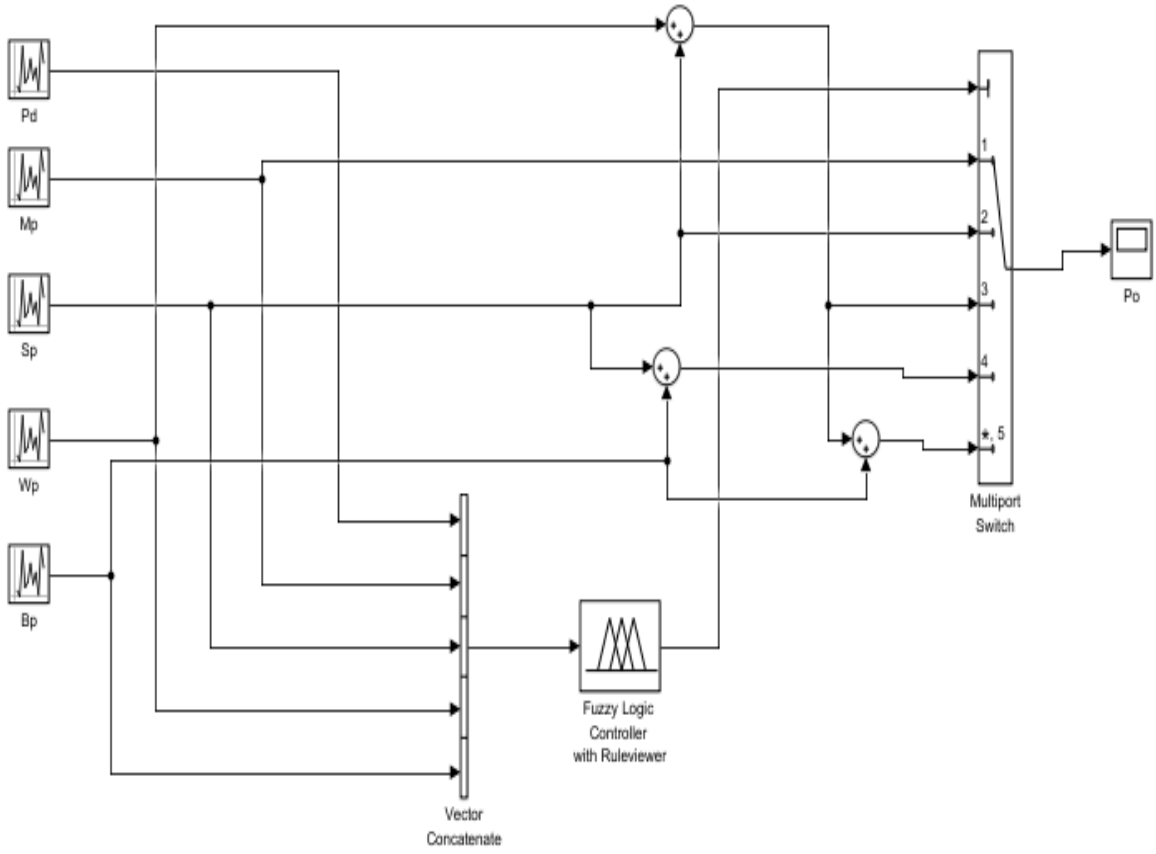


Figure 5. 13 The realization of the whole system model in Simulink

First Case

The output of the fuzzy logic controller is 1.55 KW if the Demand power (Pd) is 11.9 KW, the main power (Mp) is OFF, the wind power (Wp) is 1.69 KW, the solar power (Sp) is 8.99 KW, and the battery power (Bp) is 1.55 KW is indicated in figure 5.14.

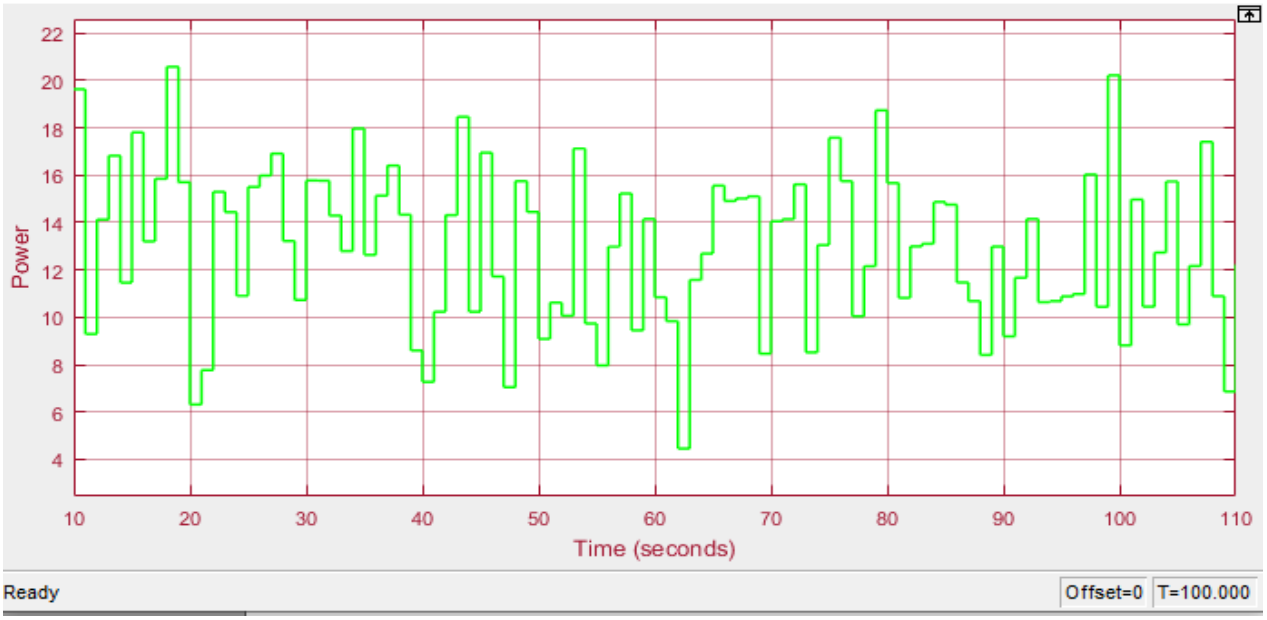


Figure 5. 14 Case one of the fuzzy logic controller output

Second Case

Figure 5.15 illustrates the fuzzy logic controller's output. The total power (Pd) is equal to 20.8 KW if the Demand power (Pd) is 20.8 KW, the main power (Mp) is OFF, the wind power (Wp) is 8.76 KW, the solar power (Sp) is 6.22 KW, and the battery power (Bp) is 6.82 KW.

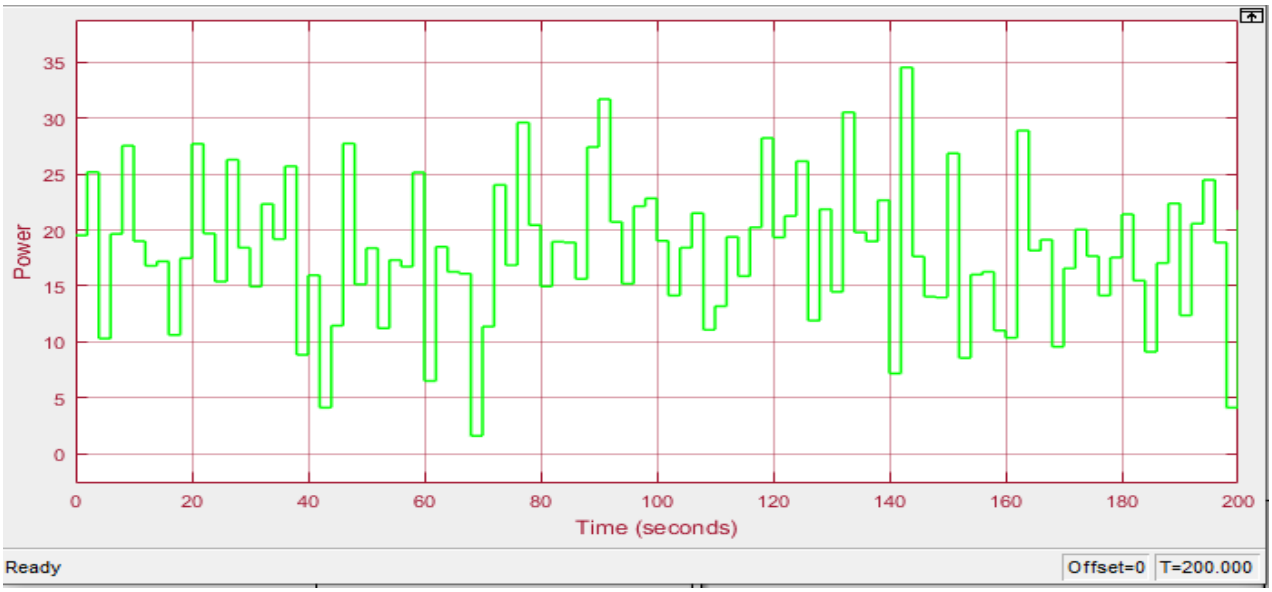


Figure 5. 15 Case two of the fuzzy logic controller output

Third Case

In figure 5.16 illustrates the fuzzy logic controller's output if the battery power (Bp) is 10.7 KW, the solar power (Sp) is 15.9 KW, the wind power (Wp) is 9 KW, and the demand power (Pd) is 34.3 KW.

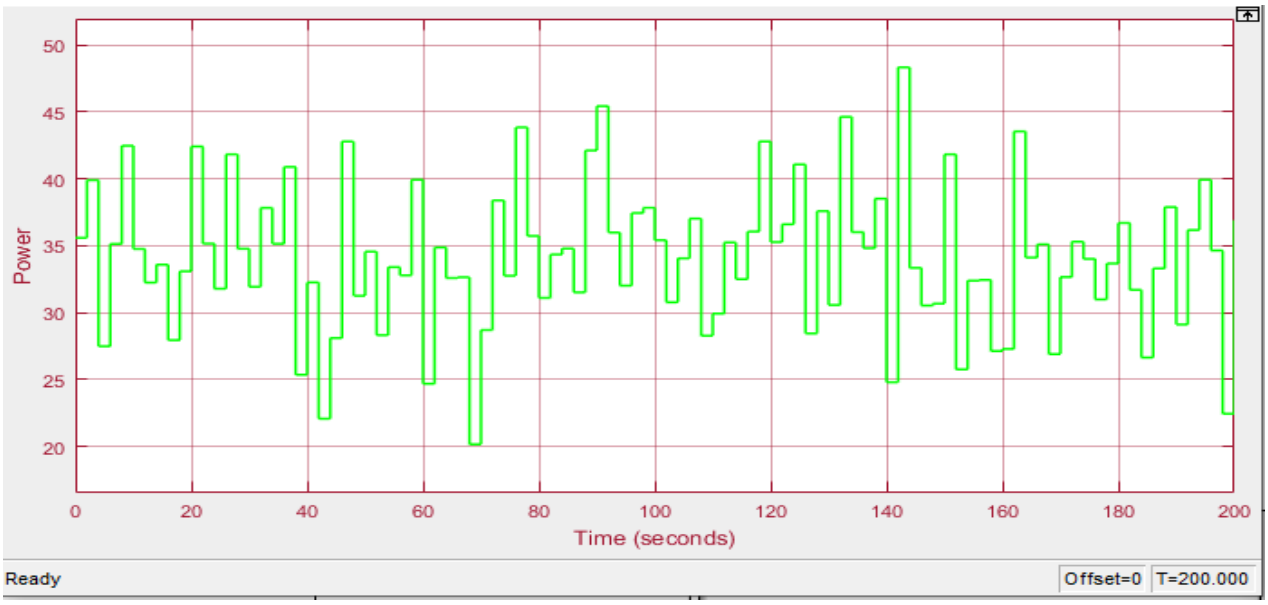


Figure 5. 16 Fuzzy logic controller output case three

Generally FLC manage the output power of the system PV, wind, battery, and utility or hydro power. The hybrid system, administration and control of the power distribution system are essential. Therefore, the out put load will be satisfies if the available power sources of the grid connected system. When the commercial utility is just not available, the load demand for the power generated by these PV, wind, and battery storage energy sources combined is to be met using the hybrid components. Fuzzy logic controllers are utilized to make wise decisions on the availability of energy sources to efficiently utilize the electricity provided.

CHAPTER SIX

CONCLUSION AND RECOMMENDATION

6.1. Conclusion

This paper employed a fuzzy logic controller for a solar/wind hybrid smart grid. By detecting the kind and amount of resources that are accessible and then selecting the best alternative source, fuzzy logic controllers are utilized to make intelligent use of the generated power. This was achieved by modeling each part of the proposed hybrid system in Matlab/Simulink, & fuzzy rules were created in the fuzzy rule editor. To switch the multi-port switch utilizing a combined hybrid-grid system of solar, wind, and battery controlled fuzzy-based systems, an intelligent choice may be made to determine the load demands, the presence of renewable energy sources, as well as the accessibility of essential utilities.

6.2. Recommendation

Large-scale renewable energy resources, including photovoltaic, geothermal, wind, & hydro, can be used to better the lives of the local populace provided they are handled wisely. Anyone with an interest in these projects is welcome to utilize one of the several intelligent controllers and offer their expertise to improve intelligent energy control methods.

6.3. Future work

Future work can make use of various hybrids of the energy resources currently available. A hybrid solar/wind system was developed for this work as a backup to the primary utility power. This study investigates whether there is a real need to begin utilizing renewable energy sources effectively, as well as whether businesses and individuals in remote areas may develop their own system models using a variety of intelligent control techniques.

REFERENCE

[1] Muralikrishna, M., and V. Lakshminarayana. "Hybrid (solar and wind) energy systems for rural electrification." ARPN Journal of Engineering and Applied Sciences 3, no. 5 (2008): 50-58.

[2] M. Shikur, "Simulation, Modeling and Control of Distributed Hybrid Generation System Case Study: Berehet Woreda," Master of Science, Electrical and Computer Engineering, Addis Ababa University, June 2015.

[3] Negi, Swati, and Lini Mathew. "Hybrid renewable energy system: a review." Int J Electron Electr Eng 7 (2014): P-8.

[4] Kumar, Sandeep. "Modeling and simulation of hybrid Wind/Photovoltaic Stand-alone generation system." Master's thesis, National Institute Technology, 2014.

[5] Patel, Sanjukta. "Modeling and control of a grid connected wind-PV hybrid generation system." Master's thesis, National Institute Technology, 2014.

[6] L. E. Weldemariam, "Genset-solar-wind hybrid power system of off-grid power station for rural applications," international journal of electrical power and energy systems 2010.

[7] M.Sharmila, C.K.Sundarabalan, J.Prince Joshva Gladson, and J. s. kuma, "Compensation of Power quality Issues using Fuel Cell with Electrolyzer/Pv/Wind Turbine," International Journal of Engineering Trends and Technology (IJETT), vol. Volume-40 October 2016.

[8] G. B. Huka, "Design of a Photovoltaic-Wind Hybrid Power Generation System for Ethiopian Remote Area," Master of Science, Electrical and Computer Engineering, Addis Ababa, July 2011.

[9] G. S. Ssali, "Energy flow in a Hybrid Wind/ Hydrogen System for Kampala and Tororo towns in Uganda," master of science Industrial Engineering and Managment, KTH University, January 2017.

[10] S. A. Tourkia Lajnef, and Anis Ammous, "Modeling, Control, and Simulation of a Solar Hydrogen/Fuel Cell Hybrid Energy System for Grid-Connected Applications," Hindawi, vol. 2013, January 2013.

[11] H. Abatcha, A. M. Jumba, and L. Maijama'a, "Design and simulation of a hybrid PV/fuel cell energy system," Continental Journal of Engineering Sciences, vol. 6, pp. 37-45, 2011.

[12] V. Singh, "Optimization Of Wind-Pv-Fc-Battery System," International Journal of Innovations in Engineering and Technology (IJIET), vol. 11 pp. 50-57, October 2018.

[13] C. Lodha and V. Shukla, "Power management of a stand-alone photovoltaic/ fuel cell hybrid energy system," International Journal of Scientific Research Engineering & Technology (IJSRET), vol. 5, pp. 222-226, April 2016.

[14] Wagh, s., & walke, t. v. ((2017).). Review on wind-solar hybrid power system. International journal of research in science & engineering ijrise, 3(2), 71–76.

[15] Melaku Matewos Hailemariam, Tefera Mekonnen, Dr .Hadadi Sudheendra. (2015). Novel Approach to Fuzzy Logic controller based Hybrid Solar/Micro Hydro/Bio-mass Generation, A Real time analysis (Barsoma Village, Ethiopia.). International Journal of Innovative Research in Engineering & Multidisciplinary Physical Sciences(IJIRMPS) , 3(1)20-30.

[16] Medrano, m., brouwer, j., carreras-sospedra, m., rodriguez, m., dabdub, d., & samuelsen,g. s. ((2008).). a methodology for developing distributed generation scenarios in urban areas using geographical information systems. . international journal of energy technonology and policy , 6(4), 413-434.

[17] Ajenikoko, g. a., eboda, a. w., & adelowo, l. ((2018).). Development of a fuzzy logic technique for biogas generation of electrical energy. . International journal of advanced scientific and technical research, 5(8). https://doi.org/10.26808/rs.st.i8v5.03

[18] Rani, s. ((2017).). A novel method for solar energy harvesting method based on optimization, . 3, 415–422.

[19] Fossati, j. p., galarza, a., martín-villate, a., echeverría, j. m., & fontán, l. ((2015).). optimal scheduling of a microgrid with a fuzzy logic controlled storage system. . international journal of electrical power and energy systems .

[20] Ajenikoko, g. a., eboda, a. w., & adelowo, l. ((2018).). Development of a fuzzy logic technique for biogas generation of electrical energy. International journal of advanced scientific and technical research, 5(8). https://doi.org/10.26808/rs.st.i8v5.03.

[21] K. reddy, p. p., & rao, v. g. (2015). “modelling and simulation of hybrid wind solar energy” https://doi.org/10.17485/ijst/v8i23/71277. system using mppt. indian journal of science and technology, 8(23).

[22] Bergman, l., & enocksson, a (2015), Design of a PV system with variations of hybrid system at Addis Ababa institute of technology.

[23] Patel, Sanjukta. "Modeling and control of a grid connected wind-PV hybrid generation system." Master’s thesis, National Institute Technology, 2014.

[24] MHUSA, NICHOLAUS JOSEPH. "Modeling and Control of Photovoltaic-Wind Hybrid Power System Using a Neural-Fuzzy Controller." PhD diss., COHRED, JKUAT, 2016.

[25] Ovaska, Seppo. "Maximum power point tracking algorithms for photovoltaic applications." PhD diss., Aalto University, 2010.

[26] Merlin, s., mary, j., & rajesh babu, s. ((2014).). Energy management on grid connected hybrid renewable energy sources using fuzzy logic. International journal of advanced research in electrical, retrieved from www.ijareeie.com , 3(4), 9275–9283.

[27] Sharma, j. p., & gangwar, s. ((2016).). a standalone hybrid energy system modeling for academic institution. in international conference on energy system and application,icesa 2015, institute of electrical and electronics engineers , (pp.184-188).

[28] Patel, UmaShankar, Ms Dhaneshwari Sahu, and Deepkiran Tirkey. "Maximum power point tracking using perturb & observe algorithm and compare with another algorithm." In International Journal of Digital Application & Contemporary research Conference, vol. 2, no. 2. 2013.

[29] Faranda, Roberto, and Sonia Leva. "Energy comparison of MPPT techniques for PV Systems." WSEAS transactions on power systems 3, no. 6 (2008): 446-455.

[30] Karuna, Kartik. "Optimized MPPT implementation for Dye-sensitized Solar cells: Maximum Power Point Tracking for DCSs." Master's thesis, KTH Royal Institute of Technology, (2015).

[31] Jimenez, Emil, Eduardo I. Ortiz-Rivera, and Omar Gil-Arias. "A dynamic maximum power point tracker using sliding mode control." In Control and Modeling for Power Electronics, 2008. COMPEL 2008. 11th Workshop on, pp. 1-5. IEEE, 2008.

[32] Dwivedi, Laxmi Kant, Prabhat Yadav, and R. K. Saket. " MATLAB based modelling and maximum power point tracking (MPPT) method for photovoltaic system under partial shading conditions." International Research Journal of Engineering and Technology (IRJET) 03, no. 08 (August 2016).

[33] Samy, A. Karuppa, and S. Jeyadevi. "Fuzzy Logic Based Battery Power Management for PV and Wind Hybrid Power System." Asian Journal of Science and Applied Technology 3, no. 1 (2014): 21-27.

APPENDIX
CHARACTERISTICS OF SELECTED SOLAR PANEL

```
Clear
clc
close all
T = 298;
Tr = 298; % Reference temperature
S = [1000 800 600]; % Solar irradiance/m2
ki = 0.00023; % Short circuit temperature constant
Iscr = 8.56; %short circuit current
Irr = 0.000021;
k = 1.38065×10^ (-23); % Boltzmann constant
q = 1.6022×10^ (-19);
a = 2.15; % Ideality factor
Eg = 1.166;%band gap of silicon
%Np = 7; %No.of parallel connected Pv array
%Ns = 27; %No.of series connected cell of Pv
% Ipmax = 8.11; %maximum power current
% Vpmax = 18.5; %maximum power voltage
Np = 7;
Ns = 27;
Vo= (0:1:25);
for i=1:3
Iph = (Iscr+ki× (T-Tr)) × (S(i)/1000);
Irs = Irr× ((T/Tr) ^3) ×exp(q×Eg/(k×a) × ((1/Tr) -(1/T)));
Io = Np×Iph-Np×Irs× (exp(q/(k×T×a) ×Vo./Ns)-1);
Po = Vo. ×Io;
figure (1)
plot(Vo,Io);
axis ([0 25 0 105]);
```

```
xlabel('Voltage in volt');
ylabel('Current in amp');
hold on;
figure (2)
plot(Vo,Po);
axis ([0 25 0 2000]);
xlabel('Voltage in volt');
ylabel('Power in watt');
hold on;
figure (3)
plot(Io,Po);
axis ([0 105 0 2000]);
xlabel('Current in amp');
ylabel('Power in watt');
hold on;
end
```

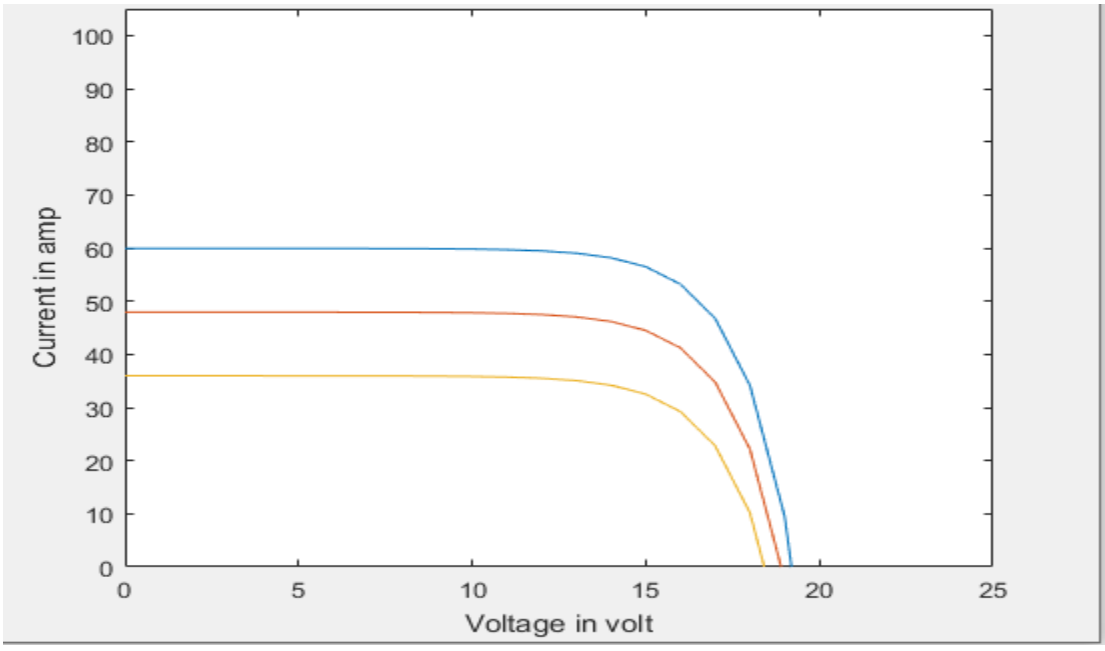


Figure A. 1 Voltage vs Current Simulation Result

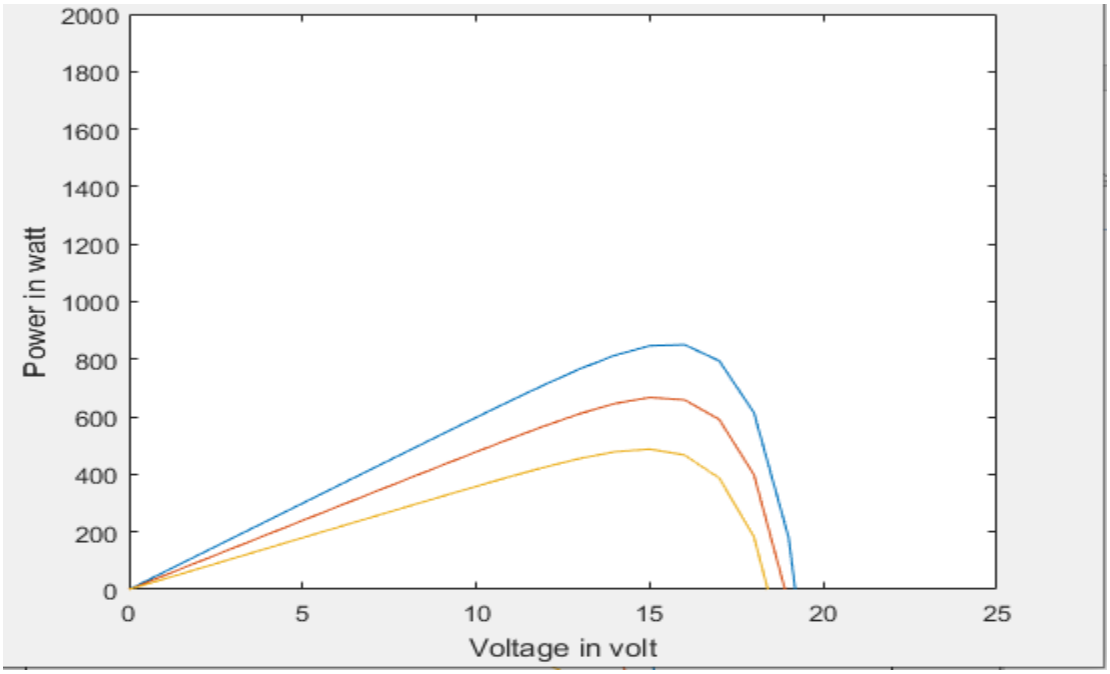


Figure A. 2 Current vs Power Simulation Result

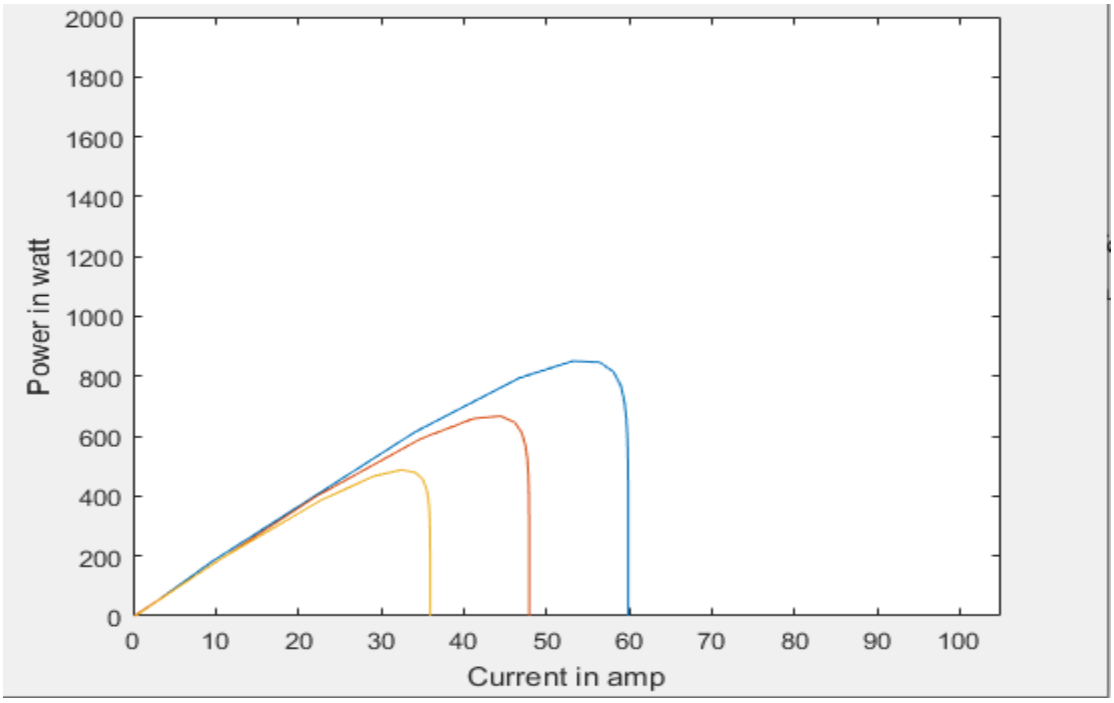


Figure A. 3 Voltage vs power Simulation Result